

Self-Consolidating Concrete (SCC) for Infrastructure Elements Report E – Hardened Mechanical Properties and Durability Performance



Prepared By:



MISSOURI UNIVERSITY OF SCIENCE AND TECHNOLOGY



Final Report Prepared for Missouri Department of Transportation
2012 August

Project TRyy1103

Report cmr 13-003

FINAL Report E

TRyy1103

Project Title: Self-Consolidating Concrete (SCC) for Infrastructure Elements

Report E: Self-Consolidating Concrete (SCC) for Infrastructure Elements: Hardened Mechanical Properties and Durability Performance

Prepared for
Missouri Department of Transportation
Construction and Materials

Missouri University of Science and Technology, Rolla, Missouri

July 2012

The opinions, findings, and conclusions expressed in this publication are those of the principal investigators and the Missouri Department of Transportation. They are not necessarily those of the U.S. Department of Transportation, Federal Highway Administration. This report does not constitute a standard or regulation.

ABSTRACT

Concrete is one of the most produced and utilized materials in the world. Due to the labor intensive and time consuming nature of concrete construction, new and innovative concrete mixes are being explored. Self-consolidating concrete (SCC) is one such method of improving the overall cost and time efficiency of concrete production. SCC is a highly flowable form of concrete. This characteristic drastically reduces the amount of labor and time needed to place the concrete. The highly flowable nature also allows for much easier placement in applications of highly congested reinforcement.

In order to test this new and innovative concrete mix, SCC was tested for both hardened material properties and durability in this investigation. The results indicated that SCC was superior to the baseline conventional concrete.

TABLE OF CONTENTS

	Page
LIST OF ILLUSTRATIONS	viii
LIST OF TABLES	xi
1. INTRODUCTION	1
1.1. BACKGROUND, PROBLEM, & JUSTIFICATION	1
1.1.1. Self-Consolidating Concrete	1
1.2. OBJECTIVES & SCOPE OF WORK	2
1.2.1. Self-Consolidating Concrete	2
1.3. RESEARCH PLAN	3
1.3.1. Self-Consolidating Concrete	3
1.4. OUTLINE	3
1.4.1. Self-Consolidating Concrete	3
2. LITERATURE REVIEW	5
2.1. SELF-CONSOLIDATING CONCRETE	5
2.2. MECHANICAL PROPERTY TESTING METHODS	11
2.2.1. Compressive Strength.....	11
2.2.2. Modulus of Elasticity	12
2.2.3. Modulus of Rupture.....	13
2.2.4. Splitting Tensile Strength.....	14
2.3. DURABILITY OF CONCRETE	15
2.3.1. Freezing and Thawing	15
2.3.2. Chloride Attack	17
2.4. DURABILITY TESTING METHODS	20
2.4.1. Resistance to Freezing and Thawing.....	20
2.4.2. Rapid Chloride Penetration	21
2.4.3. Chloride Content Analysis	23
2.4.4. Concrete Resistivity	25
2.4.5. Scaling Resistance	28
2.5. SELF-CONSOLIDATING CONCRETE	29

2.5.1. Mechanical Properties	29
2.5.2. Durability Performance	30
3. MECHANICAL PROPERTY TESTS	31
3.1. INTRODUCTION	31
3.2. MIX DESIGN	32
3.2.1. Self-Consolidating Concrete Mix Design	32
3.3. COMPRESSIVE STRENGTH TEST.....	37
3.3.1. Introduction	37
3.3.2. Fabrication.....	38
3.3.3. Testing & Procedure.....	39
3.4. MODULUS OF ELASTICITY TEST	42
3.4.1. Introduction	42
3.4.2. Fabrication.....	42
3.4.3. Testing & Procedure.....	43
3.5. MODULUS OF RUPTURE TEST.....	45
3.5.1. Introduction	45
3.5.2. Fabrication.....	45
3.5.3. Testing & Procedure.....	45
3.6. SPLITTING TENSILE TEST.....	48
3.6.1. Introduction	48
3.6.2. Fabrication.....	48
3.6.3. Testing & Procedure.....	49
4. DURABILITY TESTS.....	51
4.1. INTRODUCTION	51
4.2. RAPID FREEZING & THAWING TEST	52
4.2.1. Introduction	52
4.2.2. Fabrication.....	52
4.2.3. Testing & Procedure.....	55
4.3. ELECTRICAL INDICATION TO RESIST CHLORIDE ION PENETRATION TEST	56
4.3.1. Introduction	56

4.3.2. Fabrication.....	57
4.3.3. Testing & Procedure.....	57
4.4. PONDING TEST	60
4.4.1. Introduction	60
4.4.2. Fabrication.....	60
4.4.3. Testing & Procedure.....	61
4.5. CONCRETE RESISTIVITY TEST.....	65
4.5.1. Introduction	65
4.5.2. Fabrication.....	67
4.5.3. Testing & Procedure.....	67
5. SELF-CONSOLIDATING CONCRETE HARDENED PROPERTY AND DURABILITY RESULTS	69
5.1. COMPRESSIVE STRENGTH.....	69
5.2. MODULUS OF ELASTICITY.....	73
5.3. MODULUS OF RUPTURE	77
5.4. SPLITTING TENSILE.....	81
5.5. RAPID FREEZING & THAWING.....	84
5.6. ELECTRICAL INDICATION TO RESIST CHLORIDE PENETRATION ...	86
5.7. PONDING TEST	89
5.8. CONCRETE RESISTIVITY	92
6. EVALUATION OF SELF-CONSOLIDATING CONCRETE	98
6.1. NORMAL STRENGTH SCC.....	98
6.1.1. Mechanical Properties	99
6.1.2. Durability Performance	104
6.2. HIGH STRENGTH SCC	106
6.2.1. Mechanical Properties of High Strength Mixes	107
6.2.2. Durability Performance of High Strength Mixes	114
7. FINDINGS, CONCLUSIONS, AND RECOMMENDATIONS	117
7.1. FINDINGS AND CONCLUSIONS	117
7.1.1. Normal Strength SCC.....	117
7.1.2. High Strength SCC.....	118

7.2. RECOMMENDATIONS.....	120
7.2.1. SCC.....	120
SCC DURABILITY TEST RESULTS DATA	121
REFERENCES	165

LIST OF ILLUSTRATIONS

Figure	Page
Figure 2.1 – Slump Flow Test.....	7
Figure 2.2 – J-Ring Test.....	8
Figure 2.3 – Typical L-box Test Set-Up with Gate Removed.....	9
Figure 2.4 – Typical Segregation Column.....	10
Figure 2.7 – Typical Stress-Strain Diagram for Concrete	
Showing the Different Elastic Moduli [Mindess et al., 2002].....	12
Figure 2.8 - Typical Modulus of Rupture Testing Setup [ASTM C 78–10].....	14
Figure 2.9 - The Relative Volumes of Various Iron Oxides.....	
from Mansfield [1981], Corrosion 37(5), 301-307.	18
Figure 2.10 - Typical RCT Setup.....	22
Figure 2.11 - Schematic Representation of the Four-Probe Resistivity Method [Broomfield, 2007].....	27
Figure 3.1 - Compressive Strength Testing Setup	41
Figure 3.2 - High Strength Compressive Strength Specimens Post-Test	42
Figure 3.3 – 4 in. (102 mm) x 8 in. (203 mm) Cylinder Mold	
Compared to 6 in. (152 mm) x 12 in. (305 mm) Cylinder Mold.....	43
Figure 3.4 - Typical Compressometer	44
Figure 3.5 - Prepared Modulus of Rupture Specimen	46
Figure 3.6 - Modulus of Rupture Testing Setup	47
Figure 3.7 - Modulus of Rupture Specimen Post-Test	47
Figure 3.8 - Typical Splitting Tensile Test Setup.....	49
Figure 3.9 - Splitting Tensile Specimens Post-Test.....	50
Figure 4.1 - Freezing and Thawing Specimen Molds.....	53
Figure 4.2 - Freezing and Thawing Specimen with Protruding Bolt.....	54
Figure 4.3 - Setting Coating Being Applied to Concrete Specimens	58
Figure 4.4 - Typical Completed Specimen	59
Figure 4.5 – Typical RCT Setup.....	59
Figure 4.6 - Typical Ponding Specimen	62

Figure 4.7 - Concrete Core and Resulting Void in the Concrete Specimen	62
Figure 4.8 - Depths at which Powder Samples Were Collected.....	63
Figure 4.9 - Canin ⁺ Wenner Probe.....	66
Figure 4.10 - Wenner Probe Grid	68
Figure 5.1 - Compressive Strength Profile for Normal Strength Mixes.....	70
Figure 5.2 - Compressive Strength Profile for High Strength Concrete Mixes.....	72
Figure 5.3 – Example of RCT Results	87
Figure 5.4 – Average Chloride Content vs. Depth of Conventional Mixes.....	91
Figure 5.5 – Average Chloride Content vs. Depth of High Strength Mixes.....	92
Figure 5.6 - Individual Specimen Results for Concrete Resistivity for C6-58L Mix.....	93
Figure 5.7 - Individual Specimen Results for Concrete Resistivity for S6-48L Mix	94
Figure 5.8 – Averaged Results for Concrete Resistivity for Normal Strength Mixes	95
Figure 5.9 - Individual Specimen Results for Concrete Resistivity for C10-58L Mix.....	96
Figure 5.10 - Individual Specimen Results for Concrete Resistivity for S10-48L Mix ...	96
Figure 5.11 – Averaged Results for Concrete Resistivity for High Strength Mixes	97
Figure 6.1 – Compressive Strength vs. Modulus of Elasticity	101
Figure 6.2 – Compressive Strength vs. Modulus of Rupture.....	102
Figure 6.3 – Compressive Strength vs. Splitting-Tensile Strength.....	103
Figure 6.4 – Average Chloride Content vs. Depth of Conventional Mixes.....	105
Figure 6.5 – Average Resistivity of Normal Strength Concrete Mixes.....	106
Figure 6.6 - Compressive Strength vs. Modulus of Elasticity	110
Figure 6.7 – High Strength Mixes Compared to ACI-363 Equations.....	111
Figure 6.8 – Compressive Strength vs. Modulus of Rupture.....	112
Figure 6.9 – Compressive Strength vs. Splitting-Tensile Strength.....	113
Figure 6.10 – Average Chloride Content vs. Depth of High Strength Mixes.....	115
Figure 6.11 – Average Resistivity of High Strength Concrete Mixes	116
Figure A.1 – C6-58L-EC1TOP RCT Data	137
Figure A.2 – C6-58L-EC1MIDDLE RCT Data	138
Figure A.3 – C6-58L-EC2TOP RCT Data	139
Figure A.4 – C6-58L-EC2MIDDLE RCT Data	140
Figure A.5 – S6-48L-EC1TOP RCT Data.....	141

Figure A.6 – S6-48L-EC1MIDDLE RCT Data	142
Figure A.7 – S6-48L-EC2TOP RCT Data	143
Figure A.8 – S6-48L-EC2MIDDLE RCT Data	144
Figure A.9 – C10-58L-EC1TOP RCT Data	145
Figure A.10 – C10-58L-EC1MIDDLE RCT Data	146
Figure A.11 – C10-58L-EC2TOP RCT Data	147
Figure A.12 – C10-58L-EC2MIDDLE RCT Data	148
Figure A.13 – S10-48L-EC1TOP RCT Data	149
Figure A.14 – S10-48L-EC1MIDDLE RCT Data	150
Figure A.15 – C6-58L-FT1 Data	153
Figure A.16 – C6-58L-FT2 Data	154
Figure A.17 – C6-58L-FT3 Data	155
Figure A.18 – S6-48L-FT1 Data	156
Figure A.19 – S6-48L-FT2 Data	157
Figure A.20 – S6-48L-FT3 Data	158
Figure A.21 – C10-58L-FT1 Data	159
Figure A.22 – C10-58L-FT2 Data	160
Figure A.23 – C10-58L-FT3 Data	161
Figure A.24 – S10-48L-FT1 Data	162
Figure A.25 – S10-48L-FT2 Data	163
Figure A.26 – S10-48L-FT3 Data	164

LIST OF TABLES

Table	Page
Table 2.1 Effect of w/cm Ratio on the Air Void System in Concrete	17
Table 2.2 Chloride Ion Penetrability Based On Charge Passed [ASTM C1202–10]	22
Table 2.3 Chloride Limits for New Construction in % Chloride by Mass of Cement [ACI, 2001]	24
Table 2.4 Correlation Between Percent Water Soluble Chloride	24
by Mass of Concrete and Corrosion Risk [Broomfield, 2007]	24
Table 2.5 Correlation Between Concrete Resistivity and the Rate of Corrosion for a Depassivated Steel Bar Embedded within the Concrete [Broomfield, 2007]	28
Table 2.6 Rating Scale for Scaling Resistance [MoDOT]	29
Table 3.1 Test Matrix for Mechanical Properties	32
Table 3.2 Mix Design per Cubic Yard for SCC Investigation	33
Table 3.3 Typical Fresh Concrete Properties for Conventional Concrete Mixes	36
Table 3.4 Typical Fresh Concrete Properties for Self-Consolidating Concrete Mixes	37
Table 4.1 Test Matrix for Durability Performance	52
Table 5.1 Individual Compressive Strength Results for Normal Strength Mixes	69
Table 5.2 Averaged Compressive Strength Results for Normal Strength Mixes	70
Table 5.3 Individual Compressive Strength Results for High Strength Concrete Mixes ..	71
Table 5.4 Averaged Compressive Strength Results for High Strength Concrete Mixes ..	71
Table 5.5 Individual Modulus of Elasticity Results for Normal Strength Mixes	73
Table 5.6 Average Modulus of Elasticity Results for Normal Strength Mixes	74
Table 5.7 Normalized Modulus of Elasticity for Conventional Concrete Mixes	75
Table 5.8 Normalized AASHTO Modulus of Elasticity for Conventional Concrete Mixes	75
Table 5.9 Individual Modulus of Elasticity Results for High Strength Concrete Mixes ..	76
Table 5.10 Average Modulus of Elasticity Results for High Strength Concrete Mixes ...	76
Table 5.11 Normalized Modulus of Elasticity for High Strength Concrete Mixes	76
Table 5.12 Normalized AASHTO Modulus of Elasticity for High Strength Concrete Mixes	77

Table 5.13 Individual Modulus of Rupture Results for Normal Strength Mixes	77
Table 5.14 Averaged Modulus of Rupture for Normal Strength Mixes	78
Table 5.15 Normalized Modulus of Rupture for Normal Strength Mixes.....	78
Table 5.16 Normalized AASHTO Modulus of Rupture for Normal Strength Mixes	79
Table 5.17 Individual Modulus of Rupture Results for High Strength Concrete Mixes ..	80
Table 5.18 Average Modulus of Rupture Results for High Strength Concrete Mixes	80
Table 5.19 Normalized Modulus of Rupture Results for High Strength Concrete Mixes	80
Table 5.20 Normalized AASHTO Modulus of Rupture for High Strength Mixes.....	81
Table 5.21 Individual Splitting-Tensile Test Results for Normal Strength Concrete Mixes	82
Table 5.22 Averaged Splitting-Tensile Test Results for Normal Strength Concrete Mixes	82
Table 5.23 Normalized Splitting-Tensile Results for Normal Strength Concrete Mixes .	83
Table 5.24 Individual Splitting-Tensile Test Results for High Strength Concrete Mixes	83
Table 5.25 Averaged Splitting-Tensile Test Results for High Strength Concrete Mixes.	84
Table 5.26 Normalized Splitting-Tensile Results for High Strength Concrete Mixes	84
Table 5.27 Individual Results of Rapid Freezing and Thawing Test for Normal Strength Mixes.....	85
Table 5.28 Averaged Durability Factors for Normal Strength Mixes	85
Table 5.29 Individual Results of Freezing and Thawing Test for High Strength Mixes..	86
Table 5.30 Averaged Durability Factors for High Strength Mixes	86
Table 5.31 Individual RCT Results for Normal Strength Mixes	88
Table 5.32 Averaged Results of RCT and Permeability Class of Conventional Mixes ...	88
Table 5.33 Individual Results of RCT for High Strength Mixes.....	89
Table 5.34 Averaged Results of RCT and Permeability Class for High Strength Mixes.	89
Table 5.35 Correlation Between Percent Chloride by	90
Mass of Concrete and Corrosion Risk [Broomfield, 2007]	90
Table 5.36 Average Chloride Content at Specified Depths of Normal Strength Mixes...	90
Table 5.37 Average Chloride Content at Specified Depths of High Strength Mixes	91
Table 5.38 Final Resistivity of Normal Strength Concrete Mixes.....	95
Table 5.39 Final Resistivity of High Strength Concrete Mixes.....	97

Table 6.1 Outline of Results of Normal Strength Concrete Mixes.....	99
Table 6.2 Normalized Mechanical Properties Compared to Respective ACI Coefficients	100
Table 6.3 Normalized Mechanical Properties Compared to Respective AASHTO Coefficients	104
Table 6.4 Outline of Results of High Strength Concrete Mixes.....	107
Table 6.5 Normalized Mechanical Properties Compared to Respective ACI Coefficients	108
Table 6.6 Normalized Mechanical Properties Compared to Respective AASHTO Coefficients	113
Table A.1 C6-58L-1R (Weeks 1-7)	122
Table A.2 C6-58L-1R (Weeks 8-14)	122
Table A.3 C6-58L-1R (Weeks 15-21)	122
Table A.4 C6-58L-1R (Weeks 22-24)	123
Table A.5 C6-58L-2R (Weeks 1-7)	123
Table A.6 C6-58L-2R (Weeks 8-14)	123
Table A.7 C6-58L-2R (Weeks 15-21)	124
Table A.8 C6-58L-2R (Weeks 22-24)	124
Table A.9 C6-58L-3R (Weeks 1-7)	124
Table A.10 C6-58L-3R (Weeks 8-14)	125
Table A.11 C6-58L-3R (Weeks 15-21)	125
Table A.12 C6-58L-3R (Weeks 22-24)	125
Table A.13 S6-48L-1R (Weeks 1-7).....	126
Table A.14 S6-48L-1R (Weeks 8-14).....	126
Table A.15 S6-48L-1R (Weeks 15-21).....	126
Table A.16 S6-48L-1R (Weeks 22-24).....	127
Table A.17 S6-48L-2R (Weeks 1-7).....	127
Table A.18 S6-48L-2R (Weeks 8-14).....	127
Table A.19 S6-48L-2R (Weeks 15-21).....	128
Table A.20 S6-48L-2R (Weeks 22-24).....	128
Table A.21 C10-58L-1R (Weeks 1-7)	128

Table A.22 C10-58L-1R (Weeks 8-14)	129
Table A.23 C10-58L-1R (Weeks 15-21)	129
Table A.24 C10-58L-1R (Weeks 22-24)	129
Table A.25 C10-58L-2R (Weeks 1-7)	130
Table A.26 C10-58L-2R (Weeks 8-14)	130
Table A.27 C10-58L-2R (Weeks 15-21)	130
Table A.28 C10-58L-2R (Weeks 22-24)	131
Table A.29 C10-58L-3R (Weeks 1-7)	131
Table A.30 C10-58L-3R (Weeks 8-14)	131
Table A.31 C10-58L-3R (Weeks 15-21)	132
Table A.32 C10-58L-3R (Weeks 22-24)	132
Table A.33 S10-48L-1R (Weeks 1-7).....	132
Table A.34 S10-48L-1R (Weeks 8-14).....	133
Table A.35 S10-48L-1R (Weeks 15-21).....	133
Table A.36 S10-48L-1R (Weeks 22-24).....	133
Table A.37 S10-48L-2R (Weeks 1-7).....	134
Table A.38 S10-48L-2R (Weeks 8-14).....	134
Table A.39 S10-48L-2R (Weeks 15-21).....	134
Table A.40 S10-48L-2R (Weeks 22-24).....	135
Table A.41 S10-48L-3R (Weeks 1-7).....	135
Table A.42 S10-48L-3R (Weeks 8-14).....	135
Table A.43 S10-48L-3R (Weeks 15-21).....	136
Table A.44 S10-48L-3R (Weeks 22-24).....	136
Table A.45 C6-58L Chloride Content Data.....	151
Table A.46 S6-48L Chloride Content Data	151
Table A.47 C10-58L Chloride Content Data.....	151
Table A.48 S10-48L Chloride Content Data	152

1. INTRODUCTION

1.1. BACKGROUND, PROBLEM, & JUSTIFICATION

1.1.1. Self-Consolidating Concrete. Self-consolidating concrete (SCC) was developed in Japan in the late 1980's to solve the problem of a growing shortage of concrete laborers. Concrete, by its very nature, can be a challenging material to construct properly, particularly with very complex geometrical shapes or within elements containing very congested reinforcement. Placement and finishing of conventional concrete requires a significant amount of labor and is very time consuming. SCC was developed in an attempt to solve these problems. SCC is defined as a concrete that spreads easily under its own weight while still resisting segregation. The benefits of SCC include decreased labor and equipment cost during concrete placement, decreased potential for honeycombing and voids, increased production rates of precast and cast-in-place elements, and improved finish and appearance of cast and free concrete surfaces. However, concerns exist over the structural implications of SCC in cast-in-place and precast elements. Specifically, higher paste contents, higher fine contents, and the use of smaller, rounded aggregates may significantly alter the behavior of SCC compared to traditional concrete mixes with similar water to cementitious ratio (w/cm).

Consequently, to achieve the benefits and potential savings with SCC, the behavior of the material needs to be evaluated relative to conventional concrete. One necessary step required to make SCC so workable is to increase the fine aggregate content while decreasing the coarse aggregate content. However, increasing the fine aggregate content is believed to reduce the modulus of elasticity, as well as the tensile strength of concrete. This decrease in coarse aggregate content could also have negative

side effects on the durability performance of SCC. Resistance to freeze-thaw is largely impacted by the type and content of the coarse aggregate used in the concrete. This change to the coarse aggregate may alter the durability performance of the material. However, some research has shown that the increased density of the paste is thought to improve durability performance with a decrease in overall porosity. As a result, a systematic evaluation of the hardened material properties and durability performance of SCC is required prior to implementing its use in transportation-related infrastructure.

1.2. OBJECTIVES & SCOPE OF WORK

1.2.1. Self-Consolidating Concrete. The main objective of this study is to investigate the mechanical properties and the durability performance of SCC in comparison to conventional concrete.

The following scope of work was implemented in an effort to attain this objective: (1) review applicable and relevant literature; (2) develop a research plan; (3) evaluate the mechanical and durability properties of both normal strength and high strength SCC mixes; (4) compare the SCC mixes with conventional concrete mixes; (5) verify the validity of using current hardened property tests on SCC; (6) analyze the information gathered throughout the testing to develop findings, conclusions, and recommendations; and (7) prepare this thesis in order to document the information obtained during this investigation.

1.3. RESEARCH PLAN

1.3.1. Self-Consolidating Concrete. The research plan entailed developing SCC mix designs based on current Missouri precast plant applications. The mix designs are described in Section 3. Several standard hardened property tests were selected to evaluate the performance of the SCC mixes in comparison to conventional concrete, including compressive strength, modulus of elasticity, modulus of rupture, and splitting-tensile strength. These tests were also used to determine their validity in predicting the performance of SCC.

Specimens were also fabricated in order to evaluate the durability performance of SCC. The tests performed on the mixes consisted of chloride penetration by electrical indication and ponding methods, freeze-thaw resistance, and concrete resistivity. Both the conventional and SCC mixes were subjected to these durability tests in order to compare their performance.

1.4. OUTLINE

1.4.1. Self-Consolidating Concrete. This report consists of seven sections and one appendix. Section 1 briefly explains the history and benefits of using SCC. Also within Section 1 are the objectives, scope of work, and research plan.

Section 2 summarizes how SCC is produced and new test methods used to evaluate the fresh properties of SCC. The mechanical property tests are also discussed in further detail. Lastly, the durability tests as well as the mechanisms behind the durability issues are discussed.

Section 3 explains the development of the SCC mix designs including the selection of chemical admixtures. This section includes typical fresh properties measured

during this investigation. Also, the mechanical property tests are discussed in more detail as well as equations used to estimate the behavior of concrete.

Section 4 consists of discussing the tests used to evaluate the durability performance in further detail.

Section 5 presents the results of both the mechanical property tests as well as the durability tests. Also presented in this section are the normalized results of the mechanical property tests in comparison to traditional relationships used to estimate the behavior of concrete.

Section 6 outlines the results of the investigation and evaluates the data based on a statistical analysis. Also, the results of the investigation are discussed to propose a theory on the outcome of the tests in order to recommend how to successfully implement SCC.

Section 7 consists of the conclusion of the investigation as well as any recommendations based on the findings from the mechanical tests as well as the durability performance of the SCC mixes in comparison to conventional concrete.

There is one appendix contained in this thesis. Appendix A contains additional test data associated with the durability tests of the SCC mixes.

2. LITERATURE REVIEW

2.1. SELF-CONSOLIDATING CONCRETE

Self-consolidating concrete (SCC) is a relatively new mix of concrete which is characterized by its high degree of workability. SCC is very flowable and doesn't require any vibration when placing in the formwork. SCC also finishes very smoothly, leaving a glassy finish after curing. SCC originated in Japan in the 1980's due to Japan's decreasing labor force [Khayat, 1999]. In order to achieve the high workability of SCC while maintaining cohesiveness, the composition of SCC has to be altered. This can be done one of three ways: chemically, materially, or a combination of the two. To produce SCC chemically, two admixtures are used, High Range Water Reducers (HRWR) and Viscosity Modifying Admixtures (VMA). In concrete, the cement particles typically carry either positive or negative charges. The attraction between particles causes them to agglomerate. Water is trapped inside these particles and is not able to add to the workability of the fresh concrete. HRWRs place a like charge on the cement particles causing them to repel each other. This frees the water in the paste to add to the workability of the concrete. VMAs are used to increase the viscosity of the water, which prevents the highly flowable mix from segregating. These two admixtures allow for SCC to have the high flowability necessary to be beneficial while maintaining cohesiveness. This can also be achieved through purely physical means. To achieve the flowability of SCC, the water to cementitious material ratio (w/cm) must be increased. In order to maintain cohesiveness in such a relatively wet mix, the fine aggregate content must be increased. It is typical to see SCC mixes that contain more fine aggregate than coarse aggregate, which is completely opposite of conventional concrete. Most SCC mixes

today are produced using the third technique, which is a combination of altering the physical composition of the mix as well as the addition of chemical admixtures. These SCC mixtures maintain the high fine aggregate content while using a low w/cm ratio. The highly flowable behavior is achieved through the addition of a HRWR. This creates SCC that is both flowable and doesn't need vibration while maintaining a low w/cm, which can yield stronger and more durable concrete.

Due to the highly flowable nature of SCC, most of the conventional fresh property tests are not applicable to SCC. For this reason, several new property tests were derived in order to test the fresh properties of SCC, which included tests to evaluate properties specific to SCC. These new properties include flowability, passability, and resistance to segregation. In order to test the flowability, which is comparable to the slump of conventional concrete, the slump flow test was created. This test is outlined in ASTM C 1611-09, "Standard Test Method for Slump Flow of Self-Consolidating Concrete." Using a standard Abram's cone, either in the upright or inverted position, the SCC is placed into the cone in a single lift with no tamping or vibration. The cone is then lifted from the slump flow plate and the diameter of the spread is measured. The slump flow test is also used to note the resistance of SCC to segregation. If an SCC mix has segregation problems, most of the coarse aggregate will stay towards the center of the circle. The time it takes for the SCC spread to reach a diameter of 20 in. (50 cm) is also recorded. This reading indicates the ability of the SCC to fill molds and remain stable. The typical target value for the spread of SCC ranges from 22 in. (56 cm) to 29 in. (74 cm). A typical SCC slump flow spread can be seen in **Figure 2.1**.



Figure 2.1 – Slump Flow Test

Another test used in correlation with the slump flow test is the J-Ring test. This test is outlined in ASTM C 1621-09, “Standard Test Method for Passing Ability of Self-Consolidating Concrete by J-Ring.” In this test, the slump flow test is performed but a circular ring with vertical bars is placed on the slump flow plate. The concrete is allowed to spread into a circle but must pass through the J-Ring. This test is to simulate reinforcing bars, altering the flow of the SCC. A poor performing SCC mix will maintain a noticeable amount of the coarse aggregate within the J-Ring, allowing only the mortar fraction (cement, sand, and water) to pass through. This behavior indicates a lack of cohesiveness, which would prove detrimental if used in the field. The diameter of the spread using the J-Ring is also measured, and in addition to the behavior of the coarse aggregate during the test, a successful test typically requires the J-Ring diameter to measure no more than 2 in. (51 mm) less than the value recorded for the corresponding slump flow. A typical J-Ring spread can be seen in **Figure 2.2**.



Figure 2.2 – J-Ring Test

Other fresh property tests include the L-box test and the segregation column to measure passability and stability, respectively. The L-box is a non-ASTM test outlined in ACI 237-07 which is used to determine the passing and filling ability of an SCC mix. The vertical column of the L-box is first filled with SCC in a single lift, without vibration or tamping. A gate is then lifted allowing the SCC to flow out of the vertical column and into the horizontal trough of the L-box. At the gate there are three bars simulating reinforcing steel that the SCC must pass through. The SCC must reach the end of the horizontal section of the L-box in order for it to pass. Additionally the ratio of the height of the SCC at the end of the trough over the height of the SCC at the gate is measured. This is referred to as the “blocking ratio”. A SCC mix must have a minimum blocking ratio of 0.8 to be considered acceptable. The closer the blocking ratio is to 1.0 the better performance a SCC mix can be expected to show. A typical L-box is shown in **Figure 2.3**.

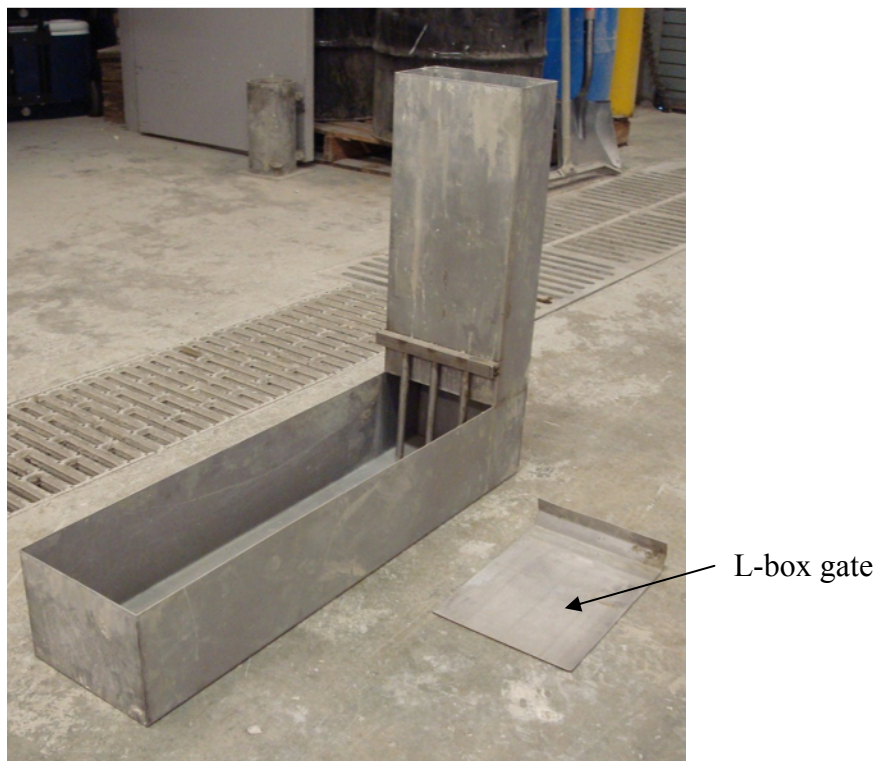


Figure 2.3 – Typical L-box Test Set-Up with Gate Removed

The segregation column is used to determine the ability of the SCC mix to resist static segregation. This test is outline in ASTM C 1610-10, “Standard Test Method for Static Segregation of Self-Consolidating Concrete Using Column Technique.” A column measuring 26 in. (660 mm) in height and 8 in. (200 mm) in diameter is filled in one lift with SCC. This column is made up of three separate sections, the top and bottom sections measuring 6.5 in. (165 mm) in height and the middle section measuring 13 in. (330 mm) in height. The segregation column can be seen in **Figure 2.4**. Once the column is filled, the SCC is then allowed to sit for 15 minutes. The SCC from the top and bottom sections of the column is then collected separately and rinsed over a No. 4 sieve in order to separate the paste from the aggregate. The aggregate from the top and bottom column

sections is then dried and weighed. Using these weights the static segregation is calculated in accordance with **Eq. 2.1**.

$$S = 2 \left[\frac{(CA_B - CA_T)}{(CA_B + CA_T)} \right] \times 100, \text{ if } CA_B > CA_T \quad (2.1)$$

$$S = 0, \text{ if } CA_b \leq CA_T$$

Where S is the static segregation in percent, CA_T is the mass of coarse aggregate in the top section of the column, and CA_B is the mass of coarse aggregate in the bottom section of the column. Although an acceptable standard for static segregation has not yet been established, an SCC mix is generally considered acceptable if the static segregation is less than 10%.



Figure 2.4 – Typical Segregation Column

2.2. MECHANICAL PROPERTY TESTING METHODS

2.2.1. Compressive Strength. The compressive strength of concrete is the most important of all the mechanical properties. Measuring compressive strength is influenced by many factors including specimen size, curing conditions, load rate, etc. In order to control variations in testing and consequently variations in results, a standard test method was developed by ASTM International. The standard for determining the compressive strength of concrete is outlined in ASTM C 39–11, “Standard Test Method for Compressive Strength of Cylindrical Concrete Specimens.” This standard requires cylindrical specimens for testing. The specimens used in laboratory testing measure either 4 in. (102 mm) in diameter x 8 in. (203 mm) in height or 6 in. (152 mm) in diameter x 12 in. (305 mm) in height. The specimens are prepared by filling the molds in equal lifts and rodding each lift a specified number of times. The numbers of lifts and extent of rodding depends on the diameter and cross sectional area, which is specified in ASTM C 192-07 “Standard Practice for Making and Curing Concrete Test Specimens in the Laboratory.” After each lift, the mold is also struck with a mallet to ensure consolidation. After 24 hours in a moist curing chamber, the specimens are de-molded and returned to the moist curing chamber until the proper test date. Common testing dates for measuring a concrete’s strength gain profile are 1, 7, and 28 days after batching. The cylindrical specimens are ground flat or capped before testing. This flat surface reduces localized stress on the specimen. Capping can be done with sulfur capping compound or neoprene pads. Dimensions of the specimens are taken before being loaded at a constant rate until

failure. The load recorded at failure is divided by the cross-sectional area to find the compressive strength of the concrete.

2.2.2. Modulus of Elasticity. Due to the nonlinear inelastic behavior of concrete, the modulus of elasticity (MOE) can be different depending on how it is measured. The MOE is the slope of the stress–strain curve between two designated points. An example of the different moduli of elasticity that can be measured can be seen in **Figure 2.7**.

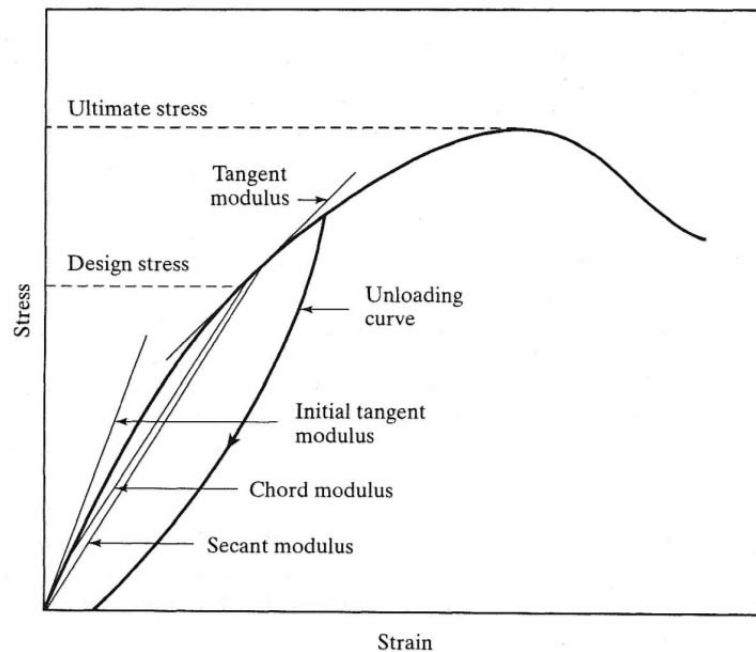


Figure 2.7 – Typical Stress-Strain Diagram for Concrete, Showing the Different Elastic Moduli [Mindess et al., 2002]

In order to standardize the measured modulus of elasticity, ASTM International developed a standard test method ASTM C 469-10, “Standard Test Method for Static Modulus of Elasticity and Poisson’s Ratio of Concrete in Compression.” This test method measures what is known as the chord modulus of elasticity. The specimens used in this

test are the same type used in the compressive strength test. Either the 4 in. (102 mm) or 6 in. (152 mm) diameter cylindrical specimens can be used. Specimens are fabricated and cured in the same manner as the compressive strength specimens. After 28 days of moist curing, specimens are prepared for testing. Using a Compressometer, the strain produced at 40% of the ultimate load is recorded. Also, the stress that produces a measured strain of 0.00005 in./in. is recorded. Using these values, the chord modulus of elasticity can be calculated in accordance with **Eq. 2.2**.

$$E_c = \frac{(S_2 - S_1)}{(\epsilon_2 - 0.00005)} \quad (2.2)$$

2.2.3. Modulus of Rupture. The modulus of rupture is an important property in the calculation of the cracking moment of concrete and thus determining how a concrete member will behave post-cracking. ASTM International has created a standard for testing the modulus of rupture known as ASTM C 78-10, “Standard Test Method for Flexural Strength of Concrete (Using Simple Beam with Third-Point Loading).” This approach is an indirect way to measure the tensile strength of concrete. The specimen has to have an overall depth of a third of the span length. The span length shall be such that it measures three times the distance in between the load points of the testing apparatus. Also, the specimen shall overhang the supports by at least 1 in. (25 mm). The schematic diagram in **Figure 2.8** summarizes these requirements.

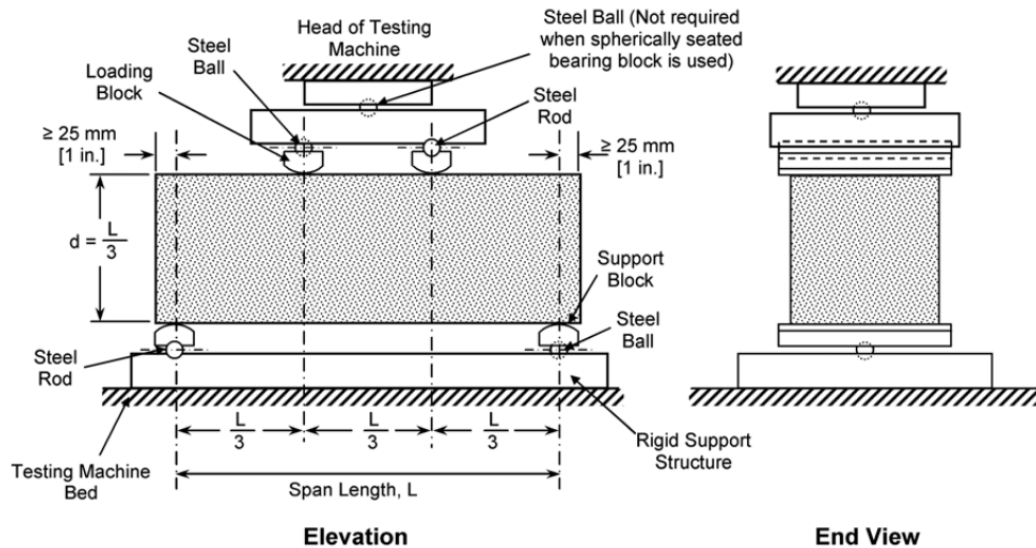


Figure 2.8 - Typical Modulus of Rupture Testing Setup [ASTM C 78–10]

The specimen is then loaded until failure. After testing, the dimensions are recorded and the modulus of rupture is computed in accordance with **Eq. 2.3**. While this test method overestimates the “true” tensile strength of concrete, the test does simulate the most common way concrete is placed into tension, through flexure.

$$R = \frac{PL}{bd^2} \quad (2.3)$$

2.2.4. Splitting Tensile Strength. While the modulus of rupture test described in Section 2.3.3 tests for the tensile strength of concrete indirectly, the splitting tensile test uses a much more direct manner. This test is outlined in ASTM C 496–11, “Splitting Tensile Strength of Cylindrical Concrete Specimens.” The cylindrical specimens measure either 4 in. (102 mm) in diameter by 8 in. (203 mm) in height or 6 in. (152 mm) in diameter and 12 in. (305 mm) in height. The method for preparing the specimens used in the splitting-tensile test is outline in ASTM C 192. Specimens are

stored in a moist curing chamber and tested after 28 days. Diametral lines are drawn on the specimens to ensure that they are in the same axial plane. The dimensions of the specimens are then taken. The specimens are then placed on top of a 1 in. (25 mm) wide x 3/8 in. (10 mm) thick plywood strip within the testing apparatus. A second plywood strip is then placed on top of the specimen so the two strips align with the diametral lines. This ensures that the load is distributed in one plane of the specimen. The peak load is recorded and the tensile strength is then calculated in accordance with **Eq. 2.4**.

$$T = \frac{2P}{\pi LD} \quad (2.4)$$

2.3. DURABILITY OF CONCRETE

2.3.1. Freezing and Thawing. Concrete is a porous material which allows water to permeate into its microstructure. When concrete containing moisture is subjected to repeated cycles of freezing and thawing, severe deterioration can occur. Initially researchers believed that this damage was caused by the expansion of water when it transitioned into ice. The trapped water would freeze and expand in the capillary pores and exert hydraulic pressure on the hardened paste. This theory of hydraulic pressure was proposed by T.C Powers [Mindess et al., 2002]. Later, Powers developed a new theory based on osmotic pressure [Powers, 1956]. He proposed this theory after observing that concrete paste, when frozen, shrank first than expanded. He also observed that air entrained cement paste would shrink indefinitely and the same deterioration is observed when liquids that do not expand when frozen were used to saturate the concrete. Investigators developed two possible explanations for these observations. The first is

osmotic pressure. As water is drawn to the freezing sites through osmosis, osmotic pressure is built up. This eventually would cause the concrete to crack. Another possible explanation is vapor pressure. The ice that begins to form in the pores has less chemical potential than the supercooled water in the unfrozen pores. This creates a lower vapor pressure. This condition causes the relative humidity at the freezing pores to lower, which draws water towards them to maintain equilibrium. This pressure would also cause the concrete to begin to crack.

The introduction of air entraining admixtures has had a positive effect on the resistance of concrete to freezing and thawing deterioration. The air bubbles in the concrete allow for excess space for the water to move and freeze without damaging the concrete. These bubbles must be spaced at certain intervals to be effective in protecting the concrete. If the bubbles are too far apart, the water cannot move to these “safety valves” and the pressure cannot be relieved. The air-entraining system becomes ineffective in fully saturated concrete due to all the pores and air bubbles containing water. Many other factors influence a concrete’s resistance to freezing and thawing attack, the most important of which is the permeability of the concrete. With concretes having a low water/cement ratio and usually a low permeability, freeze/thaw resistance generally increases [Mindess et al., 2002]. This relationship can be seen in **Table 2.1**.

Table 2.1 Effect of w/cm Ratio on the Air Void System in Concrete

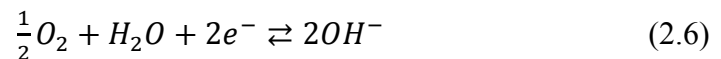
w/c ratio	Air content (%)	Spacing factor mm (in.)	Liner expansion per freeze – thaw cycle
0.35	4.8	0.11 (0.0043)	0.00004
0.45	4.7	0.14 (0.0055)	0.00014
0.55	5.2	0.15 (0.0059)	0.00021
0.65	4.9	0.18 (0.0071)	0.00026
0.75	5.3	0.23 (0.0091)	0.00036

1 in. = 2.54 cm.

2.3.2. Chloride Attack. Chloride ions attack the passive layer that forms on reinforcing steel placed within a high pH environment, such as concrete. Chloride ions are most commonly introduced into concrete through deicing salts. These salts can remain on bridge decks for days or even weeks, penetrating into the concrete structure and eventually destroying the passive layer of the reinforcing steel. Corrosion in steel begins with the iron being oxidized at an anode as shown in **Eq. 2.5**.



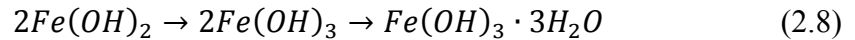
At the cathode, water is reduced into hydroxyl (OH^{-}) ions as shown in **Eq. 2.6**.



These hydroxyl ions then flow from the cathode to the anode. At the anode, the ferrous ions and the hydroxyl ions react to form ferrous hydroxide as shown in **Eq. 2.7**.



When oxygen and water are introduced the ferrous hydroxide will spontaneously oxidize into hydrated ferric oxide (rust) as shown in **Eq. 2.8**.



This hydrated ferric oxide, or red rust that is commonly seen, is known to have six times the volume of the original iron [Broomfield, 2007]. The increased volume induces expansive stresses in the concrete, eventually leading to cracking and progressive deterioration. The volume of iron and various forms of oxidized irons can be seen in

Figure 2.9.

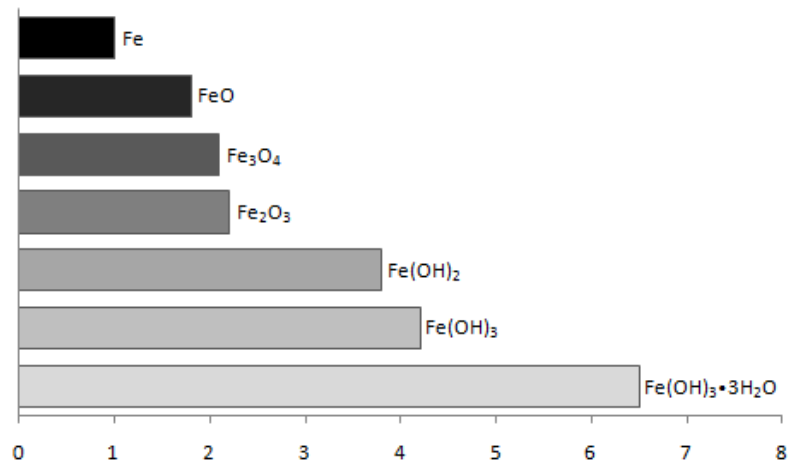
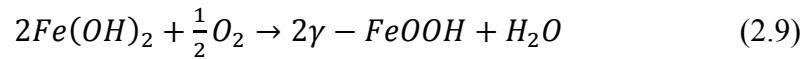


Figure 2.9 - The Relative Volumes of Various Iron Oxides from Mansfield [1981], Corrosion 37(5), 301-307.

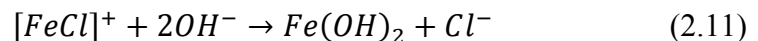
This reaction can be largely avoided in concrete structures. Conventional concrete is highly alkaline which allows for the formation of a passive oxide film (FeOOH) on the reinforcement. The Fe(OH)₂ is oxidized to create this film as shown in **Eq. 2.9**.



Chlorides effectively destroy this passive layer allowing for the reinforcement to corrode. Chlorides react with ferrous ions to create a soluble iron-chloride complex as shown in **Eq. 2.10**.



This complex in turn reacts with the hydroxyl to form the ferrous hydroxide which oxidizes into expansive rust as shown in **Eq. 2.11**.



The largest factor influencing the effect of chlorides in concrete is the permeability of the concrete. The permeability relates to the amount and rate of oxygen, moisture, and chloride penetration into the microstructure of the concrete over time. Permeability is most influenced by the water to cementitious material ratio (w/cm). The lower the w/cm ratio of the concrete, the lower the porosity [Powers et al., 1954]. Decreasing the permeability of concrete will improve its durability. Water can carry harmful chemicals,

such as chlorides, into the concrete's pores. The diffusion of chemicals into hardened concrete is described by *Fick's Second Law* as shown in **Eq. 2.12**.

$$\frac{\partial c}{\partial t} = K_d \frac{\partial^2 c}{\partial x^2} \quad (2.12)$$

Where C is the concentration, t is the time, K_d is the diffusion coefficient, and x is the depth. The solution of this equation is shown in **Eq. 2.13** [Broomfield 2007].

$$\frac{C_{max}-C_d}{C_{max}-C_{min}} = erf\left(\frac{x}{\sqrt{4D_c t}}\right) \quad (2.13)$$

Where C_d is the chloride concentration at depth (x), x is the specified depth, t is the time, D_c is the diffusion coefficient of concrete, C_{max} is the maximum chloride content of the concrete, C_{min} is the baseline chloride content of the concrete, and erf is the error function. Using this function the chloride penetration over time can be estimated. This equation has proved to estimated chloride contents extremely accurately when compared to field results [Berke and Hicks, 1996].

2.4. DURABILITY TESTING METHODS

2.4.1. Resistance to Freezing and Thawing. In order to evaluate the potentially devastating effects of freezing and thawing cycles, ASTM International developed a standardized test to simulate these conditions in the lab. This test is outlined in ASTM C 666–03 “Standard Test Method for Resistance of Concrete to Rapid Freezing and Thawing.” Specimens used in this test are prisms that are made and cured in

accordance with ASTM C 192. The dimension requirements of these specimens are specified in ASTM C 666. The specimens are cured for 14 days before testing unless otherwise specified. This test subjects the specimens to 300 freezing and thawing cycles. Every 36 cycles, the specimens are removed and properties of the concrete are measured. These properties include the transverse frequency, total length change, and total weight change. These specimens can be tested using two different procedures, A or B. Procedure A specifies that the specimens be surrounded by water during the freezing and thawing cycles, while Procedure B specifies that the specimens be surrounded by air during freezing and water during thawing. Between the testing intervals, both the relative dynamic modulus of elasticity and the durability factor are calculated. Using these values, the concrete can be evaluated for its durability performance. The test calls for the cycles to be stopped when the measured durability factor falls below 50. Every Department of Transportation has its own criteria for acceptable durability factor and sets a minimum for acceptance. The acceptability criteria for the state of Missouri and for this investigation will be discussed in Sections 6.1.2 and 6.2.2.

2.4.2. Rapid Chloride Penetration. The diffusion of chlorides can be extremely damaging, as stated previously. However the process is very slow, and testing the chloride penetration accurately can take years. In order to test a concrete's ability to resist chloride penetration, ASTM International developed a testing method that could be performed much more quickly. This testing method is outlined in ASTM C 1202-10, "Standard Test Method for Electrical Indication of Concrete's Ability to Resist Chloride Ion Penetration." This test is also known as the Rapid Chloride Test (RCT). The test specimens consist of concrete disks subjected to a constant voltage to determine their

resistance to chloride penetration. The disks are cut from concrete cylinders that are fabricated and cured according to ASTM C 192. The disks, measuring 4 in. (102 mm) in diameter and 2 in. (51 mm) thick, are prepared according to ASTM C 1202 and subjected to 60 V for 6 hours as shown in **Figure 2.10**.



Figure 2.10 - Typical RCT Setup

During the test, the current is recorded every 30 minutes. Using a plot of current versus time, the total charge passed is calculated and used to determine the permeability class of the concrete. There is a correlation between the amount of charge passed and the chloride ion penetrability of concrete. This correlation can be seen in **Table 2.2**.

Table 2.2 Chloride Ion Penetrability Based On Charge Passed [ASTM C1202–10]

Charge Passed (coulombs)	Chloride Ion Penetrability
>4000	High
2000-4000	Moderate
1000-2000	Low
100-1000	Very Low
<100	Negligible

2.4.3. Chloride Content Analysis. While the test outlined in ASTM C 1202 is an adequate test when the results are required quickly, it does not subject the concrete to realistic conditions. ASTM C 1202 is only suitable for research and development. One studies have indicates that ASTM C 1202 gives false indications for concretes made with supplementary cementitious materials, such as fly ash, slag, silica fume, and slag [Shi, 2002]. This study showed that cement containing supplementary cementitious material would yield falsely high results than what was observed in the field. Researchers found that the change in chemical composition due the addition of supplementary cementitious material affected the results of the Rapid Chloride Test. In order to properly evaluate a concrete's ability to resist chloride penetration, it should tested directly using ASTM C 1543–10, “Standard Test Method for Determining the Penetration of Chloride Ion into Concrete by Ponding.” This test method involves subjecting concrete specimens to a 5% by weight sodium chloride solution for 120 days. The specimens are then cored and powder samples are collected to determine the chloride content at multiple levels. According to Broomfield [2007], it is recommended that a minimum of four data points be used in developing a chloride profile in order to obtain an accurate representation of the chloride distribution. A chloride content analysis is then performed on the powder samples in order to determine the chloride profile of the concrete. Two types of chloride analyses can be performed on the concrete powder; acid-soluble and water-soluble. Acid-soluble tests will determine the total chloride content, including those chlorides trapped in the aggregate and paste (C_3A). Water-soluble tests will only determine those chlorides free to deteriorate the passive layer of the concrete, thus promoting corrosion. In some

cases, the acid-soluble test will overestimate the corrosion potential of a concrete and in others provide a reasonable evaluation. ACI has developed limits on chloride content for new construction for varying applications of concrete. These limitations can be seen in **Table 2.3**.

**Table 2.3 Chloride Limits for New Construction in % Chloride by Mass of Cement
[ACI, 2001]**

	Test method	
	Acid Soluble	Water Soluble
Concrete Application	ASTM C1152	ASTM C1218
Pre-stressed concrete	0.08	0.06
Reinforced concrete in wet conditions	0.10	0.08
Reinforced concrete in dry conditions	0.20	0.15

For in place structures, classifications were developed based on chloride contents and the corrosion risk. These classifications can be seen in **Table 2.4**. [Broomfield, 2007]

**Table 2.4 Correlation Between Percent Water Soluble Chloride
by Mass of Concrete and Corrosion Risk [Broomfield, 2007]**

% Chloride by mass of concrete	Corrosion Risk
<0.03	Negligible
0.03-0.06	Low
0.06-0.14	Moderate
>0.14	High

The chloride profile determined from this test method indicates the concentration of the chloride ions in the concrete as a function of depth from the surface. As stated in Section 2.4.2, chlorides will destroy the passive layer on the reinforcement in the concrete, exposing the steel to elements that will initiate corrosion. The chloride profile determined from this test method will indicate the amount of ions at specified depth to determine a concrete's ability to resist diffusion and therefore chloride ingress. In general, this test is a comparative test and does not necessarily indicate the response of a structure in service.

2.4.4. Concrete Resistivity. Electrical resistance also plays an important role in the ability of concrete to resist corrosion. When hydroxyl ions (OH⁻) are created at the cathode, they must move to the anode to cause the oxidation process to begin. The slower these ions are transported, the slower the corrosion process. This ionic current is similar to electrical current. Therefore, the rate of corrosion of the reinforcement can be estimated by the electrical resistance of the concrete [Whiting and Nagi, 2003].

Three methods have been developed to analyze the electrical resistance of concrete: single-electrode method, two-probe method, and the four probe method. Of the three methods the two-probe method is the most labor intensive and least accurate [Broomfield, 2007]. The two-probe method works by measuring the potential between two electrodes by passing an alternating current between them. If aggregates are located near the electrodes this can cause a false reading. Aggregates have a higher resistivity than concrete paste and will therefore cause a reading to be much higher than the actual resistivity. In order to counteract this problem, shallow holes can be drilled to place the electrodes into. However this is what makes the two probe method labor intensive.

The single-electrode method is a more advanced method to determine a concrete's resistivity. This method uses a disk placed on the concrete's surface as an electrode and the embedded steel reinforcement as the second electrode. The resistivity of the concrete is measured using **Eq. 2.14**.

$$\text{Resistivity } (\Omega\text{cm}) = 2RD \quad (2.14)$$

Where R is the resistance drop between the embedded reinforcement and the surface electrode, and D is the diameter of the surface electrode.

The third method is the four-probe method developed by Frank Wenner. This method was developed in 1916 and was designed for geophysical studies. This method has become widely accepted by the industry and is known as the Wenner method. The probe used in this method has four equally spaced electrodes on a single rod. The two outer electrodes send an alternating current through the concrete while the middle two electrodes measure the change in potential. The resistivity is then calculated using **Eq. 2.15**.

$$\rho = \frac{2\pi sV}{I} \quad (2.15)$$

Where ρ is the resistivity (Ωcm), s is the spacing between the electrodes (cm), V is the voltage (V), and I is the applied current (A). When the current is applied through the concrete it travels in a hemispherical pattern. This can be seen in **Figure 2.11**. This

allows for a greater area of concrete to be measured and thus avoids the influence of highly resistive aggregates.

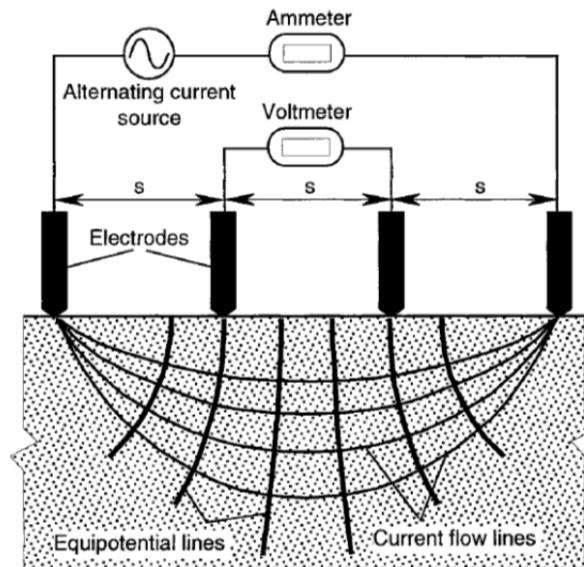


Figure 2.11 - Schematic Representation of the Four-Probe Resistivity Method [Broomfield, 2007]

The four-probe method is based on the theory that the resistivity values measured by the equation above are accurate if the current and potential fields exist in a semi-infinite volume of material [Whiting and Nagi, 2003]. This assumption indicates that larger concrete specimens will yield more accurate results. This condition has been found to be true. Measuring relatively thin concrete members or near edges produces noticeable errors. It is recommended that the spacing between the electrodes of the probe do not exceed $\frac{1}{4}$ of the smallest concrete section dimension. Another source of error is the non-homogeneous composition of concrete. While the assumption of the Wenner method is that the material will have a consistent resistivity, this is not the case for concrete. Highly resistive aggregates are surrounded by low-resistivity paste which affects the

measurements. According to research, this source of error can be avoided by using a probe where the spacing between electrodes is greater than 1.5 times the aggregate maximum size. This approach will maintain a coefficient of variation less than 5% [Whiting and Nagi, 2003]. A correlation was developed between measured concrete resistivity and the corrosion rate of embedded reinforcement. This classification can be seen in **Table 2.5**. This relationship was developed by Langford and Broomfield in 1987 and is widely used in the field.

Table 2.5 Correlation Between Concrete Resistivity and the Rate of Corrosion for a Depassivated Steel Bar Embedded within the Concrete [Broomfield, 2007]

Concrete Resistivity	Rate of Corrosion
>20 kΩcm	Low
10-20 kΩcm	Low to Moderate
5-10 kΩcm	High
<5 kΩcm	Very High

2.4.5. Scaling Resistance. The presence of salt solutions on concrete can cause additional damage besides corrosion of the reinforcing steel. The surface of the concrete can become pitted and roughened by a mechanism called scaling. In addition to leaving the surface scarred and rough, it can also increase the permeability of the concrete. To evaluate a concrete's resistance to scaling ASTM has created a test method ASTM C 672-03, "Standard Test Method for Scaling Resistance of Concrete Surfaces Exposed to Deicing Chemicals." This test method requires specimens to have at least 72 in² (46,452 mm²) of surface area and be at least 3 in. (76 mm) deep. The specimens are broom finished and a dike is built up around the perimeter of the specimen. This dike

must be at least 0.75 in. (19 mm) tall and approximately 1 in. (25 mm) wide. The specimen is then moist cured for 14 days and then air cured for 14 days. When the curing duration is over the surface of the specimen is covered with a solution having a concentration of 5.34 oz /gal (0.04 g/mL) of anhydrous calcium chloride. The specimen is then subjected to 50 cycles of freezing and thawing. After every 5 cycles, the solution is completely replaced and the condition of the surface is evaluated. After 50 cycles the surface of the concrete is evaluated and given a rating based on the scaling resistance. The rating scale can be seen in **Table 2.6**.

Table 2.6 Rating Scale for Scaling Resistance [MoDOT]

Rating	Condition of Surface
1	No scaling
2	Very slight scaling
3	Slight to moderate scaling
4	Moderate scaling
5	Moderate to severe scaling

2.5. SELF-CONSOLIDATING CONCRETE

2.5.1. Mechanical Properties. Through several investigations ACI has released report ACI 237R-07, “Self-Consolidating Concrete” outlining SCC and the properties that can be expected. The document outlines both fresh properties as well as performance requirements SCC should meet to be used in the field. In the area of compressive strength, SCC tends to perform very well. In order to achieve the flowable behavior of SCC, the w/cm ratio must be lowered through the use of a HRWR. This combination can yield higher 28-day compressive strengths than conventional concrete at the same w/cm ratio. The use of a HRWR allows for more Portland cement to be

hydrated creating a denser microstructure which in turn creates a concrete stronger in compression. In the area of modulus of rupture SCC should perform better than conventional concrete. This is due to the above mentioned denser microstructure [Sonebi and Bartos, 2001]. In the area of modulus of elasticity investigations have reported conflicting conclusions. According to Bennenck [2002], SCC mixes of equal compressive strengths to conventional concrete showed a lower modulus of elasticity by as much as 15%. This result is most likely due to the high fine aggregate content that it takes to maintain cohesiveness in SCC. However, Persson [1999] as well as Mortsell and Rodum [2001] found that the modulus of elasticity of SCC was very similar to conventional concrete of equal compressive strengths.

2.5.2. Durability Performance. With a denser microstructure created by the very nature of the concrete, SCC is believed to have better durability performance than conventional concrete. Khayat [2002] found that with a proper air-void system SCC shows excellent freeze-thaw resistance when subject to 300 cycles. It has been seen that SCC tends to have lower chloride diffusion than conventional concrete [Audenaert, 2003]. This result indicates that SCC should perform well in the area of the electrical indication of chloride penetration test as well as the ponding test. This reduction in chloride penetration is due to the denser microstructure found in SCC as mentioned previously. This denser microstructure should also lead to better resistivity than conventional concrete when measured with the Wenner probe.

3. MECHANICAL PROPERTY TESTS

3.1. INTRODUCTION

This section discusses the mechanical property tests used to evaluate the performance of the specialized concrete – self-consolidating concrete (SCC). The mechanical property comparison was important because these properties are essential to estimating the behavior of concrete in the field. These also serve as a good indicator of the quality of the concrete. The following mechanical property tests were included in the scope of work of this investigation:

- Compressive Strength of Cylindrical Concrete Specimens (ASTM C 39-11a)
- Static Modulus of Elasticity and Poisson’s Ratio of Concrete in Compression (ASTM C 469-10)
- Flexural Strength of Concrete (Using Simple Beam with Third-Point Loading) (ASTM C 78-10)
- Splitting Tensile Strength of Cylindrical Concrete Specimens (ASTM C 496-11)

These are standard tests that are used to investigate the most commonly used mechanical properties of concrete. Running these tests on both the conventional concrete and the specialized concretes will not only assure the quality of the conventional concrete but also will serve as a baseline of comparison for the specialized concretes. These mechanical properties are used in many aspects of design, and the results of these tests will allow investigators to determine how applicable existing formulas are in estimating these properties.

An outline for all the mechanical tests performed on all experimental mixes is shown in **Table 3.1**. The outline identifies the number of test specimens fabricated for

each test for each concrete mix. All of the concrete specimens were moist cured until the designated testing date. The date tested is listed as number of days after batching of the concrete.

Table 3.1 Test Matrix for Mechanical Properties

Material Property	Number of Specimens	Moist Curing Duration, days	Testing Date(s), days
Compressive Strength	9, (3/date)	1, 7, 28	1, 7, 28
Modulus of Elasticity	3	28	28
Flexural Strength	3	28	28
Splitting Tensile Strength	3	28	28

3.2. MIX DESIGN

3.2.1. Self-Consolidating Concrete Mix Design. One of the most essential parts of the investigation was the determination of the mix designs to be tested. Mix designs had to adequately represent mixes used by various contractors throughout the state of Missouri. Several contractors were already using SCC in some projects. It was important to establish an idea of what was commonly being used in the state to make the results from the investigation as applicable and relevant as possible. A survey was sent to several major concrete contractors and precasters throughout Missouri asking questions with regard to their use of SCC, including details such as cement content, admixture type and dosages, and aggregate content, type, and gradation. The responses were collected and together with mixes previously used in research at Missouri University of Science and Technology, mix designs that were relevant to contractors in the state of Missouri were then created. The admixture additions to the concrete mixes were given in dosage ranges. In order to find the appropriate admixture dosages, trial batches were mixed and

admixtures were added. If the admixtures had too great of an effect, the mix was re-batched and a smaller dosage was used. If the dosage did not have the desired effect, the same was done with a greater dosage. This process was repeated until the desired plastic properties were achieved.

The final mix designs are shown in **Table 3.2**. The mix design ID is based on characteristics of each mix. The first letter of the name designates the type of concrete, C for conventional concrete, S for self-consolidating concrete. The first number designates the target strength of the mix, 6 for 6,000 psi (41.3 MPa) and 10 for 10,000 psi (68.9 MPa). The second number designates the coarse aggregate percentage as a function of the total amount of aggregate, 58 for 58% coarse aggregate content, 48 for 48% coarse aggregate content. The last letter designates the type of coarse aggregate used, with L for limestone and R for river gravel; although only limestone was considered for material property testing reported in this thesis (Another aspect of this investigation not covered in this thesis studied the effects of different types of coarse aggregates on the shear behavior of SCC.)

Table 3.2 Mix Design per Cubic Yard for SCC Investigation

	Mix Design ID			
	C6-58L	S6-48L	C10-58L	S10-48L
Cement (Type III) (lb)	750	750	840	840
Fly Ash (lb)	0	0	210	210
w/cm ratio	0.37	0.37	0.3	0.3
Coarse Aggregate, SSD (lb)	1611	1333	1440	1192
Fine Aggregate, SSD (lb)	1166	1444	1043	1291
HRWR dosage (fl. oz)	29.25	46.5	52.5	63
Air Entrainment (fl. oz)	11.25	11.25	0	0

1 lb = 0.45 kg
1 fl. oz. = 29.57 mL

For example, C6-58L stands for conventional concrete with a target strength of 6,000 psi (41.3 MPa) and a coarse aggregate content of 58% limestone. The abbreviation HRWR in the table stands for high range water reducer, which was Glenium 7700 manufactured by the BASF Corporation (BASF). The air entraining admixture used was MB-AE-90, also manufactured by BASF. The reasons these admixtures were used is explained later in this section.

For the mix designs shown in Table 3.2 a Type III cement was chosen for high early strength. The coarse aggregate was dolomitic limestone with a nominal maximum aggregate size of $\frac{3}{4}$ in. (19.05 mm) from Capital City Quarry located in Rolla, Missouri. The fine aggregate was river sand from the Missouri River. The SCC mixes contained a lower percentage of coarse aggregate and a higher percentage of fine aggregate to provide the necessary filling, passing, and flowability characteristics. It should be noted that the batch water was adjusted to account for any moisture that was present in the aggregate. The total moisture content was found by taking a representative sample of the aggregate and weighing it. The sample was then placed into an oven and dried over night. The dried sample was then re-weighed and the difference was taken as the total moisture content.

Two types of admixtures were also used in the mix design, a high range water reducer (HRWR) and an air-entraining admixture. A HRWR was added to the mix in order to achieve the high flowability of the self-consolidating concrete without increasing the water to cementitious material ratio (w/cm). This allowed the concrete to maintain a comparable strength to its conventional counterpart but have the flowable plastic behavior that makes the concrete self-consolidating. In concrete, the cement particles

typically carry either positive or negative charges. The attraction between particles causes them to agglomerate. Water is trapped inside these particles and is not able to add to the workability of the fresh concrete. HRWRs place a like charge on the cement particles causing them to repel each other. This frees the water in the paste to add to the workability of the concrete. This apparent increase in water content allows the workability to increase while maintaining the low w/cm that is necessary for high strength concrete.

To provide the necessary durability of concrete, an air-entraining admixture was also used. Concrete that is exposed to freezing and thawing temperatures is at risk of serious deterioration. One of the most effective ways to protect against that is using an air-entraining admixture. This admixture creates an air void system in the concrete paste that is composed of millions of tiny bubbles. This air void system allows for the pressure that builds up due to the freezing of water to be released into these tiny bubbles. The normal strength concrete mixes (C6-58L and S6-48L) had a target total air content of 6%, (entrapped and entrained), while the high strength concretes did not use any air entraining admixture. This number was based on ACI recommendation for air content based on the $\frac{3}{4}$ " nominal maximum size of the coarse aggregate for optimal frost resistance. These admixtures were added at trial dosages until the desired behavior and air contents were achieved. The admixtures were added to the concrete during the mixing process by adding the dosages into the batch water. This allowed the admixtures to be dispersed in the fresh concrete. The proper dosages were established using 3 ft³ (0.08 m³) mixes. When the proper dosages were found for the trial batches, the measurements were calculated for the larger pours.

Fresh concrete properties were measured during each batching operation, either within the Butler Carlton Civil Engineering Hall (BCH) Materials Lab for mixes prepared on site or within the BCH Structural Engineering High-Bay Research Laboratory (SERL), at Missouri S&T for mixes delivered by a local ready-mix supplier. These tests were performed to ensure that certain properties were achieved such as workability and air content. The following fresh property tests were performed on the conventional concrete mixes:

- Slump of Hydraulic-Cement Concrete (ASTM C 143)
- Unit of Weight of Concrete (ASTM C 138)
- Air Content of Freshly Mixed Concrete by the Pressure Method (ASTM C 173)

Typical fresh properties of the conventional concrete mixes are shown in **Table 3.3**.

Table 3.3 Typical Fresh Concrete Properties for Conventional Concrete Mixes

Property	Mix Design ID	
	C6-58L	C10-58L
Slump (in)	5.0	4.5
Air Content (%)	5.5	2.8
Unit Weight (lb/ft ³)	144.7	148.4

$$1 \text{ in} = 2.54 \text{ cm}$$

$$1 \text{ lb/ft}^3 = 16.02 \text{ kg/m}^3$$

Due to its unique nature, SCC requires several additional fresh property tests. These tests were done to ensure both adequate flowability and resistance to segregation. The following fresh property tests were performed on the self-consolidating concrete mixes:

- Slump Flow of Self-Consolidating Concrete (ASTM C 1611)
- Passing Ability of Self-Consolidating Concrete by J-Ring (ASTM C 1621)

- Static Segregation of Self-Consolidating Concrete Using Column Technique (ASTM C 1610)
- Unit Weight of Concrete (ASTM C 138M)
- Air Content of Freshly Mixed Concrete by the Pressure Method (ASTM C 173M)

Typical fresh properties of the SCC mixes are shown in **Table 3.4**.

Table 3.4 Typical Fresh Concrete Properties for Self-Consolidating Concrete Mixes

	Mix Design ID	
	S6-48L	S10-48L
Slump flow (in)	25.5	28.5
J Ring (in)	25.0	28.5
Segregation Column (%)	12.3	31.2
Unit Weight (lb/ft ³)	139.6	146.4
Air Content (%)	5.5	2.2

$$1 \text{ in.} = 2.54 \text{ cm.}$$

$$1 \text{ lb/ft}^3 = 16.02 \text{ kg/m}^3$$

The unit weight and air content tests were modified for the SCC mixes. Both ASTM tests call for the air pot to be filled in three equal lifts, with each lift rodded 24 times. The sides of the air pot were also to be struck smartly 12 to 15 times per lift. Due to the unique nature of SCC, the air pot was filled in a single lift and was neither rodded nor struck with a rubber mallet. A similar modification was used for fabrication of the compressive strength cylinders.

3.3. COMPRESSIVE STRENGTH TEST

3.3.1. Introduction. The compressive strength test was used in several different aspects of the research project. It was used as a quality control and quality assurance, (QC/QA) tool. The compressive strength results from the experimental mixes

were compared to target values to assure the strengths were within the desired limits. These values can also be compared to other strengths of similar mixes to evaluate behavior. The compressive strength was also used to assure the quality of the concrete by observing any drastic differences between the target and actual strengths. The compressive strength of concrete is also an important factor in many tests that were used in this investigation, such as shear, bond, and creep.

3.3.2. Fabrication. A minimum of 9 compressive strength cylinders were cast for each mix design. All specimens were prepared in accordance with ASTM C 192-07, “Standard Practice for Making and Curing Concrete Test Specimens in the Laboratory” using 4 in. (102 mm) diameter by 8 in. (203 mm) long plastic cylinder molds. The molds were lubricated using form release oil prior to the placement of concrete. The concrete was rodded in order to reduce air voids and to assure the concrete would be sufficiently consolidated. The sides of the mold were also struck smartly for each lift with a rubber mallet in order to consolidate the concrete. It should be noted that the compressive strength specimens made with the self-consolidating mixes were not rodded or struck due to the plastic highly flowable behavior of the concrete. Instead these mixes were placed in one continuous lift. Immediately after casting, plastic lids were placed over the molds and the specimens were covered with plastic. After allowing for 16 to 24 hours of setting time, the concrete specimens were removed from the molds using compressed air and placed inside a temperature-controlled moist curing room until the designated testing date.

3.3.3. Testing & Procedure. The testing of the compressive strength of the experimental mixes was performed in accordance with ASTM C 39-11, “Standard Test Method for Compressive Strength of Cylindrical Concrete Specimens.” A minimum of 3 compressive strength cylinders were used at each test age. Testing occurred at 1, 7, and 28 days after batching. These are typical testing dates for compressive strength tests. Prior to testing, the specimens had to be capped in order to provide a flat surface for testing. The two methods used to cap specimens in this project were sulfur capping and neoprene pad capping.

Neoprene pads were used to cap any specimens constructed with a high strength concrete mix. Any specimens that were constructed with normal strength concrete were sulfur capped. Prior to using the neoprene pads, the concrete specimens were ground smooth using a concrete grinding machine. Once the ends were removed off all rough spots, the cylinders were placed into steel retaining rings with a neoprene pad between the specimen and the steel. With the steel retaining rings and neoprene pads on both the top and bottom of the concrete specimen, it was loaded into the compressive strength testing machine. Specimens that were sulfur capped were placed into liquid sulfur capping compound to create a smooth liquid cap that hardened within seconds and could be tested in a few hours. At least two hours before the compressive strength test was to occur, the concrete specimens were removed from the moist curing chamber and the moisture was removed from the ends. When the specimens were ready to be capped, an ample amount of sulfur capping compound was poured into the capping mold. The specimen was quickly held against the mold to ensure it was level and it was gently but quickly lowered in the capping compound. The capping compound hardened very

quickly, so capping the cylinders needed to be done in a swift manner. Once the capping compound hardened around the concrete specimen, it was removed and the process was repeated on the other end. Once the specimen was capped on both ends, it was returned to the moist curing chamber. In order for the capping compound to reach its maximum strength, the capped specimens had to sit in the moist curing chamber for a minimum of two hours. After this time, the concrete specimens could be tested for compressive strength.

Before the compressive strength tests were run, the dimensions of the specimens were measured. The diameter was measured three times and the average was used to compute the compressive strength. From the measured diameter, the cross sectional area was calculated. The height was also measured. The specimens were then loosely wrapped in a canvas wrap (not shown) and placed in the testing apparatus, as shown in **Figure 3.1**. A Forney 600 kip (2,669 kN) compression testing machine was used. Steel plates were placed on the load deck in order to minimize the distance traveled. The specimen was then placed in the apparatus, centered, and brought to just below the upper plate.



Figure 3.1 - Compressive Strength Testing Setup

When the setup was complete, the specimen was loaded at a load rate specified for 4 in. (102 mm) diameter specimens. The target load rate was 525 lb/sec. (238 kg/sec.). The specimen was loaded at the specified rate until it could no longer sustain a load and the load rate dropped to a negative value. The machine was turned off and the peak load was recorded. Completed test specimens are show in **Figure 3.2**.



Figure 3.2 - High Strength Compressive Strength Specimens Post-Test

The load was then divided by the cross sectional area to get the measured compressive strength in pounds per square inch. A minimum of three specimens were tested at a given test age and the results were averaged to get the final measured compressive strength.

3.4. MODULUS OF ELASTICITY TEST

3.4.1. Introduction. The modulus of elasticity is an important property to investigate as it is used to determine the anticipated amount of deflection in design. This is important in designing for serviceability of a structure. The modulus of elasticity of concrete is determined by testing specimens in the linear elastic range. Specimens are loaded to a specified stress while the strain is measured. The slope of the stress–strain curve is taken as the modulus of elasticity.

3.4.2. Fabrication. Specimens used to measure the modulus of elasticity were fabricated according to ASTM C 192–07. These are the same type of specimens that were used for compressive strength testing. A minimum of three specimens were created for each mix design. For the modulus of elasticity test, the specimens could be fabricated

either using 4 in. (102 mm) diameter by 8 in. (203 mm) long cylinders or 6 in.(152 mm) diameter by 12 in.(305 mm) long cylinders. The two types of cylinder molds can be seen in **Figure 3.3**. It should be noted that for the SCC mixes, 4 in. (102 mm) x 8 in. (203 mm) specimens were used.



Figure 3.3 – 4 in. (102 mm) x 8 in. (203 mm) Cylinder Mold Compared to 6 in. (152 mm) x 12 in. (305 mm) Cylinder Mold

Specimens were de-molded after 24 hours and placed in the moist curing chamber for 28 days before testing. Before the test was conducted, all test specimens were sulfur capped in the same manner as the compressive strength cylinders.

3.4.3. Testing & Procedure. After the specimens were allowed to cure for 28 days, the specimens were tested in accordance with ASTM C 469–10, “Standard Test Method for Static Modulus of Elasticity and Poisson’s Ratio of Concrete in Compression.” The dimensions of the specimens were measured, and before loading, the specimen was fitted with a compressometer in order to measure the deflection of the cylinder during loading. A typical compressometer can be seen in **Figure 3.4**.



Figure 3.4 - Typical Compressometer

The specimen was then placed into a compression loading apparatus and loaded at a constant rate. The load was recorded when the deflection of the specimen reached 0.0004 in. (0.01 mm). The specimen was continually loaded until the load reached 40% of the ultimate strength of the concrete. The value of the ultimate strength was determined from compressive strength tests of companion specimens. When the load on the specimen reached 40% of the measured ultimate load, the deflection was recorded. This test was then performed three additional times on the same specimen. The data recorded during the first test run on each specimen was disregarded and only the following three tests were used for averaging. Using these deflections, the strains were calculated and the corresponding stresses were used to calculate the modulus of elasticity using Eq. 3.1.

$$E_c = \frac{(S_2 - S_1)}{(\varepsilon_2 - 0.00005)} \quad (3.1)$$

Where S_2 is the stress measured at 40% of the ultimate load and S_1 is the stress measured when the deflection of the specimen reached 0.0004 in. (0.01 mm) and ϵ_2 is the strain produced by S_2 . The results from the individual tests were then averaged and the averages from the three tests were then averaged to obtain the measured modulus of elasticity.

3.5. MODULUS OF RUPTURE TEST

3.5.1. Introduction. The modulus of rupture test is used to determine the flexural strength or tensile strength of the concrete. This is an important mechanical property to investigate. The modulus of rupture is important in design for estimating the cracking moment of the concrete when subjected to flexure.

3.5.2. Fabrication. The specimens used for the modulus of rupture test were fabricated in accordance with ASTM C 78–10, “Standard Test Method for Flexural Strength of Concrete (Using Simple Beam with Third-Point Loading).” Three specimens were fabricated for every concrete mix. The specimens measured 6 in. (152 mm) x 6 in. (152 mm) in cross section with a length of 24 in. (610 mm). The specimens were filled with two lifts, each lift being rodded 72 times. It should be noted that the SCC was not rodded when specimens were cast. The specimens were cast in one single lift. The specimens were de-molded after 24 hours and stored in a moist curing chamber for 28 days. After 28 days they were prepared for testing.

3.5.3. Testing & Procedure. After 28 days, the specimens were removed from the moist curing chamber. The supports on the testing apparatus were 18 in. (457 mm) apart. In order to align the specimen on the supports, it had to be divided into thirds. The

first 3 in. (76 mm) of either end of the specimen were not included in the measuring. This caused the 18 in. (457 mm) span to be divided into 3, 6 in. spans. The load points would be placed on the 6 in. mark and the 12 in. mark, creating the third-point loading. The prepared specimen can be seen in **Figure 3.5**.

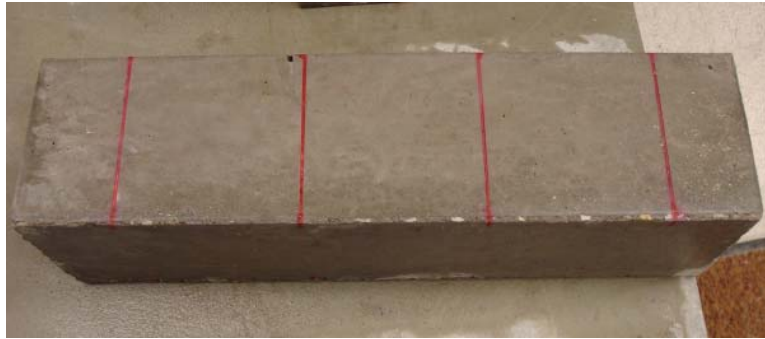


Figure 3.5 - Prepared Modulus of Rupture Specimen

The specimen was rotated and loaded into the testing machine on a formed side to provide the smoothest surface and thus prevent localized forces on the beam. The load was applied at the aforementioned points. A leather pad was placed in between the concrete specimen and the load points in order to help distribute the load. The test setup can be seen in **Figure 3.6**. It is important to note that during the set-up, the specimen was kept moist in order to prevent any internal stresses from developing.

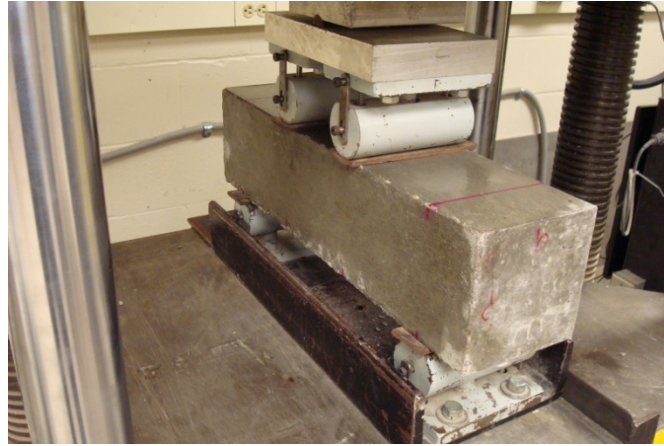


Figure 3.6 - Modulus of Rupture Testing Setup

The load head was then lowered until it made contact with the leather pads. The beam was then loaded at a constant rate until failure. If the beam failed within the middle third, the test was accepted. It should be noted that all beams tested in this investigation failed in the middle third of the beam. A post failure specimen can be seen in **Figure 3.7**. The failure load was recorded and subsequently used to calculate the modulus of rupture using **Eq. 3.2**.



Figure 3.7 - Modulus of Rupture Specimen Post-Test

The beam was removed from the testing apparatus and its dimensions were measured. The width and depth of the beam were measured three times and averaged. The modulus of rupture was then calculated using **Eq. 3.2**.

$$R = \frac{PL}{bd^2} \quad (3.2)$$

Where P is the peak load, L is the distance between supports, b is the average width of the beam after testing, and d is the average depth of the beam after testing.

3.6. SPLITTING TENSILE TEST

3.6.1. Introduction. ASTM has not yet specified a standardized test to find the direct tensile strength of concrete. There is a standardized test for an indirect tension test known as the splitting tensile test. This test involves loading a cylindrical specimen along its longitudinal axis until failure. This test is thought to measure a greater tensile strength than a direct tensile strength. However it is usually lower than a measured strength from a modulus of rupture test. The splitting tensile test is a good indication of a concrete's tensile strength but should be performed alongside other tests such as the modulus of rupture test.

3.6.2. Fabrication. The specimens used for the splitting tensile test were fabricated in accordance with ASTM C 496–11, “Standard Test Method for Splitting Tensile Strength of Cylindrical Concrete Specimens.” A minimum of three specimens were made for each concrete mix. The specimens were made using 4 in. (102 mm) diameter by 8 in. (203 mm) long cylindrical molds. The specimens used for the splitting

tensile test were the same types of specimens used for the compressive strength test. The specimens were fabricated according to ASTM C 192. After 24 hours, the specimens were de-molded and placed in a moist curing chamber for 28 days, at which time they were then tested.

3.6.3. Testing & Procedure. After the specimens were allowed to cure for 28 days, the specimens were removed from the curing chamber for testing. The diameter and height of the specimens were recorded. The diameter of the specimen was marked on the top of the specimen. Two lines were then drawn down the long side of the specimen from the previously drawn line. This was done to assist in lining up the specimen in the testing apparatus. The specimen was then loaded into the testing apparatus on the line drawn down its vertical axis. The specimen was placed on a piece of plywood. Another plywood strip was placed on the top of the specimen between it and the load platen. These strips were used so the load would be distributed along the axis of the specimen. The test setup can be seen in **Figure 3.8**.



Figure 3.8 - Typical Splitting Tensile Test Setup

The specimen was then loaded at a rate between 100 (45 kg) and 200 lb /min. (91 kg/min.) until failure. The load at failure was recorded as the peak load, and the tensile strength was calculated using **Eq. 3.3**.

$$T = \frac{2P}{\pi LD} \quad (3.3)$$

Where P was the peak load, L is the length of the specimen, and D is the diameter of the specimen. A post failure specimen can be seen in **Figure 3.9**.



Figure 3.9 - Splitting Tensile Specimens Post-Test

4. DURABILITY TESTS

4.1. INTRODUCTION

This section discusses the durability tests used to evaluate the performance of self-consolidating concrete (SCC). The durability performance of these specialized concretes is a crucial aspect in investigating the possibility of implementing these new materials into transportation-related infrastructure, such as bridges, roadways, culverts, and retaining walls. The following durability tests were included in the scope of work for this investigation:

- Resistance of Concrete to Rapid Freezing and Thawing (ASTM C 666-08)
- Electrical Indication of Concrete's Ability to Resist Chloride Ion Penetration (ASTM C 1202-10)
- Determining the Penetration of Chloride Ion into Concrete by Ponding (ASTM C 1543-10)
- Concrete Resistivity (Non-ASTM)

The outline for the durability tests is shown in **Table 4.1**. The outline identifies the number of test specimens fabricated for each test for each concrete mix. The table also includes the required curing conditions and durations, as well as the specimen age at the start of testing and the duration of the test, if applicable.

Table 4.1 Test Matrix for Durability Performance

Durability Property	Number of Specimens	Moist Curing Duration, days	Dry Curing Duration, days	Testing Date, days	Testing Duration, days
Freezing and Thawing	3	35	0	35	N/A ¹
Electrical Chloride Penetration	2 (4 disks)	28	0	28	N/A ²
Ponding	3	14	14	28	120
Concrete Resistivity	3	14	21	35	168

Notes: 1. Test duration based on cycles
2. Duration of test is 6 hours

4.2. RAPID FREEZING & THAWING TEST

4.2.1. Introduction. The rapid freeze-thaw test was one of the most critical durability tests performed in this investigation. The climate in Missouri is susceptible to multiple freeze-thaw cycles, which is a more severe environment for concrete durability than continuous freezing. The test involves subjecting specimens to multiple freeze-thaw cycles in order to measure the resistance of the material to deterioration caused by the expansion of the free water freezing inside the specimens. This resistance was measured using three parameters: the length change of the specimens, change in the fundamental transverse frequency of the specimens, and mass change of the specimens. Using these parameters the resistance to freeze-thaw can be quantified as a durability factor.

4.2.2. Fabrication. The specimens for the rapid freeze-thaw test were fabricated according to ASTM C 666–03, “Standard Test Method for Resistance of Concrete to Rapid Freezing and Thawing.” The molds used in the fabrication of these specimens were loaned to the project by the Construction & Materials Division of the

Missouri Department of Transportation (MoDOT) and can be seen in **Figure 4.1**. These stainless steel molds measured 3.5 in. (8.9 cm) in width, 4.5 in. (11.43 cm) in height, and 16 in. (40.64 cm) in length and conformed to ASTM C 666 requirements for specimen dimensions.



Figure 4.1 - Freezing and Thawing Specimen Molds

The ends of each mold contained a threaded hole to install a specialized bolt. This bolt contained a rounded end, and when the concrete specimens were de-molded, the end of this bolt protruded from both ends of the prism as shown in **Figure 4.2**. The embedded bolt provides a mechanism to measure the length change of the concrete prism as it was subjected to freezing and thawing cycles.

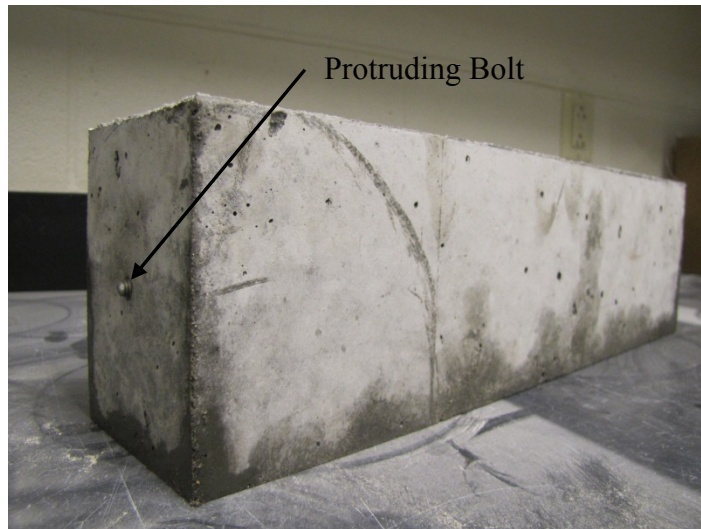


Figure 4.2 - Freezing and Thawing Specimen with Protruding Bolt

Once the specimens were formed and de-molded, they were placed in a temperature controlled moist curing room for 35 days prior to testing. It should be noted that this moist curing duration is a standard for MoDOT and a modification of ASTM C 666. The ASTM specifies that the prisms should be moist cured for 14 days unless otherwise specified. It should also be noted that the typical MoDOT procedure requires that specimens that will be subjected to the rapid freeze-thaw test be submersed in a lime water solution while they cure for the 35 days. However, due to space restraints in the University laboratory, the specimens were only moist cured. This change was deemed acceptable provided all specimens received the same treatment. Between 14 and 21 days, the prisms were transported from the University's moist curing chamber to the Construction & Materials testing lab of MoDOT in Jefferson City, Missouri. To be transported, the specimens were wrapped in burlap that was saturated in a 5% by weight lime water solution. The specimens were then placed into a cooler and immediately driven to the MoDOT lab and placed into the moist curing chamber to complete the 35-

day moist curing regime. All rapid freezing and thawing tests were performed by MoDOT employees of the Construction & Materials Division.

4.2.3. Testing & Procedure. All specimens were tested in accordance with ASTM C 666, Procedure B. When the specimens reached the appropriate age, they were brought to the target thaw temperature. The fundamental transverse frequency, mass, length, and cross section of the specimen were measured. The freeze-thaw specimens were then subjected to the appropriate freezing and thawing cycles. Each specimen was subject to 300 cycles of freezing and thawing. Every 36 cycles the specimens would be removed in the thawed state and properties of the specimen would be measured. The properties measured were fundamental transverse frequency, length change, and mass change. The specimens were then placed back into the testing apparatus and the cycles continued. The test was halted if the specimen deteriorated so extensively that the test could not continue. The relative dynamic modulus of elasticity was then calculated using **Eq. 4.1.**

$$P_c = \frac{n_1^2}{n^2} \times 100 \quad (4.1)$$

Where P_c is the relative dynamic modulus of elasticity at, c , cycles of freezing and thawing. N_1 is the fundamental transverse frequency after, c , cycles of freezing and thawing and n is the fundamental transverse frequency after 0 cycles of freezing and thawing. Using the relative dynamic modulus of elasticity, the durability factor of the freezing and thawing specimen was also calculated using **Eq. 4.2.**

$$DF = \frac{PN}{M} \quad (4.2)$$

Where DF is the durability factor, P is the relative dynamic modulus of elasticity at N cycles, N is the number of cycles at which the specified value of P is reached or the specified number of cycles is reached, whichever is less, and M is the number of cycles until termination. The higher the measured durability factor, the greater resistance the concrete will have to freezing and thawing attack.

4.3. ELECTRICAL INDICATION TO RESIST CHLORIDE ION PENETRATION TEST

4.3.1. Introduction. Chloride penetration of concrete is one of the leading durability issues facing many concrete specimens. Concrete members that are exposed to chlorides such as concrete piers in the ocean or concrete bridge decks exposed to de-icing salts all face chloride penetration. If sufficient chloride is allowed to penetrate into a concrete member, it can cause the embedded steel reinforcement to corrode and the expanding corrosion product will result in internal stresses, which in turn will cause cracking of the concrete. Over time this will cause concrete spalling and eventual failure. The electrical indication of concrete's ability to resist chloride penetration is a rapid method to determine the permeability of the concrete and its ability to withstand chloride penetration. This test is often used in correlation with the ponding test as it was in this investigation. Due to the ponding test's longer duration, this electrical test is a rapid method to estimate the durability of concrete. This test is also known as the Rapid Chloride Test (RCT).

4.3.2. Fabrication. The test specimens consisted of cylinders fabricated and prepared according to ASTM C 192–07, “Standard Practice for Making and Curing Concrete Test Specimens in the Laboratory.” Two 4 in. (10.16 cm) diameter x 8 in. (20.32 cm) long cylinders were used for this test for every concrete mix. These cylinders were prepared alongside the compressive strength specimens. These specimens were demolded after 24 hours and placed in the moist curing chamber for 28 days. In between 14 and 21 days after batching, these cylinders were transported to the Construction & Materials testing lab in Jefferson City to finish the curing cycle and begin testing. These specimens were wrapped in burlap that was saturated in a 5% by weight lime water solution. The specimens were then placed into a cooler and immediately driven to the Jefferson City MoDOT lab and placed into the moist curing chamber to complete the 28-day moist curing regime. All electrical chloride tests were performed by MoDOT employees of the Construction & Materials Division.

4.3.3. Testing & Procedure. The testing of specimens for the electrical indication of a concrete’s ability to resist chloride ion penetration is outlined in ASTM C 1202-10, “Standard Test Method for Electrical Indication of Concrete’s Ability to Resist Chloride Ion Penetration.” The test specimens consist of 4 in. (102 mm) diameter by 2 in. (51 mm) thick concrete disks. These disks were cut from specimens cast according to ASTM C 192. Two disks were cut from each concrete cylinder, with two concrete cylinders cast from each mix, which resulted in a total of 4 concrete disks for each concrete mix. One disk was cut from the top of the cylinder and the other from the middle. These disks were labeled with the mix design name and noted as either middle or

top. The specimens were allowed to surface dry for at least 1 hour before the sides of the disks were coated with a setting coating as seen in **Figure 4.3**.



Figure 4.3 - Setting Coating Being Applied to Concrete Specimens

After the coating dried, the specimens were placed into a vacuum desiccator and vacuumed for 3 hours. The pressure of the vacuum was at least 0.96 psi (6650 Pa). At the end of the 3 hour desiccation period, de-aerated water was poured into the water stockpot of the vacuum until the specimen was covered. The stockpot was closed and the vacuum was maintained for another hour. The vacuum was then turned off and air was allowed to enter the desiccator. The specimen was then allowed to soak in the de-aerated water for 18 ± 2 hours. The specimen was then blotted dry and placed into the voltage cell. A sealant was then applied to the specimen-cell boundary. The exposed face of the specimen was then covered while the sealant was allowed to dry. Once the sealant was dry, the process was repeated to the other face of the specimen. The final specimen can be seen in **Figure 4.4**.

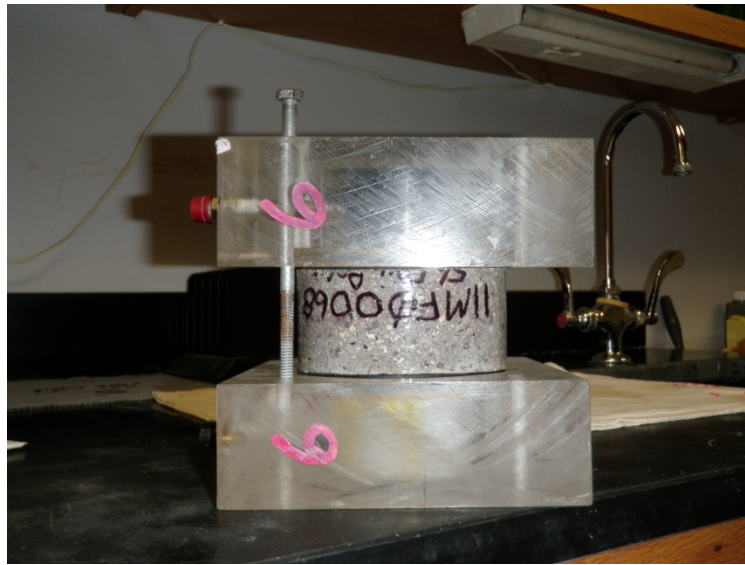


Figure 4.4 - Typical Completed Specimen

The side of the cell that is connected to the negative terminal is then filled with 3.0% NaCl solution while the side connected to the positive terminal is filled with 0.3 N NaOH solution. The test setup can be seen in **Figure 4.5**. The power is then turned on and the voltage is set to 60 V. The initial current is recorded and then recorded at 30 minute intervals.

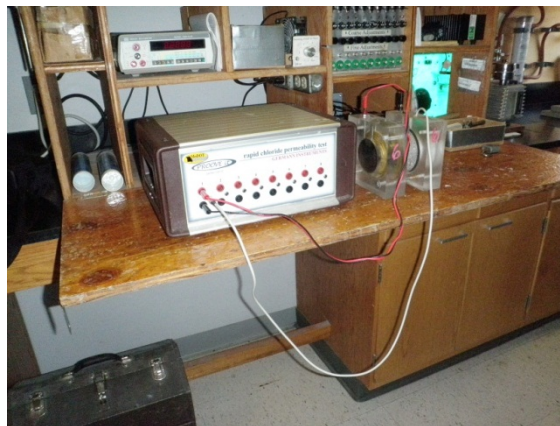


Figure 4.5 – Typical RCT Setup

The test is conducted for 6 hours unless the temperature in the solution exceeds 190°F. This temperature is only exceeded when the concrete is extremely permeable. The data that is recorded is then used to calculate the total charge passed through the specimen in coulombs. This is discussed further in Section 5.6.

4.4. PONDING TEST

4.4.1. Introduction. A serious problem facing Missouri concrete bridge decks is spalling and deterioration caused by chloride penetration and subsequent corrosion of the underlying steel. During winter months, de-icing salts are used to remove snow and ice from bridge and roadway surfaces. The chlorides contained in these de-icing salts diffuse into the concrete, eventually breaking down the passive layer of the reinforcing steel and causing corrosion. The corrosion product expands to approximately six times the original volume, resulting in internal stresses and eventually cracking. Over time, this process will lead to spalling and deterioration of the concrete. The ponding test subjects concrete specimens to a similar environment to investigate the ability of the concrete to resist chloride penetration. This test is a valuable indicator of the resistance of the concrete to chloride ingress and thus the durability of the material. Although this test requires a longer period of time compared to other methods to predict the resistance of concrete to chloride penetration, it is the most realistic test method.

4.4.2. Fabrication. The concrete specimens for the ponding test were fabricated according to ASTM C 1543-10, “Standard Test Method for Determining the Penetration of Chloride Ion into Concrete by Ponding.” Three specimens were made for each concrete mix. The test requires that the specimens have a surface area of at least

45.6 in² (30,000 mm²). The specimens must also be at least 3.54 ± 0.6 in. (90 ± 15 mm) tall. The specimens created for the ponding test in this investigation measured 18 in. (457 mm) wide x 18 in. (457 mm) long x 4 in. (102 mm) tall. Also, the test procedure required a dike along the top of the specimen with a height of at least 0.79 in. (20 mm) high. To accomplish this, a 0.75 in.-thick (19 mm) foam panel measuring 16 in. (406 mm) x 16 in. (406 mm) in plan was placed on a sheet of plywood that would serve as the base of the mold. Walls constructed from 2 in. (51 mm) x 4 in. (102 mm) pieces of wood were then connected to the panel to arrive at the overall dimension of 18 in. (457 mm) x 18 in. (457 mm) in plan. When the concrete was placed in the mold, the foam created a void in what would become the top of the specimen. The foam formed the reservoir for the chloride solution. The concrete was placed into the formwork and consolidated as necessary. After 24 hours, the concrete specimens were de-molded and placed in a moist curing chamber at 100% relative humidity. After 14 days of moist curing, the specimens were transported to a temperature and humidity controlled environment where they would dry cure at 75°F (23.8°C) and 65% relative humidity for another 14 days. After 28 days of curing, the specimens would then begin the ponding test.

4.4.3. Testing & Procedure. The test procedure involved placing a 5% by weight chloride solution into the ponding specimen reservoir. The solution had to be at a depth of 0.6 ± 0.2 in. (15 ± 5 mm). A typical ponded specimen can be seen in **Figure 4.6**. When the required amount of solution was poured into the reservoir, the concrete specimens were covered with plastic sheeting and the sheets were secured with elastic bands to prevent evaporation of the solution.



Figure 4.6 - Typical Ponding Specimen

Every two weeks the specimens were checked to ensure that the proper depth of the solution was maintained. If the reservoir was low, additional solution was added. After 60 days of ponding, the reservoir was vacuumed dry and fresh solution was added. The sheeting was replaced and the specimens were monitored every two weeks. After another 60 days, the chloride solution was vacuumed off and the specimen allowed to air dry. A few days later, a core was taken from the center of the specimen. A typical core and core location can be seen in **Figure 4.7**.



Figure 4.7 - Concrete Core and Resulting Void in the Concrete Specimen

The core was removed using an industry standard core driller with a medium flow of water to ensure proper blade lubrication as well as creating the proper slurry. Powder samples were then taken from the cores at specified depth intervals. The intervals were 0.25 in. (6 mm), 0.75 in. (19 mm), 1.5 in. (38 mm), and 2 in. (51 mm) from the surface of the core. A sample was also taken from the surface of the core. These depths are shown in **Figure 4.8**.

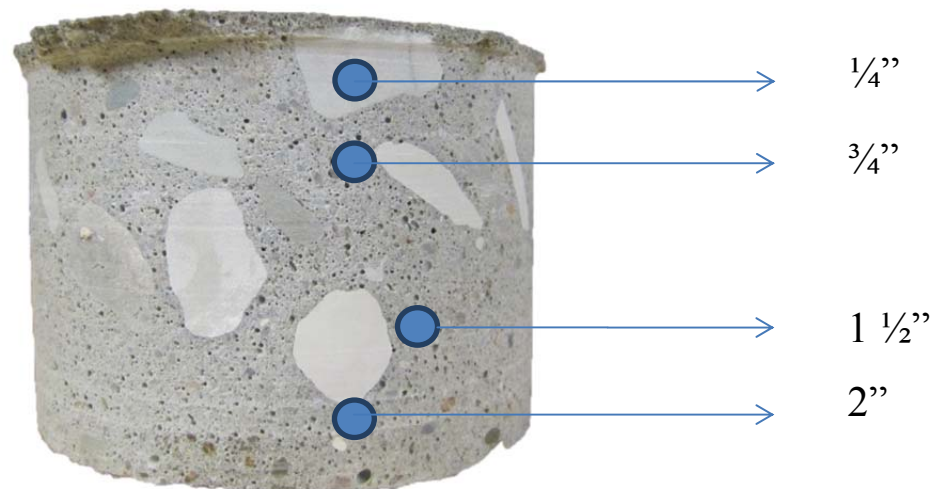


Figure 4.8 - Depths at which Powder Samples Were Collected
1 in. = 2.54 cm.

The samples had to measure at least 0.053 oz. (1.5 g) to be considered sufficient. Samples were collected using a 3/8 in. (9.5 mm) drilled bit at all locations except at the 0.25 in. (6 mm) location. At this location a 3/16 in. (5 mm) drill bit was used. A paper plate was used to collect the dust and a steel plate was placed in between the core and the vise to confine the concrete and prevent spalling. A hole was cut in the paper plate and placed

over the mark to be drilled. The paper plate was then taped to the concrete specimen as to create a seal between the paper and concrete surface. This was done in order to catch the concrete dust created by drilling the hole. The drilling locations were placed on a point on the cylinder as to not drill directly into a piece of coarse aggregate unless absolutely necessary. After each hole was drilled, it was sealed using masking tape to prevent cross contamination with the other samples. Samples were also taken from the surface of the core. This was done by drilling the surface of the core to a depth of no deeper than 0.125 in. (3 mm). Samples were collected from several locations on the surface of the core to obtain the necessary sample size. A chloride analysis was then performed on the powder samples to obtain the chloride content in the concrete at the respective sample depths.

The chloride analysis of water soluble chlorides was performed using the Rapid Chloride Testing (RCT) equipment made by Germann Instruments, Inc. The 0.053 oz. (1.5 g) sample was poured into a vial containing 0.304 fl-oz. (9 mL) of the extraction liquid. The vial was shaken vigorously for 5 minutes. The extraction liquid and powder slurry were then filtered into a buffer solution by pouring the slurry through a filter paper and into a vial containing the buffer solution. While the slurry was filtering the electrode was prepared and calibrated. The preparing of the electrode began with filling it with a wetting agent. After any air bubbles were removed the wetting agent was allowed to be released in order to fully wet the circumference of the electrode tip. After the electrode had been refilled with the wetting agent, the preparation was complete. In order to calibrate the electrode and develop a scale to determine the chloride content of the specimens, the electrode was inserted into four calibration solutions of known chloride content. The four calibration liquids contained 0.005%, 0.02%, 0.05%, and 0.5% chloride

content. The electrode was inserted into each solution and the voltage was read. The four calibration liquids produced a voltage of approximately 100 mV, 72 mV, 49 mV, and -5 mV respectively. This data was used then plotted on a log chart in order to develop a scale for the rest of the testing. An example of this log chart can be seen in Appendix B. After the preparing and the calibrating the electrode was ready to use. When the filtering process was complete the electrode was inserted into the buffer solution vial which contained the buffer solution and filtered slurry and was held steady until the voltage reading stabilized. Using the recorded voltage and the developed scale, the chloride content was determined. After every use the electrode was sprayed with distilled water, blotted dry and stored in an empty vial. This data collected from each depth was used to develop a chloride profile and determine chloride penetration into the concrete.

4.5. CONCRETE RESISTIVITY TEST

4.5.1. Introduction. A concrete's electrical resistance may be measured in an attempt to quantify the rate at which a bare, depassivated steel bar, embedded within the concrete, corrodes. The corrosion process is dependent upon the ability of charged ions, such as hydroxyl ions OH^- , to flow from the cathode to the anode. The faster the ions can flow from the cathode to the anode, the faster the corrosion process may proceed, provided the cathode is supplied with a sufficient amount of oxygen and water. The transport of electricity through concrete closely resembles that of ionic current; therefore, it is possible to classify the rate of corrosion of a bar embedded within concrete by quantifying the electrical resistance of the surrounding concrete.

The four probe resistivity meter, also known as the Wenner probe and shown in **Figure 4.9**, is generally regarded as the most accurate method of measuring concrete resistivity. The probe contains four equally spaced electrodes that are positioned along a straight line. The two outer electrodes send an alternating current through the concrete while the inner electrodes measure the drop in potential. The resistivity is then calculated using **Eq. 4.3**.

$$\rho = \frac{2\pi sV}{I} \quad (4.3)$$

Where ρ is the resistivity (Ωcm) of the concrete, s is the spacing of the electrodes (cm), V is the recorded voltage (V), and I is the applied current (A).



Figure 4.9 - Canin⁺ Wenner Probe

4.5.2. Fabrication. The concrete specimens for the resistivity test were fabricated according to ASTM C 1543–10 “Standard Test Method for Determining the Penetration of Chloride Ion into Concrete by Ponding”. The molds used to create these specimens were the same molds to create the specimens for the ponding test. The specimens were prepared the same way, using the same procedure. They were cured in the moist curing chamber for 14 days then transported to a humidity and temperature controlled environment to dry cure for an additional 21 days before testing. Testing began when the specimens reached an age of 35 days.

4.5.3. Testing & Procedure. One day prior to the beginning of the test, the specimens were ponded with just enough distilled water to coat the bottom of the reservoir. The specimens sat with water in them for 24 hours. The following day the water was vacuumed off using a shop vacuum cleaner. The Wernner probe was then used to take the initial resistivity measurements. The measurements were taken in a systematic manner, from left to right, then top to bottom, using the Plexiglas template shown in **Figure 4.10**. Three measurements were taken from left to right, once on the far left, once in the middle and once on the far right. Three measurements were then taken from top to bottom, once on the top, once in the middle, and once on the bottom.



Figure 4.10 - Wenner Probe Grid

This procedure was done in the same order, once every week. The measurements were taken weekly until the resistivity measurements became constant. However, due to time constraints the duration of the test was limited to 24 weeks.

5. SELF-CONSOLIDATING CONCRETE HARDENED PROPERTY AND DURABILITY RESULTS

5.1. COMPRESSIVE STRENGTH

The compressive strength was determined in accordance with ASTM C 39-11. A minimum of three, and many times four, replicate specimens were tested for each testing date for each experimental mix. The compressive strength was tested at 1, 7, and 28 days. The specimen strengths were averaged and reported as the compressive strength of the experimental mix. The normal strength conventional concrete (C6-58L) was compared to the normal strength self-consolidating concrete (S6-48L). A strength profile was developed in order to analyze and compare the strength gain of each mix. The individual specimen results of the normal strength mixes can be seen in **Table 5.1**.

Table 5.1 Individual Compressive Strength Results for Normal Strength Mixes

	Mix Design ID							
	C6-58L				S6-48L			
1 Day Compressive Strength (psi)	4,270	4,330	4,430	4,790	4,050	4,090	4,560	4,390
7 Day Compressive Strength (psi)	6,110	6,270	6,210	6,080	5,970	6,340	6,570	6,640
28 Day Compressive Strength (psi)	7,300	7,670	7,850	7,580	8,310	8,130	7,930	8,180

1 psi = 6.89 kPa

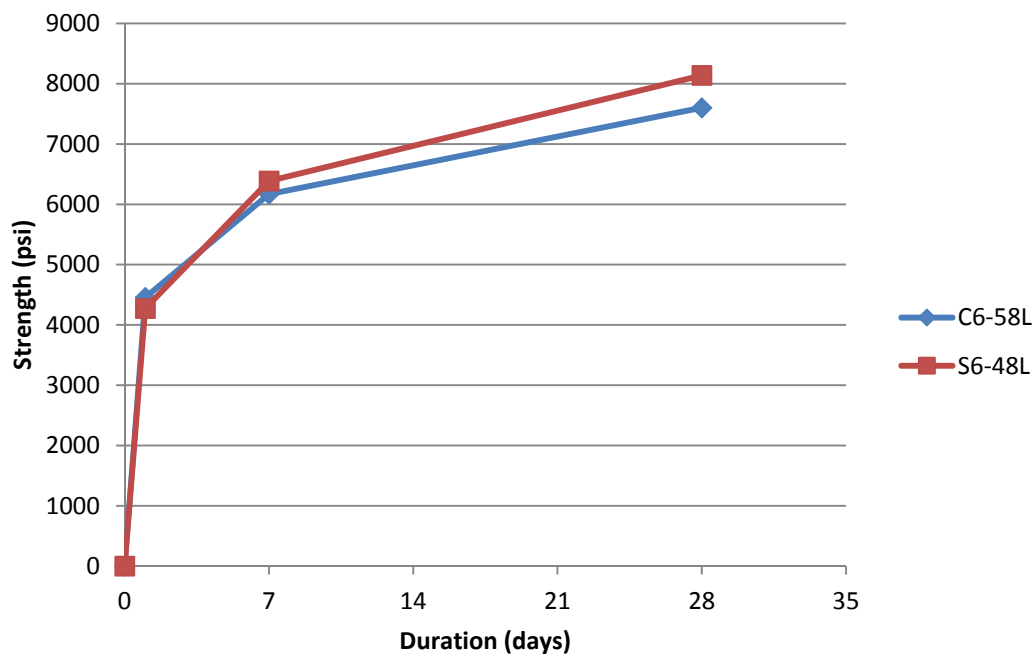
The individual results were then averaged and reported as the compressive strength of the experimental mix. The averaged values can be seen in **Table 5.2**.

Table 5.2 Averaged Compressive Strength Results for Normal Strength Mixes

Mix Design ID	1 Day Strength (psi)	7 Day Strength (psi)	28 Day Strength (psi)
C6-58L	4,450	6,170	7,600
S6-48L	4,270	6,390	8,140

1 psi = 6.89 kPa

These values were then plotted in order to develop a strength gain profile for the normal strength mixes, both conventional and SCC. The strength profiles for both mixes are shown in **Figure 5.1**.

**Figure 5.1 - Compressive Strength Profile for Normal Strength Mixes**

The compressive strength was also determined for the high strength experimental mixes, C10-58L and S10-48L. These tests were conducted in the same way, according to ASTM C 39. The individual specimen results can be seen in **Table 5.3**.

**Table 5.3 Individual Compressive Strength Results for
High Strength Concrete Mixes**

	Mix Design ID							
	C10-58L				S10-48L			
1 Day Compressive Strength	5,680	5,970	4,830	4,850	7,520	7,270	7,310	7,400
7 Day Compressive Strength (psi)	8,650	8,270	9,000	8,820	10,360	10,910	11,590	11,540
28 Day Compressive Strength (psi)	11,270	10,510	10,190	11,320	13,140	13,540	13,760	-

1 psi = 6.89 kPa

The individual results were then averaged and reported as the compressive strength. The averaged compressive strength results can be found in **Table 5.4**.

**Table 5.4 Averaged Compressive Strength Results for
High Strength Concrete Mixes**

Mix Design ID	1 Day Strength (psi)	7 Day Strength (psi)	28 Day Strength (psi)
C10-58L	5,330	8,690	10,820
S10-48L	7,380	11,100	13,480

1 psi = 6.89 kPa

From this data, the compressive strength profile was developed, with both mixes shown in **Figure 5.2**.

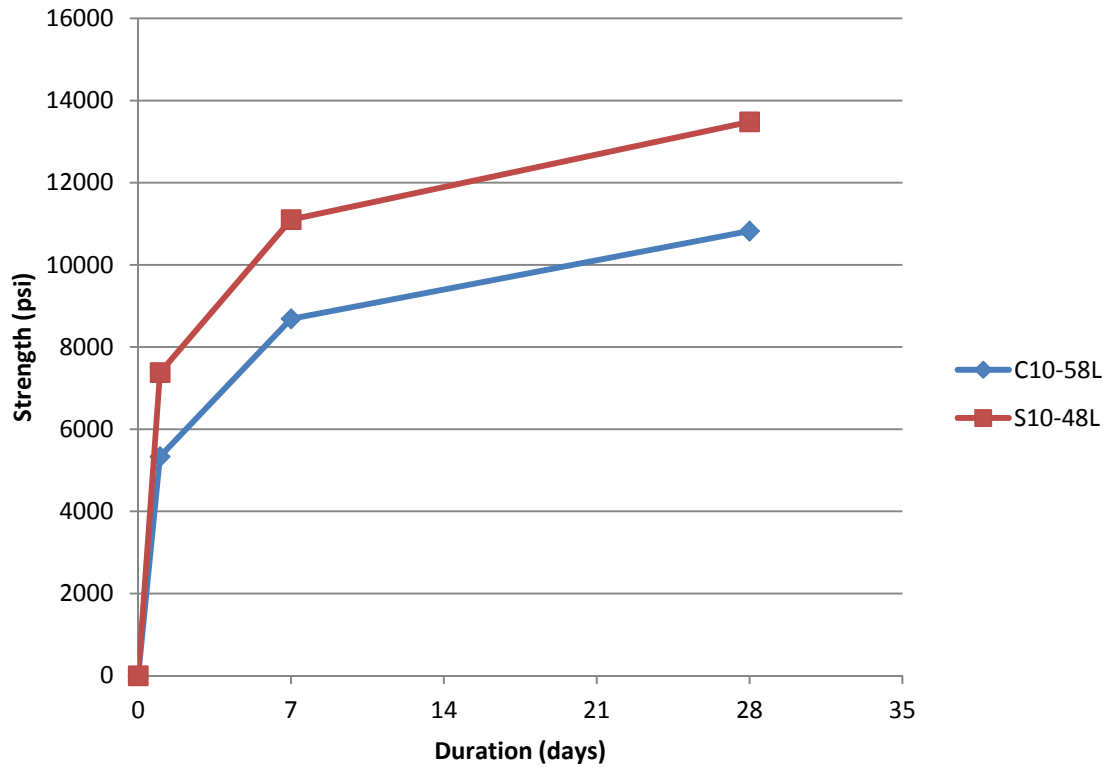


Figure 5.2 - Compressive Strength Profile for High Strength Concrete Mixes

From the strength profiles, the effect of the Type III cement is evident in the early strength gains for both the normal strength and high strength mixes. Both of the normal strength mixes exceeded the target strength of 6,000 psi (41.4 MPa), with the self-consolidating concrete performing slightly better than the conventional mix. The C6-58L mix also showed a more rapid strength gain than the S6-48L mix. The high strength mixes showed different behavior. The S10-48L mix gained much more strength early on than the C10-58L mix and far surpassed it in ultimate strength. However, both of these mixes surpassed the 10,000 ksi (68.9 MPa) target strength.

5.2. MODULUS OF ELASTICITY

The modulus of elasticity was tested and calculated in accordance with ASTM C 469-10. Test specimens consisted of 4 in. (102 mm) x 8 in. (203 mm) cylinders. The specimens were tested after 28 days. During testing, both the load at 50×10^{-6} strain and the length change at 40% of the ultimate strength were measured. Using these values the modulus of elasticity was calculated using **Eq. 5.1**.

$$E = \frac{(S_2 - S_1)}{(\epsilon_2 - 0.000050)} \quad (5.1)$$

Where S_2 is the stress at 40% of the ultimate load, S_1 is the stress measured at 50×10^{-6} strain, and ϵ_2 is the strain at S_2 . The results for the normal strength experimental mixes can be seen in **Table 5.5**.

Table 5.5 Individual Modulus of Elasticity Results for Normal Strength Mixes

Mix Design ID	Specimen ID	Test 1			Test 2		
		S_2 (psi)	S_1 (psi)	ϵ_2 ($\times 10^{-4}$)	S_2 (psi)	S_1 (psi)	ϵ_2 ($\times 10^{-4}$)
C6-58L	MOE-1	2,990	231	8.66	2990	211	8.54
	MOE-2	3,040	198	8.66	3040	198	8.66
S6-48L	MOE-1	3,290	192	10.5	3290	192	10.5
	MOE-2	3,250	190	10.2	3250	187	10.1

$$1 \text{ psi} = 6.89 \text{ kPa}$$

The values for S_2 were based on results of the companion compressive strength tests. The modulus of elasticity test and compressive strength tests were performed back to back, so the values for S_2 vary slightly from test to test. Using this data and **Eq. 5.1**, the modulus

of elasticity was calculated and averaged from the two tests. The averaged results can be seen in **Table 5.6**.

Table 5.6 Average Modulus of Elasticity Results for Normal Strength Mixes

Batch ID	Modulus of Elasticity (psi)
C6-58L	3,450,000
S6-48L	3,130,000

1 psi = 6.89 kPa

The results were also normalized using the respective measured compressive strengths. This step was performed in order to compare the coefficients with the ACI 318-08 recommended value of 57,000, as shown in **Eq. 5.2**. This equation assumes a unit weight of concrete of 145 pcf. It should be noted that while none of the concrete mixes had a unit weight of 145 pcf all were very close and it was decided that the difference would not be significant.

$$E_c = 57,000\sqrt{f'_c} \quad (5.2)$$

Where E_c is the modulus of elasticity and f'_c is the compressive strength of concrete. The measured modulus of elasticity was divided by the square root of the strength of the respective mix and then compared to the ACI coefficient. The results can be seen in **Table 5.7**.

Table 5.7 Normalized Modulus of Elasticity for Conventional Concrete Mixes

	C6-58L	S6-48L	ACI Coefficient
Normalized Results	39,580	34,700	57,000

$$1 \text{ psi} = 6.89 \text{ kPa}$$

The measured modulus of elasticity for the conventional concrete was also compared to the recommended AASHTO coefficient of 1,820 as shown in **Eq. 5.3**.

$$E_c = 1,820\sqrt{f'_c} \quad (5.7)$$

The measured modulus of elasticity was divided by the strength of the respective mix and the compared to the AASHTO coefficient. The results can be seen in **Table 5.8**.

Table 5.8 Normalized AASHTO Modulus of Elasticity for Conventional Concrete Mixes

	C6-58L	S6-48L	AASHTO Coefficient
Normalized Results	1,251	1,097	1,820

The same procedure was also performed for the high strength experimental mixes. The results of the individual tests can be seen in **Table 5.9**.

Table 5.9 Individual Modulus of Elasticity Results for High Strength Concrete Mixes

Mix Design ID	Specimen ID	Test 1			Test 2		
		S ₂ (psi)	S ₁ (psi)	ϵ_2 (x10 ⁻⁴)	S ₂ (psi)	S ₁ (psi)	ϵ_2 (x10 ⁻⁴)
C10-58L	MOE-1	4,360	230	11.2	4360	233	11.4
	MOE-2	4,270	227	10.6	4270	223	10.7
S10-48L	MOE-1	4,410	237	12.5	4410	248	12.5
	MOE-2	4,390	222	11.2	4390	237	11.8

1 psi = 6.89 kPa

Using this data, the average modulus of elasticity was calculated. The average modulus of elasticity for each high strength experimental mix can be found in **Table 5.10**.

Table 5.10 Average Modulus of Elasticity Results for High Strength Concrete Mixes

Mix Design ID	Modulus of Elasticity (psi)
C10-58L	3,900,000
S10-48L	3,630,000

1 psi = 6.89 kPa

The values for the high strength mixes were also normalized using the respective strengths. These values were then compared to the ACI coefficient of 57,000. The results can be seen in **Table 5.11**.

Table 5.11 Normalized Modulus of Elasticity for High Strength Concrete Mixes

	C10-58L	S10-48L	ACI Coefficient
Normalized Results	37,500	31,290	57,000

1 psi = 6.89 kPa

The same procedure was also performed on the high strength mixes and compared to the AASHTO coefficient of 1,820. The results for the high strength mixes can be seen in

Table 5.12.

Table 5.12 Normalized AASHTO Modulus of Elasticity for High Strength Concrete Mixes

	C10-58L	S10-48L	AASHTO Coefficient
Normalized Results	1,186	987	1,820

5.3. MODULUS OF RUPTURE

The modulus of rupture test was performed in accordance with ASTM C 78-10.

The modulus of rupture was calculated using the formula stated in Section 3.5.3. The values used in the equation measured for each individual test can be seen in **Table 5.13.**

Table 5.13 Individual Modulus of Rupture Results for Normal Strength Mixes

Mix Design ID	Specimen ID	L (in.)	Peak Load (lb.)	b ₁ (in.)	b ₂ (in.)	b ₃ (in.)	b _{avg} (in.)	d ₁ (in.)	d ₂ (in.)	d ₃ (in.)	d _{avg} (in.)
C6-58L	MOR-1	18	9,589	5.94	5.97	5.96	5.96	6.32	6.29	6.28	6.29
	MOR-2	18	8,824	6.06	6.08	6.08	6.07	5.98	5.97	5.98	5.98
	MOR-3	18	9,267	6.22	6.24	6.21	6.22	5.93	5.95	5.95	5.94
S6-48L	MOR-1	18	8,047	6.04	6.01	6.02	6.02	5.97	5.95	5.93	5.95
	MOR-2	18	8,731	6.29	6.32	6.39	6.34	5.94	5.95	5.97	5.95
	MOR-3	18	7,775	6.11	6.11	6.13	6.12	5.93	5.97	5.96	5.95

$$1 \text{ psi} = 6.89 \text{ kPa}$$

The modulus of rupture was calculated using the values in **Table 5.13** and then averaged for each concrete type. The average modulus of rupture for the normal strength mixes can be seen in **Table 5.14.**

Table 5.14 Averaged Modulus of Rupture for Normal Strength Mixes

Mix Design ID	Modulus of Rupture (psi)
C6-58L	740
S6-48L	670

1 psi = 6.89 kPa

The results were also normalized using the respective measured compressive strengths. This step was done in order to compare the coefficients with the ACI 318-08 recommended coefficient of 7.5, which appears in the equation to estimate the modulus of rupture, as seen in **Eq. 5.3**.

$$f_r = 7.5\sqrt{f'_c} \quad (5.3)$$

Where f_r is the modulus of rupture and f'_c is the compressive strength of concrete. ACI 318-08 states that any values between 6 and 12 are acceptable as coefficients. After the modulus was measured, the values were divided by the average measured compressive strength of the respected mix. This normalized the results, and these results were compared to the ACI coefficient of 7.5. The results of the normal strength mixes can be seen in **Table 5.15**.

Table 5.15 Normalized Modulus of Rupture for Normal Strength Mixes

	C6-58L	S6-48L	ACI Coefficient
Modulus of Rupture (psi)	8.5	7.4	7.5

1 psi = 6.89 kPa

The modulus of rupture was also normalized and compared to the AASHTO coefficient of 0.24 as seen in **Eq. 5.4**.

$$f_r = 0.24\sqrt{f'_c} \quad (5.4)$$

The measured modulus of rupture was divided by strength of the respective mix and then compared to the AASHTO coefficient. The results of the normal strength concrete can be seen in **Table 5.16**.

Table 5.16 Normalized AASHTO Modulus of Rupture for Normal Strength Mixes

	C6-58L	S6-48L	AASHTO Coefficient
Normalized Result	0.27	.23	.24

The same procedure and calculations were performed for the high strength experimental mixes. The results for the individual tests can be seen in **Table 5.17**.

The modulus of rupture was calculated from the values in **Table 5.17** and then averaged to give a measured modulus of rupture for each mix. The averaged modulus of rupture for the high strength experimental mixes can be seen in **Table 5.18**.

**Table 5.17 Individual Modulus of Rupture Results for
High Strength Concrete Mixes**

Mix Design ID	Specimen ID	L (in.)	Peak Load (lb.)	b ₁ (in.)	b ₂ (in.)	b ₃ (in.)	b _{avg} (in.)	d ₁ (in.)	d ₂ (in.)	d ₃ (in.)	d _{avg} (in.)
C10-58L	MOR-1	18	12,791	6.18	6.14	6.13	6.15	5.92	5.96	5.95	5.94
	MOR-2	18	12,123	6.02	6.01	5.99	6.01	5.94	5.98	5.98	5.97
	MOR-3	18	12,719	6.20	6.22	6.23	6.22	5.95	5.96	5.98	5.96
S10-48L	MOR-1	18	13,808	6.01	6.01	6.06	6.03	5.96	5.93	5.92	5.94
	MOR-2	18	13,588	6.09	6.05	6.11	6.08	5.92	5.97	5.95	5.95
	MOR-3	18	12,546	6.17	6.17	6.22	6.19	5.98	5.99	5.94	5.97

1 psi = 6.89 kPa

Table 5.18 Average Modulus of Rupture Results for High Strength Concrete Mixes

Mix Design ID	Modulus of Rupture (psi)
C10-58L	1,040
S10-48L	1,100

1 psi = 6.89 kPa

These values were also normalized with the respective compressive strengths in order to compare to the ACI coefficient of 7.5. The normalized results can be seen in **Table 5.19**.

Table 5.19 Normalized Modulus of Rupture Results for High Strength Concrete Mixes

	C10-58L	S10-48L	ACI Coefficient
Normalized Results	9.98	9.52	7.5

The modulus of rupture was also normalized and compared to the AASHTO coefficient of 0.24 as seen in **Eq. 5.4**. The measured modulus of rupture was divided by strength of

the respective mix and then compared to the AASHTO coefficient. The results of the high strength concrete can be seen in **Table 5.20**.

Table 5.20 Normalized AASHTO Modulus of Rupture for High Strength Mixes

	C10-58L	S10-58L	AASHTO Coefficient
Normalized Result	0.32	0.30	0.24

5.4. SPLITTING TENSILE

The splitting-tensile strength of the concrete mixes was tested and calculated in accordance with ASTM C 496-11. This test was performed using 6 in. (152 mm) diameter by 12 in. (305 mm) long cylindrical specimens. These specimens were loaded into the testing apparatus and loaded until failure. The splitting tensile strength was then calculated using **Eq. 5.5**.

$$T = \frac{2P}{\pi ld} \quad (5.5)$$

Where P is the maximum load applied, l is the length of the specimen, and d is the diameter. A total of 3 specimens were tested for each mix. The individual test results for the normal strength mixes are shown in **Table 5.21**.

Table 5.21 Individual Splitting-Tensile Test Results for Normal Strength Concrete Mixes

Mix Design ID	Specimen Number	Length (in)	Diameter (in)	Load (lb.)	Splitting Tensile Strength (psi)
C6-58L	1	12.1	6.0	37,155	326
	2	12.1	6.0	40,260	353
	3	12.1	6.0	49,575	435
S6-48L	1	12.1	6.0	40,890	359
	2	12.1	6.0	66,075	579
	3	12.1	6.0	49,620	435

1 in. = 2.54 cm.

1 lb = 0.45 kg

1 psi = 6.89 kPa

The results of the individual tests were then averaged, and the splitting tensile strength of the normal strength mixes can be seen in **Table 5.22**.

Table 5.22 Averaged Splitting-Tensile Test Results for Normal Strength Concrete Mixes

Mix Design ID	Splitting Tensile Strength (psi)
C6-58L	370
S6-48L	460

1 psi = 6.89 kPa

The results were also normalized using the respective measured compressive strengths. This step was done in order to compare the coefficients with the ACI coefficient of 6.7 which comes from the equation to estimate the splitting-tensile strength as seen in **Eq. 5.6**.

$$f_t = 6.7\sqrt{f'_c} \quad (5.6)$$

Where f_t is the splitting-tensile strength and f'_c is the compressive strength of concrete. After the splitting tensile strength was measured, the values were divided by the square root of the average measured strength of the respected mix. This normalized the results, and these results were compared to the ACI coefficient of 6.7. The results of the normal strength mixes can be seen in **Table 5.23**.

**Table 5.23 Normalized Splitting-Tensile Results for
Normal Strength Concrete Mixes**

Mix Design ID	C6-58L	S6-48L	ACI Coefficient
Normalized Results	4.2	5.1	6.7

The same test was carried out on the high strength concrete mixes. The individual test results can be seen in **Table 5.24**.

**Table 5.24 Individual Splitting-Tensile Test Results for
High Strength Concrete Mixes**

Mix Design ID	Specimen Number	Length (in.)	Diameter (in.)	Load (lb.)	Splitting Tensile Strength (psi)
C10-58L	1	12.2	6.0	66,675	580
	2	12.1	6.0	56,070	492
	3	12.1	6.0	66,090	580
S10-48L	1	12	6.0	95,100	841
	2	12.1	6.0	83,520	732
	3	12.2	6.0	81,345	708

1 in. = 2.54 cm.

1 lb = 0.45 kg

1 psi = 6.89 kPa

The results of the individual tests were then averaged, and the splitting tensile strength of the high strength mixes can be seen in **Table 5.25**.

Table 5.25 Averaged Splitting-Tensile Test Results for High Strength Concrete Mixes

Mix Design ID	Splitting Tensile Strength (psi)
C10-58L	550
S10-48L	760

1 psi = 6.89 kPa

These values were also normalized with the respective compressive strengths in order to compare to the ACI coefficient of 6.7. The normalized results can be seen in **Table 5.26**.

Table 5.26 Normalized Splitting-Tensile Results for High Strength Concrete Mixes

Mix Design ID	C10-58L	S10-48L	ACI Coefficient
Normalized Results	5.3	6.5	6.7

5.5. RAPID FREEZING & THAWING

The concrete's resistance to freezing and thawing was tested and calculated in accordance to ASTM C 666-08. During the freezing and thawing cycles, the relative dynamic modulus of elasticity was measured for each of the specimens using the equation stated in Section 4.2.3. Using this data, the durability factor of the specimen could be calculated using the equation stated in Section 4.2.3. The relative dynamic modulus of elasticity and durability factor of each specimen was calculated every 36 cycles. The complete data for all test specimens can be found in Appendix A. The minimum calculated durability factor was reported as the durability factor for that

specimen, and the values for the individual specimens of the normal strength mixes can be seen in **Table 5.27**.

Table 5.27 Individual Results of Rapid Freezing and Thawing Test for Normal Strength Mixes

Mix Design ID	Specimen ID	Initial Frequency	Terminal Frequency	Durability Factor	% Mass Change
C6-58L	FT-1	1973	1184	23.2	0.01
	FT-2	1947	1168	22.4	0.02
	FT-3	1980	1188	31.1	-0.01
S6-48L	FT-1	2013	1208	11.5	0.05
	FT-2	1979	1187	28.9	0.01
	FT-3	1902	1141	19.2	0.02

The average durability factor was reported using the three replicate specimens for each experimental mix. The higher the measured durability factor of the specimen, the better the mix will perform when exposed to cyclic freezing and thawing. The calculated durability factors for the normal strength mixes can be seen in **Table 5.28**.

Table 5.28 Averaged Durability Factors for Normal Strength Mixes

Mix Design ID	Durability Factor
C6-58L	25.5
S6-48L	19.9

The calculation procedure was the same for the high strength experimental mixes. The calculated durability factors for each individual specimen can be seen in **Table 5.29**.

Table 5.29 Individual Results of Freezing and Thawing Test for High Strength Mixes

Mix Design ID	Specimen ID	Initial Frequency	Terminal Frequency	Durability Factor	% Mass Change
C10-58L	FT-1	1990	1194	90.8	-0.01
	FT-2	1978	1187	93.1	-0.09
	FT-3	1988	1193	77.6	0
S10-48L	FT-1	2018	1211	43.4	0
	FT-2	1998	1199	61.5	-0.01
	FT-3	2041	1225	30.6	0.02

The average durability factors for the high strength experimental mixes can be seen in **Table 5.30**.

Table 5.30 Averaged Durability Factors for High Strength Mixes

Mix Design ID	Durability Factor
C10-58L	87.2
S10-48L	45.2

5.6. ELECTRICAL INDICATION TO RESIST CHLORIDE PENETRATION

The testing and calculations for this test were performed in accordance with ASTM C 1202-10. After the testing was complete, the measured current vs. time was plotted. A trend line was drawn through the graph and was integrated to calculate the area under the curve. The graphs plotted for each specimen can be found in Appendix A. An example of this graph can be seen in **Figure 5.3**.

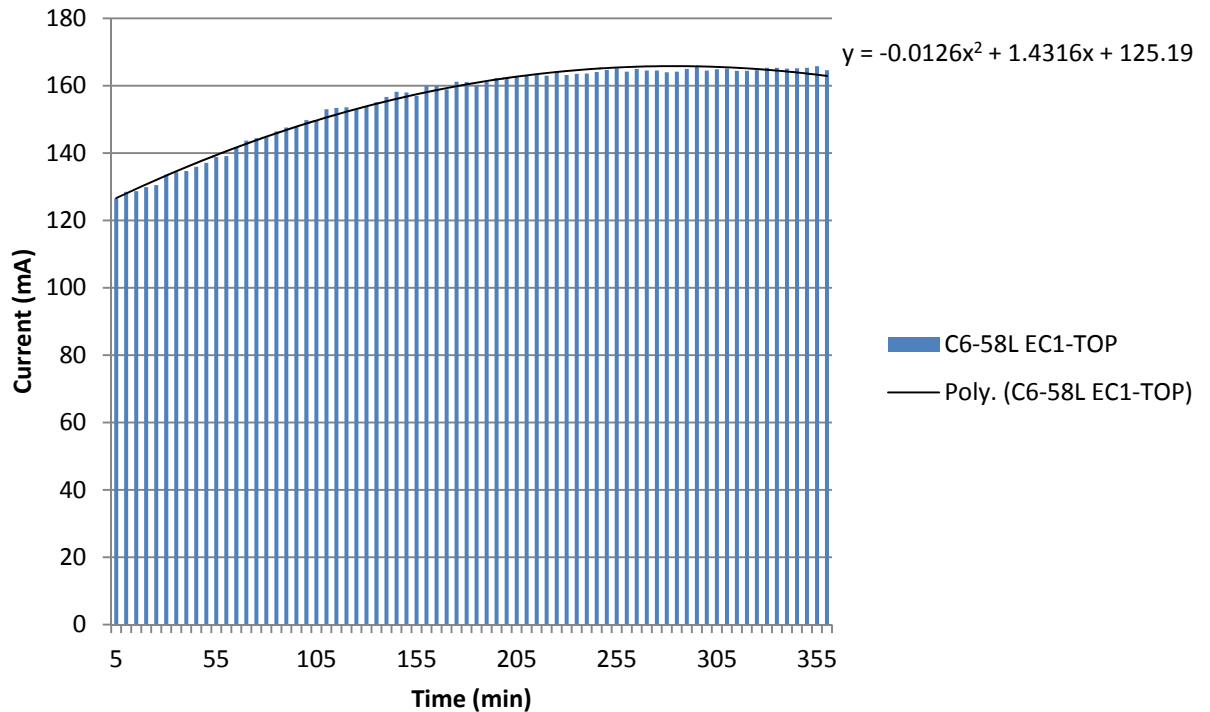


Figure 5.3 – Example of RCT Results

This area gives the total charge in coulombs to pass through the specimen during the 6 hour test. Since the diameter of the specimens used did not measure 3.75 in. (95 mm), the charge had to be adjusted using **Eq. 5.7**.

$$Q_s = Q_x \times \left(\frac{3.75}{x}\right)^2 \quad (5.7)$$

Where Q_s is the total charge through a 3.75 in. (95 mm) specimen, Q_x is the total charge passed through a specimen measuring x inches in diameter, and x is the diameter of the specimen that is tested. The total charge was then compared to ASTM C 1202 to assign a permeability rating, with a range from negligible (indicating the highest resistance to chloride penetration) to high (indicating the lowest resistance to chloride penetration).

The corrected results of the individual specimens for the normal strength mixes can be seen in **Table 5.31**.

Table 5.31 Individual RCT Results for Normal Strength Mixes

Mix Design ID	Corrected Charge Passed (Coulombs)			
	EC1-TOP	EC1-MID	EC2-TOP	EC2-MID
C6-58L	3025	3135	4050	3810
S6-48L	3990	3681	3846	3812

The average was taken of the total charge passed through all four specimens and that charge was then used to assign a permeability class. The results of the conventional mixes can be seen in **Table 5.32**.

Table 5.32 Averaged Results of RCT and Permeability Class of Conventional Mixes

Mix Design ID	Charge Passed (Coulombs)	Permeability Class
C6-58L	3505	Moderate
S6-48L	3832	Moderate

The ranges for the classes are as follows; 0-100 for negligible, 100-1000 for very low, 1000-2000 for low, 2000-4000 for moderate, >4000 for high. Both mixes fell into the moderate category. The same calculation process was performed on the high strength mix specimens. The individual specimen results can be seen in **Table 5.33**.

Table 5.33 Individual Results of RCT for High Strength Mixes

Batch ID	Corrected Charge Passed (Coulombs)			
	EC1-TOP	EC1-MID	EC2-TOP	EC2-MID
C10-58L	4314	4666	3785	4860
S10-48L	2125	2444	2391	2296

The average of the four specimens was then calculated and this value was used to assign a permeability class. The results for the high strength experimental mixes can be seen in **Table 5.34**.

Table 5.34 Averaged Results of RCT and Permeability Class for High Strength Mixes

Mix Design ID	Charge Passed (Coulombs)	Permeability Class
C10-58L	4406	High
S10-48L	2564	Moderate

5.7. PONDING TEST

The ponding test was performed in accordance with ASTM C 1543-10. After the ponding duration was complete, cores were taken from the specimens and powder samples collected at specified depths. A water soluble chloride analysis was performed on each powder sample to determine the chloride concentration. For each experimental mix, a total of 3 cores were taken from each of the three individual test specimens, with 5 powder samples taken from each core. This approach would determine an average chloride profile for each experimental mix. Using a scale set forth by Broomfield in 2007, the risk of corrosion in concrete can be determined by the amount of chloride present in concrete. The scale can be seen in **Table 5.35**.

Table 5.35 Correlation Between Percent Chloride by Mass of Concrete and Corrosion Risk [Broomfield, 2007]

% Chloride by mass of concrete	Corrosion Risk
<0.03	Negligible
0.03-0.06	Low
0.06-0.14	Moderate
>0.14	High

Using this scale, the concrete mixes were assigned corrosion risk based on the data collected in the chloride analysis. The averaged data for the normal strength mixes can be seen in **Table 5.36**. The complete table of data can be found in Appendix A. The data was also plotted in **Figure 5.4** with a line indicating a negligible corrosion risk.

Table 5.36 Average Chloride Content at Specified Depths of Normal Strength Mixes

Mix Design ID	Depth (in.)	Chloride Content (%)	Corrosion Risk
C6-58L	Surface	0.23	High
	0.25	0.07	Moderate
	0.75	0.02	Negligible
	1.5	0.009	Negligible
	2.0	0.006	Negligible
S6-48L	Surface	0.28	High
	0.25	0.09	Moderate
	0.75	0.017	Negligible
	1.5	0.011	Negligible
	2.0	0.005	Negligible

1 in. = 2.54 cm

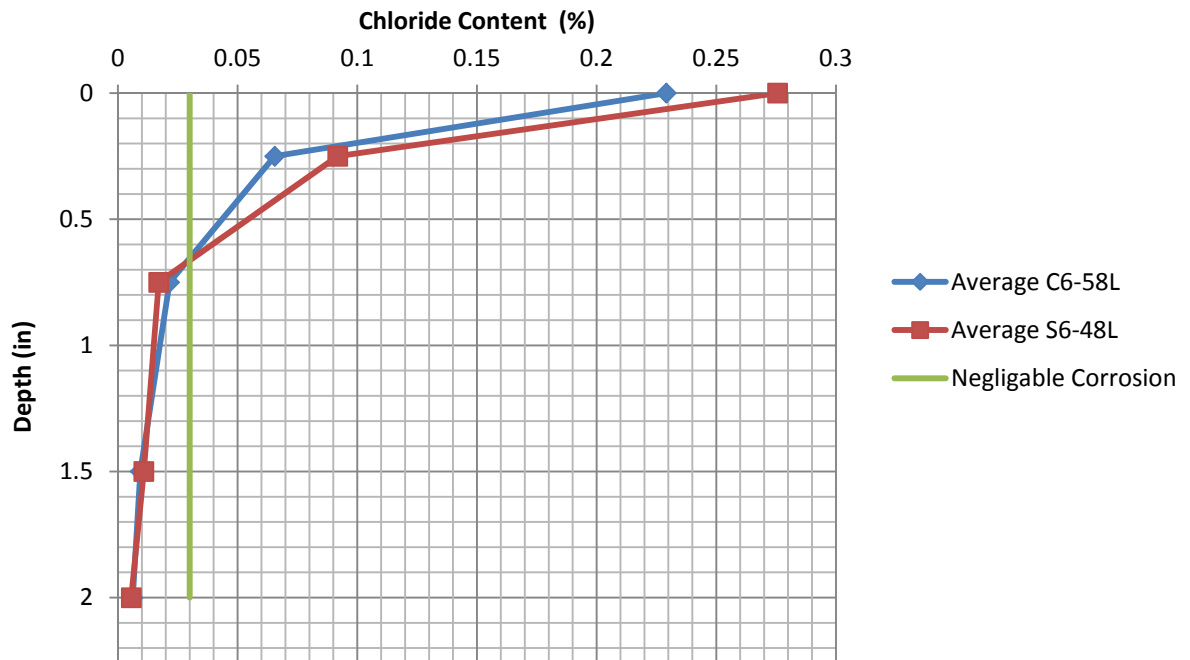


Figure 5.4 – Average Chloride Content vs. Depth of Conventional Mixes
1 in. = 2.54 cm

The same process was performed on the high strength mixes. The averaged data for the high strength mixes can be seen in **Table 5.37**. The complete table of data can be seen in Appendix A. This data was also plotted in **Figure 5.5** with a line indicating a negligible corrosion risk.

Table 5.37 Average Chloride Content at Specified Depths of High Strength Mixes

Mix Design ID	Depth (in.)	Chloride Content (%)	Corrosion Risk
C10-58L	Surface	0.24	High
	0.25	0.095	Moderate
	0.75	0.011	Negligible
	1.5	0.0074	Negligible
	2.0	0.010	Negligible

S10-48L	Surface	0.15	High
	0.25	0.016	Negligible
	0.75	0.006	Negligible
	1.5	0.0062	Negligible
	2.0	0.0044	Negligible

1 in. = 2.54 cm.

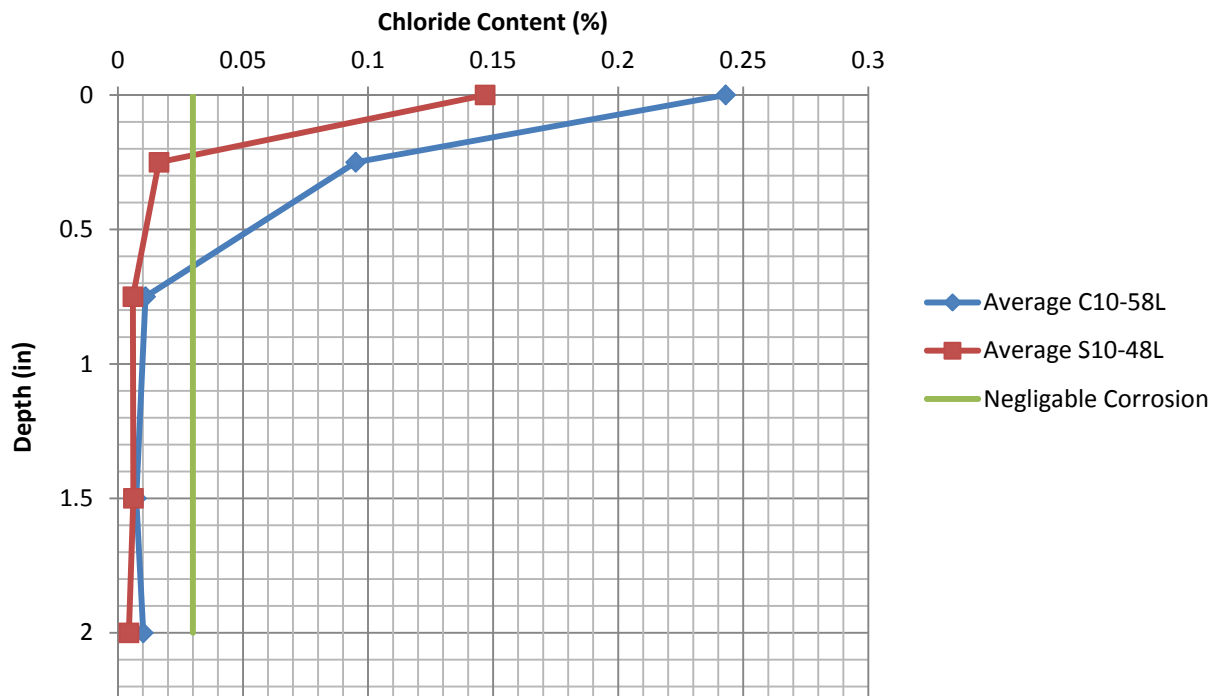


Figure 5.5 – Average Chloride Content vs. Depth of High Strength Mixes
1 in. = 2.54 cm

5.8. CONCRETE RESISTIVITY

The concrete resistivity test was a non-ASTM test method. It is however, an industry standard, and is used quite frequently. The resistivity measurements were measured over a period of 24 weeks. These measurements can be found in Appendix A.

The test was performed on three replicate specimens with the results averaged to

determine the response of the individual concrete mix. The averages for each mix were then compared between concrete types. The individual specimen results for the conventional and SCC normal strength mixes are shown in **Figure 5.6** and **Figure 5.7**, respectively.

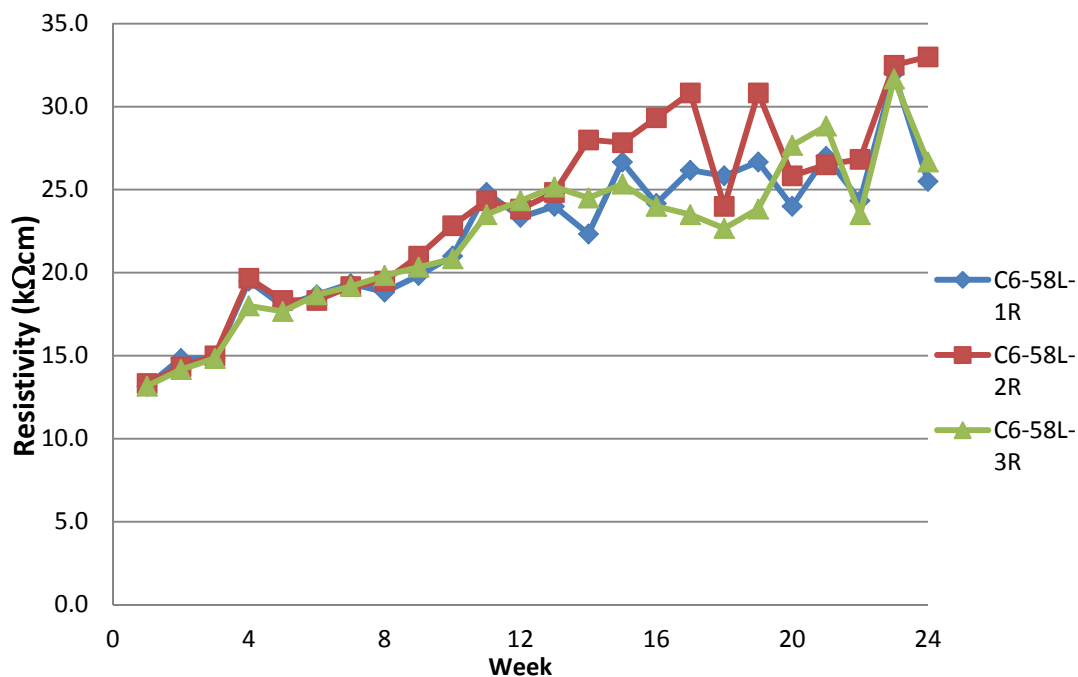


Figure 5.6 - Individual Specimen Results for Concrete Resistivity for C6-58L Mix

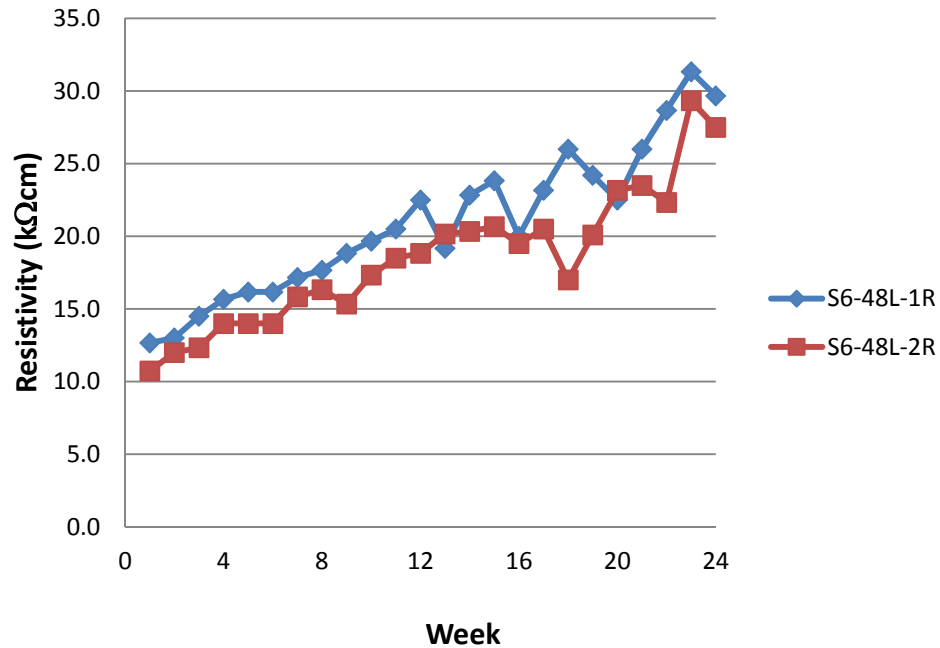


Figure 5.7 - Individual Specimen Results for Concrete Resistivity for S6-48L Mix

It should be noted that a specimen for the S6-48L mix was damaged during the de-molding process. The individual results were then averaged and graphed on the same plot for comparison purposes, which are shown **Figure 5.8**. A linear trend line of the results was also plotted in **Figure 5.8** in order to compare the rates at which the different mixes gained resistivity. According to Broomfield, any concrete that has a resistivity greater than 20 kΩcm is considered to have low corrosion potential. The final readings were taken at 24 weeks and can be seen in **Table 5.38**.

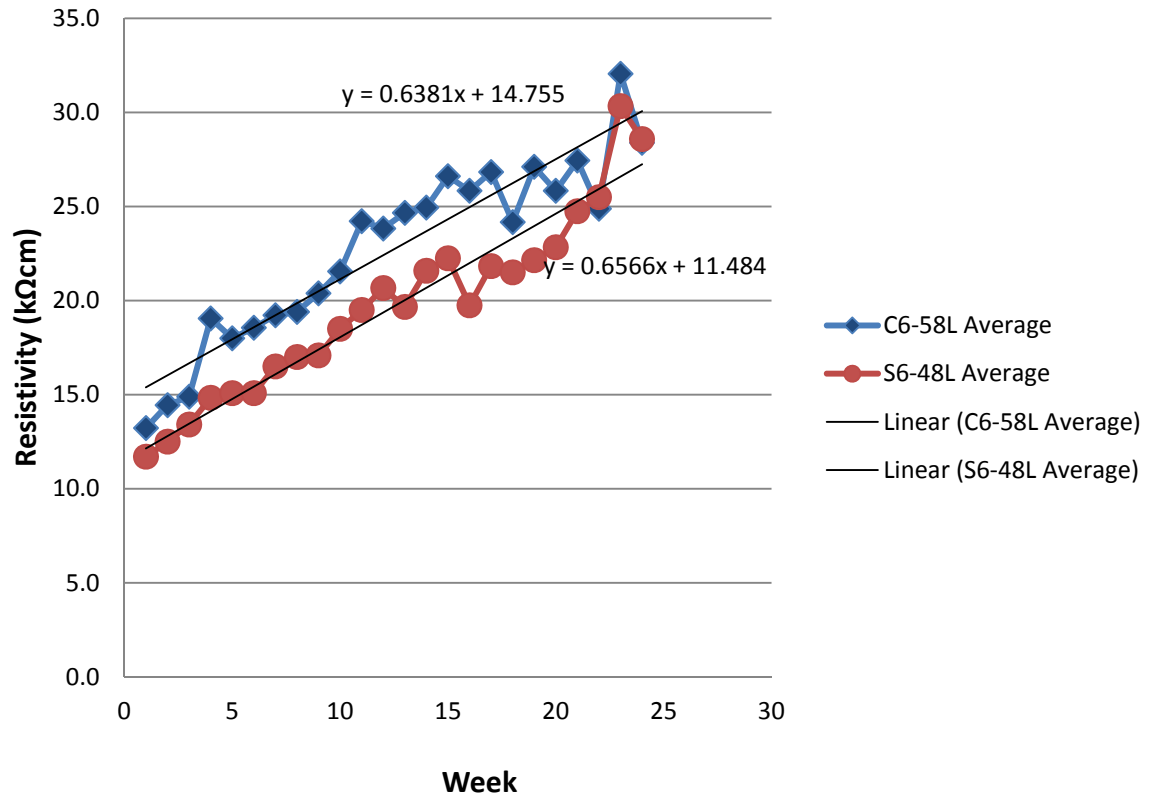


Figure 5.8 – Averaged Results for Concrete Resistivity for Normal Strength Mixes

Table 5.38 Final Resistivity of Normal Strength Concrete Mixes

Mix Design ID	Resistivity (kΩcm)
C6-58L	28.4
S6-48L	28.6

The same procedure was used for the high strength mixes. The results of the individual specimens for the C10-58L mix and the S10-48L mix can be seen in **Figure 5.9** and **Figure 5.10**, respectively.

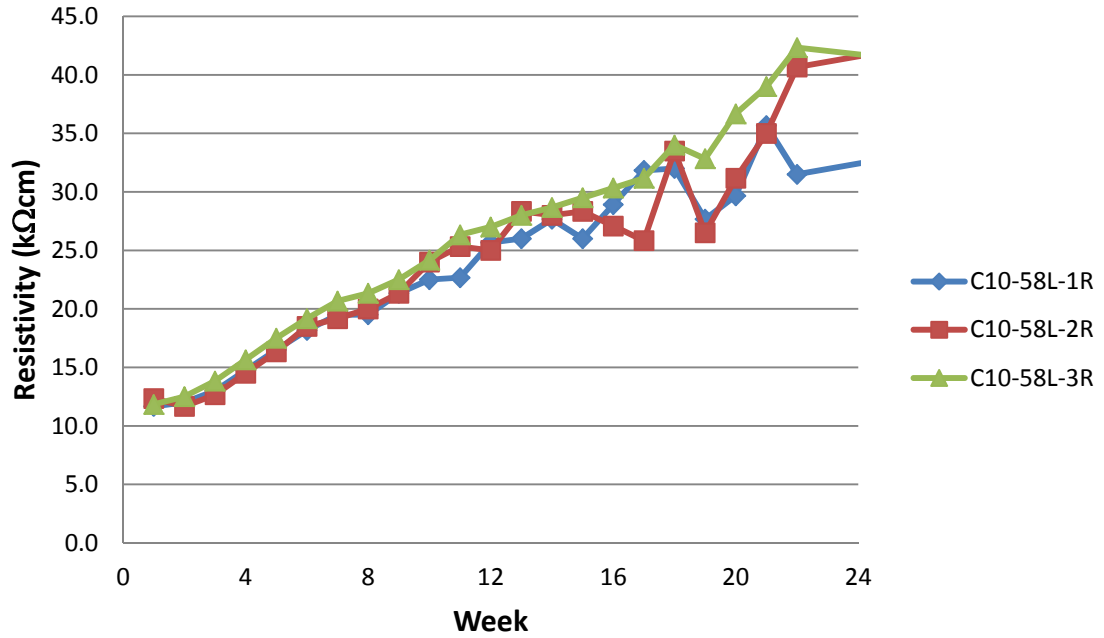


Figure 5.9 - Individual Specimen Results for Concrete Resistivity for C10-58L Mix

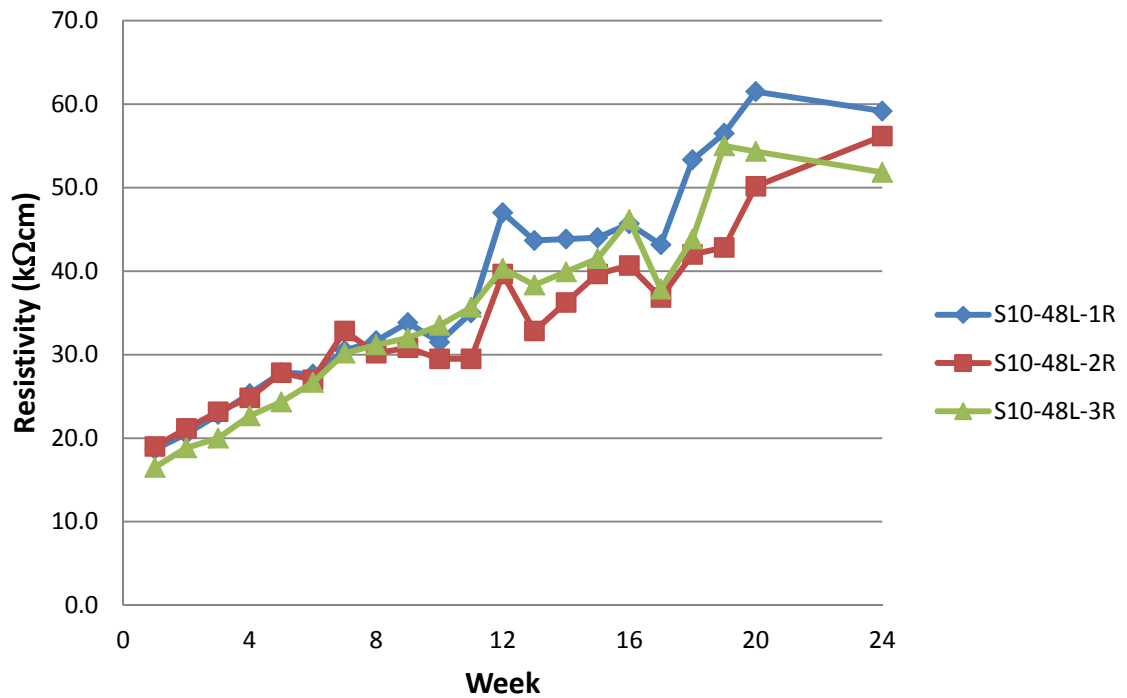


Figure 5.10 - Individual Specimen Results for Concrete Resistivity for S10-48L Mix

The measurements can be found in Appendix A. These results were then averaged and graphed on the same plot for comparison purposes, with the results for the high strength mixes shown in **Figure 5.11**. A liner trend line was plotted in order to compare the rate at which the concretes gain resistivity. The final readings were taken at 24 weeks and can be seen in **Table 5.39**.

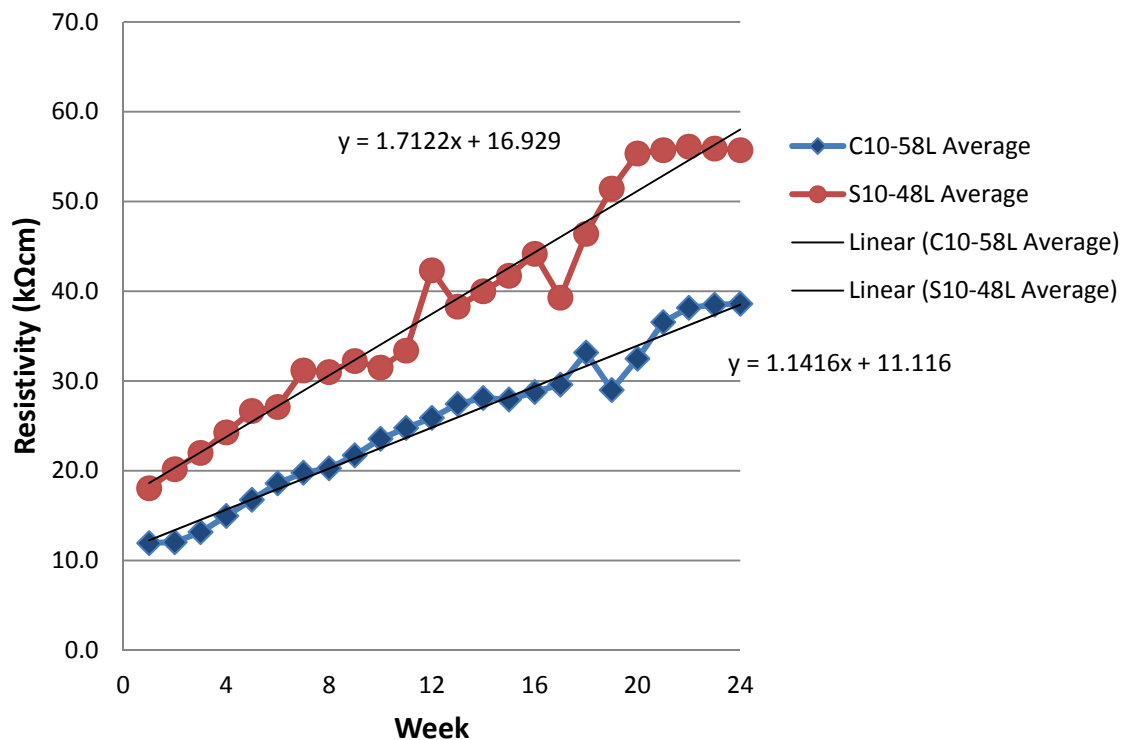


Figure 5.11 – Averaged Results for Concrete Resistivity for High Strength Mixes

Table 5.39 Final Resistivity of High Strength Concrete Mixes

Mix Design ID	Resistivity (kΩcm)
C10-58L	38.6
S10-48L	55.7

6. EVALUATION OF SELF-CONSOLIDATING CONCRETE

6.1. NORMAL STRENGTH SCC

As stated in previous sections, both the normal strength conventional concrete mix and the normal strength SCC mix were subjected to the same mechanical property and durability tests. In this way, it was possible to evaluate the performance of the SCC relative to a benchmark – the conventional normal strength concrete mix. If the SCC mix performed as well or better than the conventional concrete, than it could be reasoned that, due to the time-saving properties of SCC, it would be beneficial to use the SCC in precast applications. The results of the mechanical property and durability tests can be found in Chapter 5. An outline of these results can be seen in **Table 6.1**. As stated in previous chapters, the C6-58L and S6-48L mix design IDs represent the conventional concrete mix and SCC mix, respectively.

Table 6.1 Outline of Results of Normal Strength Concrete Mixes

Test ID	Mix Design ID	
	C6-58L	S6-48L
28 Day Compressive Strength (psi)	7,600	8,140
Modulus of Elasticity (psi)	3,337,000	3,124,000
Modulus of Rupture (psi)	741	672
Splitting Tensile (psi)	371	458
Rapid Freeze – Thaw (durability factor)	25.5	19.9
RCT (coulombs)	3,505	3,832
Ponding (Depth at 0.03% Chloride Content, in)	0.65	0.65
Concrete Resistivity (kΩcm)	28.4	28.6

1 psi = 6.89 kPa

1 in. = 2.54 cm

6.1.1. Mechanical Properties. For compressive strength, both mixes were designed to reach 6,000 psi (41.3 MPa) at 28 days, which both mixes exceeded. However, the compressive strength for the SCC mix was slightly higher than that for the conventional mix. From the strength profiles shown in **Figure 5.1** it can be seen that the early strength development was almost identical, but the SCC mix began to exceed the conventional mix at around 3 days. This early strength development is very important to precast construction. With the resulting reduction in labor, SCC would be a good candidate for precast plants when just looking at rate of strength gain. A statistical t-test was performed on the compressive strength data in order to determine if there is any statistical difference between the two mixes. The P value of the t test between the normal

strength mixes was 0.07. Any value greater than 0.05 shows the data is statistically equal. In other words, the compressive strengths of the two mixes are essentially identical. The modulus of rupture, modulus of elasticity, and splitting-tensile strengths are typically estimated in design using equations based on previous research. These equations were mentioned in Chapter 5. The results of the modulus of rupture, modulus of elasticity, and splitting-tensile strengths were subsequently normalized using the respective compressive strengths of each mix and the resulting coefficients were then compared to recommended values within ACI standards. A summary of these results can be seen in **Table 6.2**.

**Table 6.2 Normalized Mechanical Properties Compared to
Respective ACI Coefficients**

	C6-58L	S6-48L	ACI Coefficient
Modulus of Elasticity	38,280	34,630	57,000
Modulus of Rupture	8.5	7.4	7.5
Splitting Tensile Strength	4.2	5.1	6.7

Both mixes fell considerably short of the empirical relationships recommended for modulus of elasticity, with the SCC mix performing below the conventional mix. This result means that in the design of concrete structures constructed with these concretes, the modulus of elasticity for either mix would be overestimated. This situation can have negative effects on estimating deflection and serviceability of concrete in the field. However, with both concretes falling at about the same level, it can be stated that both C6-58L and S6-48L are comparable in this area. This fact leads to the conclusion that the low modulus of elasticity is more a function of the particular limestone coarse aggregate used in each mix. A statistical t-test was performed on the modulus of elasticity

coefficient data in order to determine if there was a statistical difference between the two mixes. The P value of the test between the two mixes was 0.1. This value is greater than 0.05 so the data is statistically equal. In other words, the modulus of elasticity of the two mixes is essentially identical. The measured modulus of elasticity for each specimen of each mix was also plotted against compressive strength for comparison with the ACI recommended relationship. This graph can be seen in **Figure 6.1**.

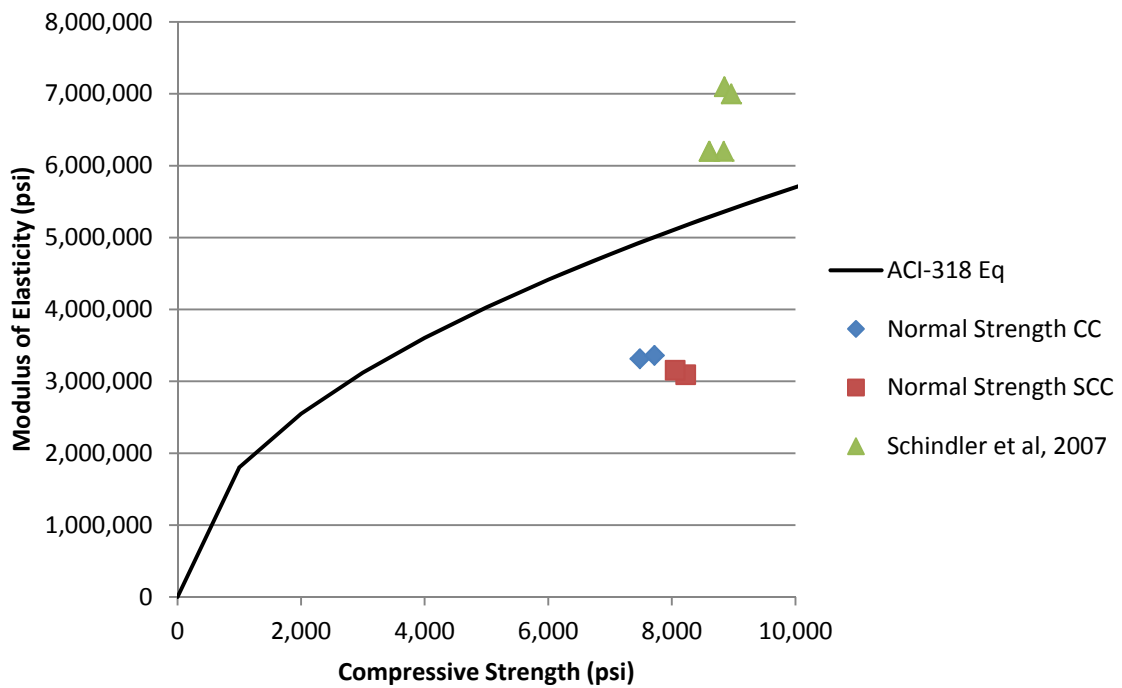


Figure 6.1 – Compressive Strength vs. Modulus of Elasticity

For the modulus of rupture, it can be seen that the C6-58L mix exceeded the ACI coefficient of 7.5 while the S6-48L mix barely fell short. It is important to note, however, that the modulus of rupture is highly variable as the coefficient can vary between 6 and 12 [Neville, 1997]. A statistical t-test was performed on the modulus of rupture coefficient data in order to determine if there was a statistical difference between the two

mixes. The P value of the test between the two mixes was 0.04. This value is less than 0.05 so the data is statistically different. The measured modulus of rupture for each specimen of each mix was also plotted against compressive strength for comparison with the ACI recommended relationship. Also included in the plot for comparison is data from another SCC study completed at Missouri S&T. This graph can be seen in **Figure 6.2**.

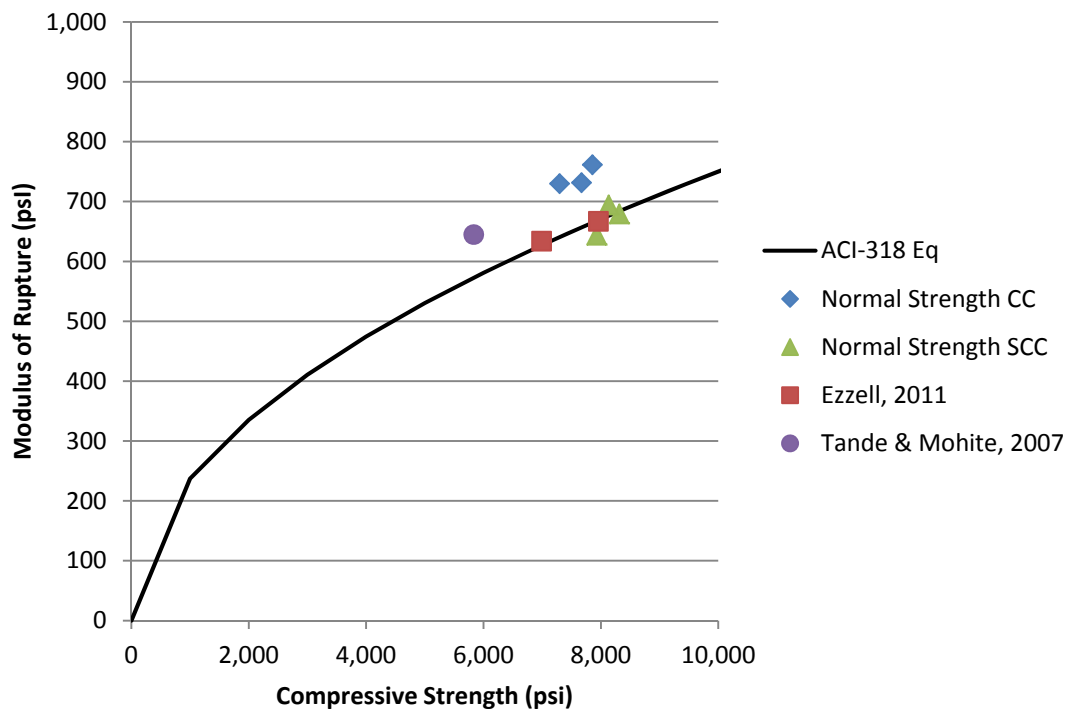


Figure 6.2 – Compressive Strength vs. Modulus of Rupture

For the splitting-tensile strength, the S6-48L mix showed a higher tensile strength than the C6-58L mix. However, both mixes fell short of the ACI coefficient used to estimate the splitting-tensile strength. However, splitting-tensile strength is also highly variable with values ranging from 5 to 9.5 [Oluokun, 1991]. A statistical t-test was performed on the splitting-tensile strength coefficient data in order to determine if there is

a statistical difference between the two mixes. The P value of the t-test between the normal strength mixes was 0.4. Any value greater than 0.05 shows the data is statistically equal. In other words, the splitting-tensile strengths of the two mixes are essential identical. The splitting-tensile strength of the specimens was also plotted against the compressive strength of the concrete. This graph can be seen in **Figure 6.3**.

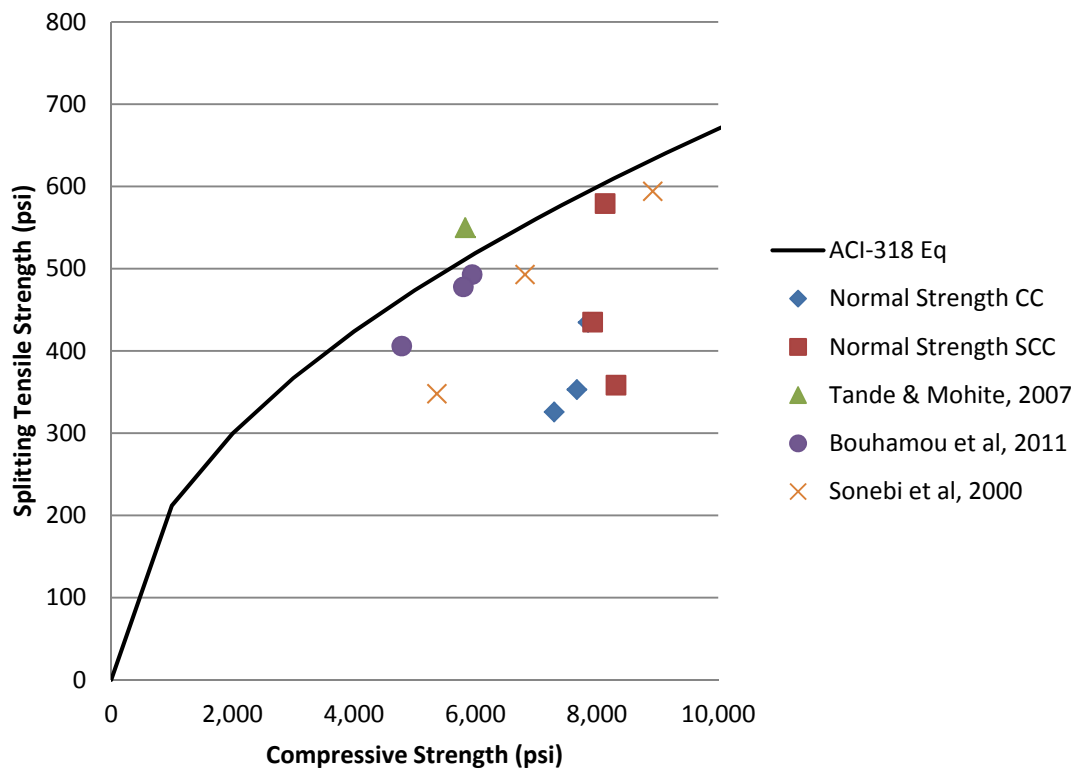


Figure 6.3 – Compressive Strength vs. Splitting-Tensile Strength

The measured modulus of elasticity and modulus of rupture were also compared to the AASHTO LRFD Design equations used to estimate these mechanical properties. These properties were normalized by dividing the measured values by the respective compressive strength and then compared to the AASHTO equations as mentioned in Chapter 5. A summary of these coefficients can be seen in **Table 6.3**.

**Table 6.3 Normalized Mechanical Properties Compared to
Respective AASHTO Coefficients**

	C6-58L	S6-48L	AASHTO Coefficient
Modulus of Elasticity	1,251	1,097	1,820
Modulus of Rupture	0.27	0.23	0.24

It can be observed that these normalized results follow a very similar trend when comparing the results to the ACI coefficients. For example, the C6-58L mix showed a slightly higher coefficient than the AASHTO coefficient while the S6-48L mix showed a slightly lower coefficient than the AASHTO coefficient. This was also seen in the ACI coefficient comparison.

6.1.2. Durability Performance. For resistance to freezing and thawing, both the C6-58L mix and the S6-48L mix did very poorly when compared to the minimum set forth by MoDOT. MoDOT specifies a minimum durability factor of 75, while the conventional and SCC mixes recorded values of 25.5 and 19.9, respectively. Although both mixes performed poorly, the SCC was comparable to the conventional concrete, which leads to the conclusion that the poor freeze-thaw performance was more a function of the particular coarse aggregate used in the mixes (Jefferson City dolomite).

With regard to permeability, both mixes were comparable. For the Rapid Chloride Test (RCT), the lower the total charge passed, the less permeable the concrete. Both concrete mixes fell in the mid-3000 range, with the C6-58L mix being slightly less permeable. The similarity in performance continued in the concrete's resistance to chloride penetration by ponding. After the concrete was analyzed for chloride content at specified depths, it was found that the two mixes performed almost identically. Both

mixes reached the goal of 0.03% chloride content by mass, indicating negligible corrosion risk, at approximately the same depth, 0.7 in. (18 mm). The S6-48L did however show slightly higher chloride contents at the first two depths indicating a slightly higher surface permeability, which is believed to be related to the finishing of the specimens. The ponding test is a relative measure of chloride permeability, and the test indicated that the SCC is comparable to the conventional control mix. The average chloride profile of the two normal strength mixes can be seen in **Figure 6.4**.

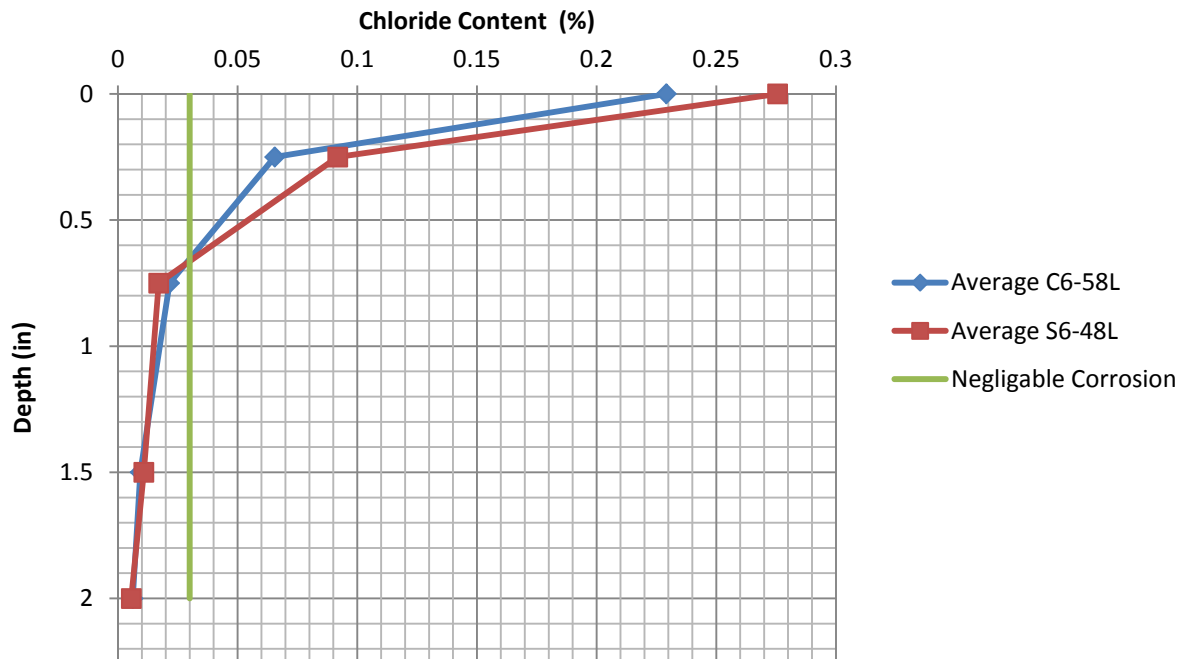


Figure 6.4 – Average Chloride Content vs. Depth of Conventional Mixes
1 in. = 2.54 cm

With regard to concrete resistivity using the Wenner probe, both concrete mixes performed very similarly. The rate at which resistivity increased was almost identical. A trend line for the resistivity was plotted for each mix and the slope for the C6-58L mix

and the S6-48L mix was 0.638 and 0.656, respectively. The results of this test can be seen in **Figure 6.5**. After 24 weeks of testing, each mix reached a resistivity of approximately 28.5 kΩcm. According to Broomfield [2007], any concrete that indicates resistivity over 20 kΩcm is to be classified as having a low rate of corrosion. Both mixes exceeded this benchmark and performed very similarly.

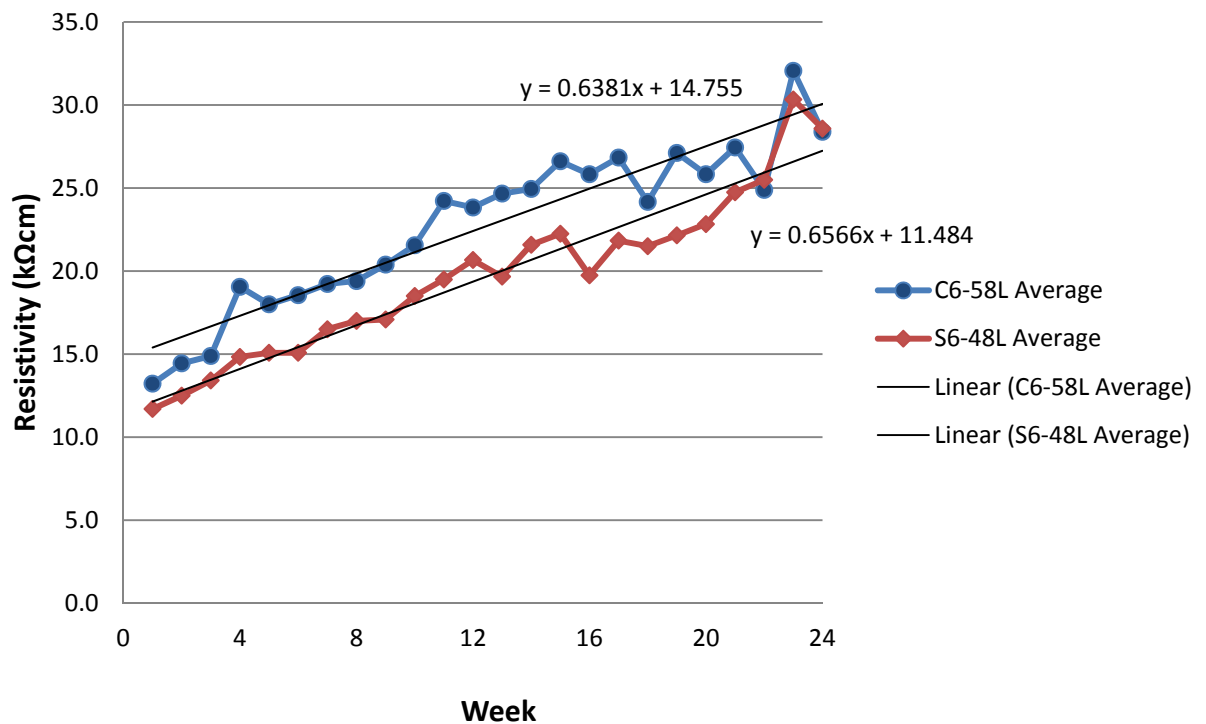


Figure 6.5 – Average Resistivity of Normal Strength Concrete Mixes

6.2. HIGH STRENGTH SCC

As stated in previous sections, both the high strength conventional concrete mix and the high strength SCC mix were subjected to the same mechanical property and durability tests. In this way, it was possible to evaluate the performance of the high strength SCC relative to a benchmark – the conventional high strength concrete mix. If

the high strength SCC mix performed as well or better than the conventional concrete, than it could be reasoned that, due to the time-saving properties of SCC, it would be beneficial to use the SCC in precast applications. The results of the mechanical property and durability tests can be found in Chapter 5. An outline of these results can be seen in **Table 6.4**. As stated in previous chapters, the C10-58L and S10-48L mix design IDs represent the high strength conventional concrete mix and high strength SCC mix, respectively.

Table 6.4 Outline of Results of High Strength Concrete Mixes

Test ID	Mix Design ID	
	C10-58L	S10-48L
28 Day Compressive Strength (psi)	10,823	13,482
Modulus of Elasticity (psi)	3,855,000	3,556,000
Modulus of Rupture (psi)	1,039	1,105
Splitting Tensile (psi)	550	760
Rapid Freezing – Thawing (durability factor)	87.2	45.2
RCT (coulombs)	4,406	2,564
Ponding (Depth at 0.03% Chloride Content, in)	0.2	0.65
Concrete Resistivity (k Ω cm)	38.6	55.7

1 psi = 6.89 kPa

1 in. = 2.54 cm

6.2.1. Mechanical Properties of High Strength Mixes. For compressive strength, both mixes were designed to reach 10,000 psi (68.9 MPa) at 28 days, which both mixes exceeded. The S10-48L exceeded this goal by a much higher margin than the C10-58L mix. The S10-48L mix also showed a much higher early strength gain, while

the later strengths for the two mixes developed at approximately the same rate. This early strength development is very important to precast construction. With the resulting reduction in labor, SCC would be a good candidate for precast plants when just looking at the rate of strength gain. A statistical t-test was performed on the compressive strength data in order to determine if there is any statistical difference between the two mixes. The P value of the t test between the high strength mixes was 0.03. Any value less than 0.05 shows the data is statistically different. In other words, the high strength SCC mix compressive strength exceeded the high strength conventional concrete mix compressive strength.

The modulus of rupture, modulus of elasticity, and splitting-tensile strengths are typically estimated in design using equations based on previous research. These equations were mentioned in Chapter 5. The results of the modulus of rupture, modulus of elasticity, and splitting-tensile strengths were subsequently normalized using the respective compressive strengths of each mix and the resulting coefficients were then compared to recommended values within ACI standards. A summary of these results can be seen in **Table 6.5**.

**Table 6.5 Normalized Mechanical Properties Compared to
Respective ACI Coefficients**

	C10-58L	S10-48L	ACI Coefficient
Modulus of Elasticity	37,070	30,660	57,000
Modulus of Rupture	9.98	9.52	7.5
Splitting-Tensile Strength	5.3	6.5	6.7

Both high strength mixes fell considerably short of the empirical relationship recommended for modulus of elasticity, with the high strength SCC mix performing below the high strength conventional mix. This result means that in the design of concrete structures constructed with these concretes, the modulus of elasticity for either mix would be overestimated. This situation can have negative effects on estimating deflection and serviceability of concrete in the field. However, with both concretes falling at about the same level, it can be stated that both C10-58L and S10-48L are comparable in this area. This fact leads to the conclusion that the low modulus of elasticity is more a function of the particular limestone coarse aggregate used in each mix. A statistical t-test was performed on the modulus of elasticity coefficient data in order to determine if there was any statistical difference between the two mixes. The P value of the t test between the high strength mixes was 0.01. Any value less than 0.05 shows the data is statistically different, which indicates there was some additional decrease in modulus between the high strength conventional concrete and SCC separate from that caused by the aggregate. The modulus of elasticity of each specimen was also plotted against compressive strength for comparison with the ACI recommended relationship. The graph can be seen in **Figure 6.6**.

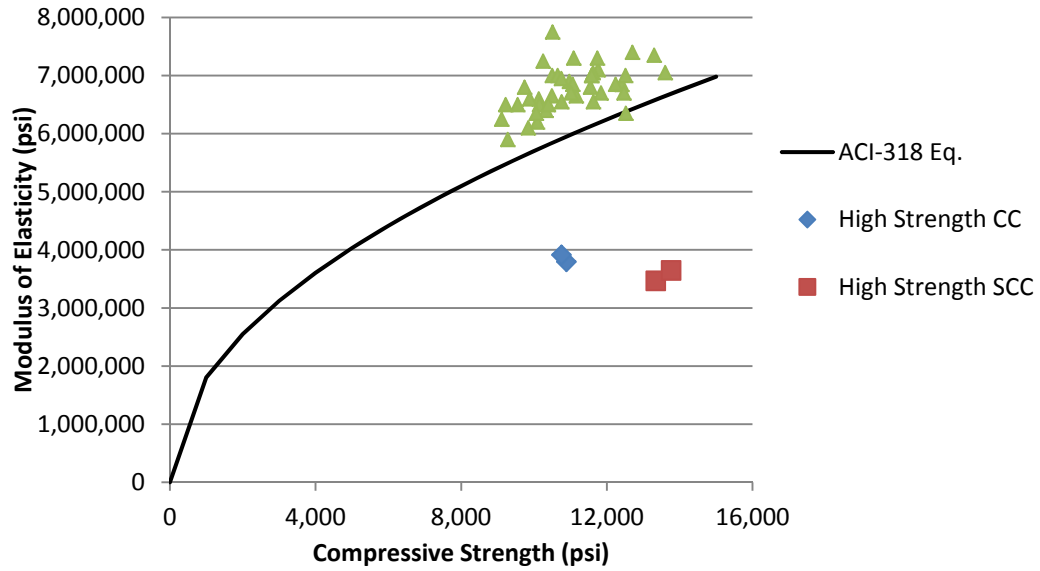


Figure 6.6 - Compressive Strength vs. Modulus of Elasticity

The high strength mixes were also compared to several modulus of elasticity equations found in ACI-363. The equations were developed specifically for high strength concretes. The following equations were used for comparison.

$$E_c = 38,200f_c'^{0.5} + 2,110,000 \quad (6.1)$$

$$E_c = 309,500f_c'^{0.3} \quad (6.2)$$

The results of this comparison can be seen in **Figure 6.7**.

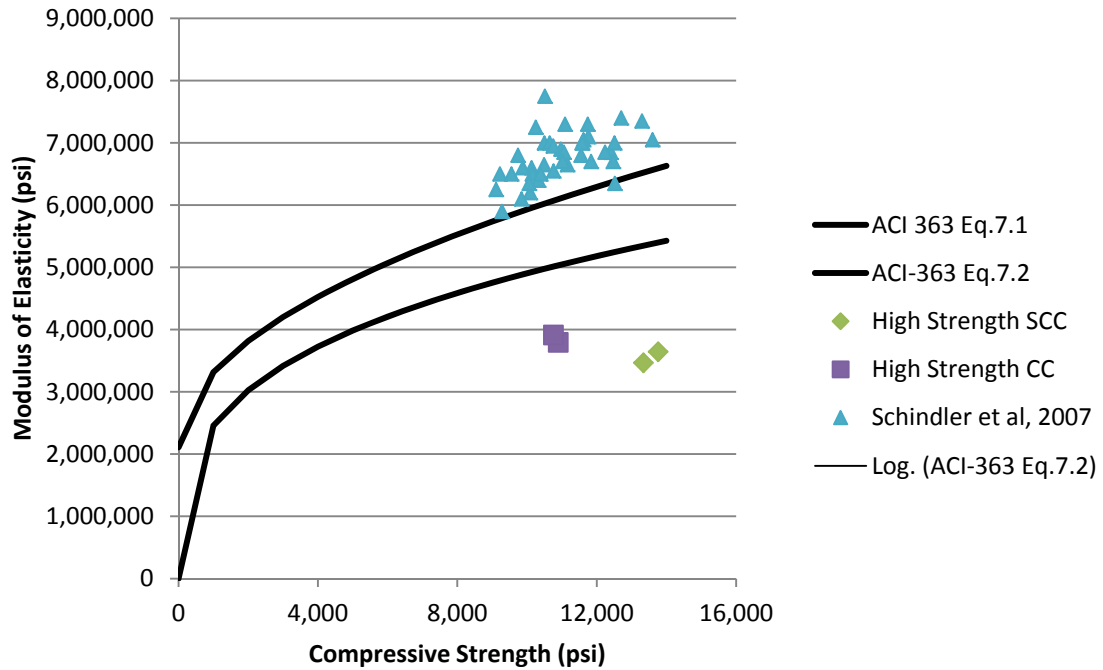


Figure 6.7 – High Strength Mixes Compared to ACI-363 Equations

For the modulus of rupture it can be seen that both mixes exceeded the recommended empirical relationship. It is important to note, however, that the modulus of rupture is highly variable as the coefficient can vary between 6 and 12 [Neville, 1997]. A statistical t-test was performed on the modulus of rupture coefficient data in order to determine if there was any statistical difference between the two mixes. The P value of the t test between the high strength mixes was 0.71. Any value greater than 0.05 shows the data is statistically equal. In other words, the modulus of rupture of the two mixes is essentially identical. The modulus of rupture for each specimen was plotted against the compressive strength for comparison with the ACI recommended relationship. The graph can be seen in **Figure 6.8**.

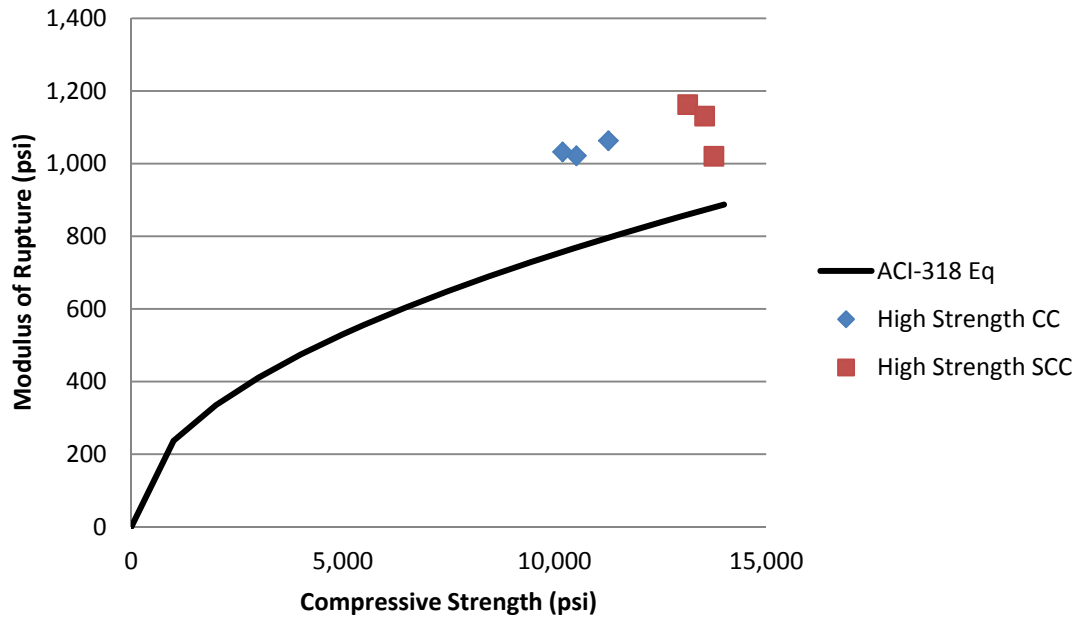


Figure 6.8 – Compressive Strength vs. Modulus of Rupture

For the splitting-tensile strength the S10-48L showed a higher tensile strength than the C10-58L mix. However both mixes fell short of the recommended ACI coefficient for estimating splitting-tensile strength, with the SCC falling very slightly below the recommended value (6.5 vs. 6.7). However, splitting-tensile strength is also highly variable with values ranging from 5 to 9.5 (Oluokun, 1991). A statistical t-test was performed on the splitting-tensile strength coefficient data in order to determine if there is a statistical difference between the two mixes. The P value of the t test between the high strength mixes was 0.12. Any value greater than 0.05 shows the data is statistically equal. In other words, the splitting-tensile strength of the two mixes are essential identical. The splitting-tensile strength of the specimens was also plotted against the compressive strength of concrete for comparison with the ACI recommended relationship. This graph can be seen in **Figure 6.9**.

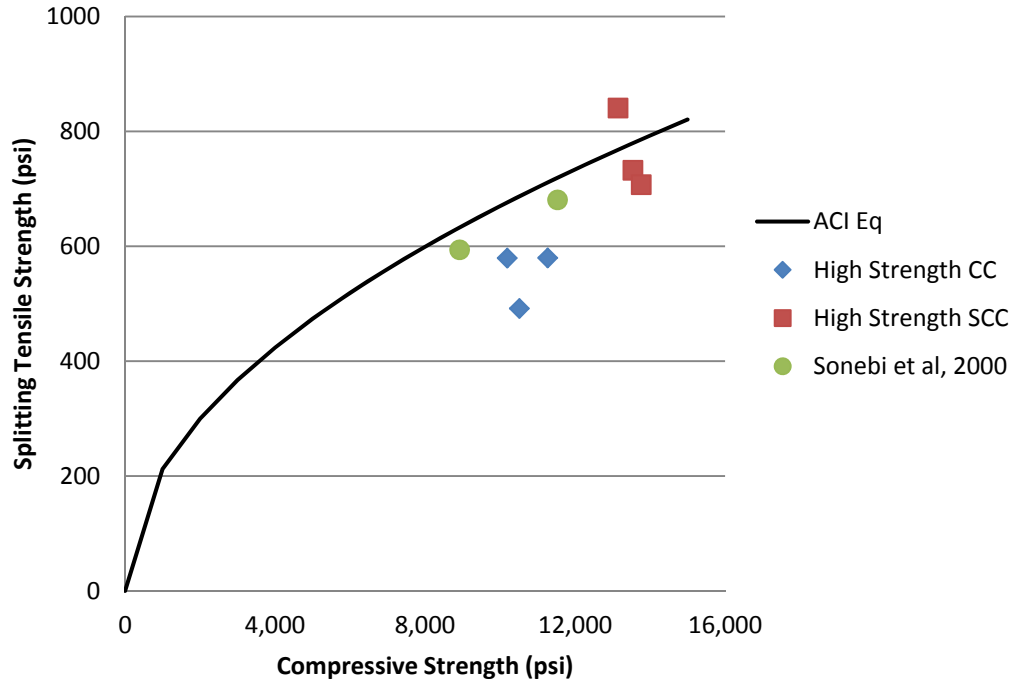


Figure 6.9 – Compressive Strength vs. Splitting-Tensile Strength

The measured modulus of elasticity and modulus of rupture were also compared to the AASHTO LRFD Design equations used to estimate these mechanical properties. These properties were normalized by dividing the measured values by the respective compressive strength and then compared to the AASHTO equations as mentioned in Chapter 5. A summary of these coefficients can be seen in **Table 6.6**.

Table 6.6 Normalized Mechanical Properties Compared to Respective AASHTO Coefficients

	C10-58L	S10-48L	AASHTO Coefficient
Modulus of Elasticity	1,186	987	1,820
Modulus of Rupture	0.32	0.30	0.24

These results also followed a very similar trend as the ACI coefficient comparison. Both the C10-58L mix and the S10-48L mix showed lower values than the AASHTO

coefficient for the modulus of elasticity while both also showed higher values for the modulus of rupture.

6.2.2. Durability Performance of High Strength Mixes. For resistance to freezing and thawing, only the C10-58L mix did well when compared to the minimum set forth by MoDOT. MoDOT specifies a minimum durability factor of 75, and while the high strength conventional mix recorded a value of 87.2, the high strength SCC only recorded a value of 45.2. With the high strength conventional concrete outperforming the high strength SCC it would suggest that the effect of the poor performing coarse aggregate used in this investigation (Jefferson City dolomite) is amplified when using SCC or, alternatively, that the higher paste content reduced the freeze-thaw resistance of the SCC.

With regard to permeability, the S10-48L mix showed a much better performance than the C10-58L mix. For the RCT, the high strength SCC mix was classified as moderate permeability and was close to being classified as low permeability, while the high strength conventional concrete was classified as high permeability. This indicates that the SCC is more resistive to the penetration of chloride ions. This was also observed in the performance for chloride penetration by ponding. The S10-48L mix showed not only a smaller surface chloride content but also reached the goal of 0.03% chloride content at a much shallower depth. The S10-48L mix reached the negligible corrosion level at approximately 0.2 in. (5 mm) while the C10-58L mix reached the same chloride content at approximately 0.65 in (17 mm). The ponding test is a relative measure of chloride permeability, and the test indicated that the high strength SCC performs better than the high strength conventional control mix. This resistance to chloride penetration is

likely due to the tighter microstructure caused by the higher fine aggregate content. This characteristic, along with the high dosage of HRWR, which frees water molecules to hydrate with the Portland cement, creates a denser paste in the concrete. This property is likely what makes the high strength SCC more resistive to chloride penetration. The average chloride profile of the high strength mixes can be seen in **Figure 6.10**.

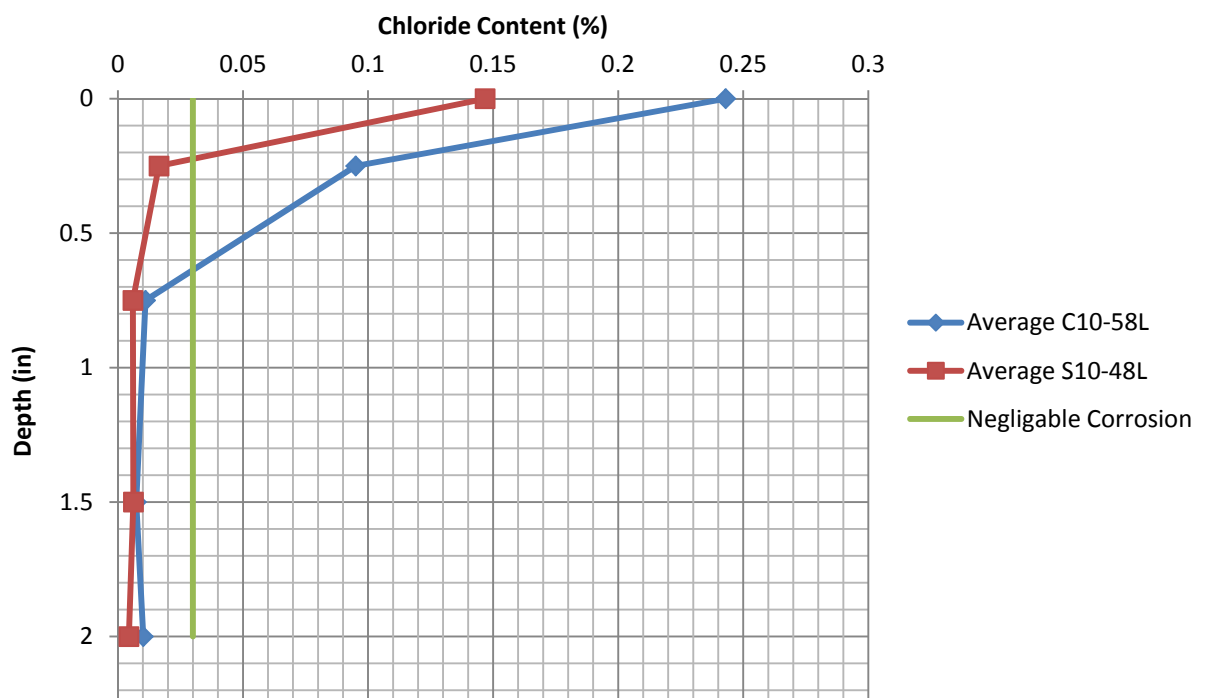


Figure 6.10 – Average Chloride Content vs. Depth of High Strength Mixes
1 in. = 2.54 cm

With regard to concrete resistivity using the Wenner probe, both concrete mixes performed exceptionally well, with the S10-48L showing a higher resistivity than the C10-58L mix. The S10-48L mix showed a higher resistivity at week 1 and also an increased rate of resistivity gain than the C10-58L mix. A trend line for the resistivity

was plotted for each mix, and the slope of the C10-58L and the S10-48L mixes were 1.17 and 1.71, respectively. The results of this test can be seen in **Figure 6.11**. After 24 weeks of testing, the final resistivity for the C10-58L and S10-48L mixes was 38.6 kΩcm and 55.7 kΩcm respectively. According to Broomfield [2007], any concrete with a measured resistivity exceeding 20 kΩcm is to be classified as having a low rate of corrosion. Both concrete mixes exceeded this benchmark with the S10-48L mix far exceeding the value.

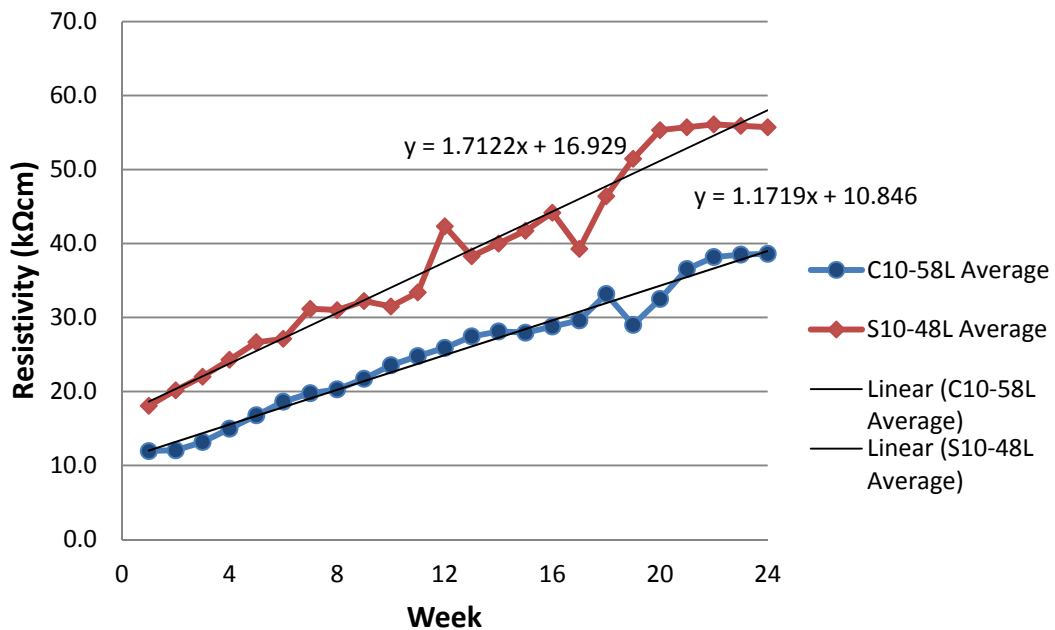


Figure 6.11 – Average Resistivity of High Strength Concrete Mixes

7. FINDINGS, CONCLUSIONS, AND RECOMMENDATIONS

7.1. FINDINGS AND CONCLUSIONS

7.1.1. Normal Strength SCC. The normal strength SCC mix in this investigation outperformed the conventional normal strength concrete in nearly every aspect tested. This finding is important for determining the plausibility of using SCC instead of conventional concrete. The S6-48L mix achieved a higher 28-day compressive strength than the C6-58L mix. With the w/cm ratio being equal, as well as the type of aggregate and cement, it is believed that the high amount of HRWR used to provide SCC with its flowable characteristics accounts for the higher strength. The HRWR allows more water to be effective in the hydration process by dispersion of cement particles. This characteristic in turn hydrates more of the Portland cement, creating a denser overall microstructure, thus improving the compressive strength of the concrete. The S6-48L mix showed a comparable modulus of elasticity to the C6-58L mix. However, both mixes fell below both the recommended ACI-318 coefficient and the AASHTO LRFD design coefficient used to estimate this property. The C6-58L mix showed a higher modulus of rupture when compared to the SCC mix and exceeded the recommended ACI coefficient used to estimate the modulus of rupture. However, in regards of the ACI-318 coefficient, the SCC mix only fell slightly below the recommended value of 7.5. These concretes also showed similar performance when compared to the AASHTO coefficient. Both concrete mixes showed comparable splitting-tensile strength, while both mixes fell below the recommended ACI-318 coefficient used to estimate the splitting-tensile strength.

The S6-48L mix showed very comparable durability behavior and even exceeded the performance of the C6-58L mix in some aspects. Both concretes performed poorly for

resistance to freeze-thaw. This result is most likely due to the aggregate source incorporated into the specimens. Jefferson City Dolomite Limestone from the Rolla quarry is known for its poor durability performance, and resistance to freeze-thaw for concrete is very dependent on the aggregate's performance. Both concrete mixes showed very similar performance with the RCT. This result was further supported by similar performance in the ponding test. While the RCT classified both concrete mixes as moderate permeability, both mixes reached negligible corrosion risk at a relatively shallow depth in the ponding test. Both mixes also performed almost identical in the area of concrete resistivity, indicating a low rate of corrosion.

7.1.2. High Strength SCC. The high strength SCC mix in this investigation outperformed the conventional high strength concrete in nearly every aspect tested. The S10-48L mix achieved a much higher 28-day compressive strength than the C10-58L mix. This increase in strength can most likely be attributed to the high dosage of HRWR used to produce the SCC. The HRWR disperses more cement particles to be effective in the hydration process. This characteristic in turn hydrates more of the Portland cement, creating a denser overall microstructure, thus improving the compressive strength of the concrete. This was also noted in the normal strength SCC mix but not to the degree observed in the high strength investigation. It could be concluded that the HRWR has a larger effect on strength gain at lower w/cm ratios. The HRWR creates a much denser paste. When this aspect is combined with the lower w/cm ratio necessary to achieve high strengths, it appears that SCC will achieve higher compressive strengths than an equivalent conventional concrete mix.

The S10-48L mix showed a lower modulus of elasticity than the C10-58L mix. This is attributed to the decreased amount of coarse aggregate present in the SCC mix. Both of the mixes were considerably lower than the recommended ACI coefficient used to estimate the modulus of elasticity. Both mixes showed comparable modulus of rupture and exceeded the recommended ACI coefficient. Both mixes also showed comparable splitting-tensile strength as well, while both mixes fell short of the recommended ACI coefficient used to estimate this property.

The S10-48L mix significantly outperformed the C10-58L mix in every durability test except resistance to freezing and thawing. During the freeze-thaw test, the S10-48L showed noticeably poorer performance when compared to the C10-58L mix. Neither mix contained an air entraining admixture. It is possible that the C10-58L mix entrapped more air during the mixing process than the S10-48L mix, improving its performance relative to the SCC mix. In all other durability aspects the S10-48L mix showed improved performance compared to the C10-58L mix. In both the RCT and ponding test, the S10-48L mix showed greater resistance to chloride penetration. The C10-58L mix was classified as highly permeable by the RCT while the S10-48L mix was classified as moderate. This classification was further supported by the ponding test. While both mixes performed well, the S10-48L mix achieved negligible corrosion risk at a third of the depth that the C10-58L mix achieved negligible corrosion risk. This increase in performance is most likely due to the denser microstructure achieved by SCC. The S10-48L mix also outperformed the C10-58L mix in concrete resistivity, most likely due to the denser microstructure.

7.2. RECOMMENDATIONS

7.2.1. SCC. After thorough mechanical property and durability testing, it is recommended that SCC be implemented in precast and prestressing applications. With SCC showing comparable results for hardened mechanical properties and slightly higher performance for durability, SCC appears to be a viable option to decrease the cost of labor and time consumption during concrete placement. This performance was observed in both normal and high strength SCC, with high strength SCC performing at a slightly higher margin over high strength conventional concrete than SCC performed over conventional concrete.

APPENDIX A
SCC DURABILITY TEST RESULTS DATA

Table A.1 C6-58L-1R (Weeks 1-7)

Date	6/23/2011	6/30/2011	7/7/2011	7/14/2011	7/21/2011	7/28/2011	8/4/2011
A1	14	15	16	21	19	20	19
A2	13	14	14	18	17	18	18
A3	13	15	15	21	18	19	19
B1	14	16	17	19	20	21	21
B2	12	14	12	18	16	16	19
B3	13	15	15	20	18	18	20
Average	13.2	14.8	14.8	19.5	18.0	18.7	19.3

Table A.2 C6-58L-1R (Weeks 8-14)

Date	8/18/2011	8/25/2011	9/1/2011	9/8/2011	9/15/2011	9/22/2011	9/29/2011
A1	19	21	22	24	25	20	20
A2	18	19	20	23	22	25	18
A3	19	19	19	25	19	27	27
B1	21	23	22	27	22	22	22
B2	18	17	19	24	25	23	24
B3	18	20	24	26	27	27	23
Average	18.8	19.8	21.0	24.8	23.3	24.0	22.3

Table A.3 C6-58L-1R (Weeks 15-21)

Date	10/6/2011	10/13/2011	10/20/2011	10/27/2011	11/3/2011	11/10/2011	11/17/2011
A1	29	36	30	33	25	25	29
A2	27	27	19	29	31	27	25
A3	26	18	29	27	29	21	24
B1	26	23	27	23	25	23	26
B2	26	17	21	22	23	23	25
B3	26	24	31	21	27	25	33
Average	26.7	24.2	26.2	25.8	26.7	24.0	27.0

Table A.4 C6-58L-1R (Weeks 22-24)

Date	11/24/2011	12/1/2011	12/8/2011
A1	27	35	29
A2	26	37	22
A3	25	27	25
B1	22	27	24
B2	24	24	24
B3	22	42	29
Average	24.3	32.0	25.5

Table A.5 C6-58L-2R (Weeks 1-7)

Date	6/23/2011	6/30/2011	7/7/2011	7/14/2011	7/21/2011	7/28/2011	8/4/2011
A1	14	15	16	19	18	20	20
A2	12	13	13	19	19	15	16
A3	14	16	17	21	20	20	21
B1	14	15	16	19	19	20	21
B2	12	12	13	19	15	16	17
B3	14	15	15	21	19	19	20
Average	13.3	14.3	15.0	19.7	18.3	18.3	19.2

Table A.6 C6-58L-2R (Weeks 8-14)

Date	8/18/2011	8/25/2011	9/1/2011	9/8/2011	9/15/2011	9/22/2011	9/29/2011
A1	20	23	24	25	23	29	30
A2	16	18	21	20	19	25	27
A3	25	23	24	27	29	24	31
B1	20	22	24	25	25	25	31
B2	16	19	20	22	22	24	27
B3	20	21	24	27	25	22	22
Average	19.5	21.0	22.8	24.3	23.8	24.8	28.0

Table A.7 C6-58L-2R (Weeks 15-21)

Date	10/6/2011	10/13/2011	10/20/2011	10/27/2011	11/3/2011	11/10/2011	11/17/2011
A1	30	30	32	24	27	28	28
A2	25	26	28	19	22	22	18
A3	31	35	38	30	42	24	40
B1	29	29	30	28	34	28	22
B2	26	26	24	21	27	24	21
B3	26	30	33	22	33	29	30
Average	27.8	29.3	30.8	24.0	30.8	25.8	26.5

Table A.8 C6-58L-2R (Weeks 22-24)

Date	11/24/2011	12/1/2011	12/8/2011
A1	27	34	30
A2	22	30	27
A3	26	44	46
B1	36	35	36
B2	21	25	28
B3	29	27	31
Average	26.8	32.5	33.0

Table A.9 C6-58L-3R (Weeks 1-7)

Date	6/23/2011	6/30/2011	7/7/2011	7/14/2011	7/21/2011	7/28/2011	8/4/2011
A1	14	15	15	19	19	20	20
A2	13	13	14	17	17	17	18
A3	13	14	16	19	18	21	21
B1	14	15	15	19	18	19	20
B2	11	12	13	16	15	16	17
B3	14	16	16	18	19	19	19
Average	13.2	14.2	14.8	18.0	17.7	18.7	19.2

Table A.10 C6-58L-3R (Weeks 8-14)

Date	8/18/2011	8/25/2011	9/1/2011	9/8/2011	9/15/2011	9/22/2011	9/29/2011
A1	20	22	18	26	27	29	24
A2	21	21	22	19	22	25	23
A3	22	22	24	25	22	29	22
B1	19	20	21	26	28	27	29
B2	17	19	21	22	22	17	22
B3	20	18	19	23	25	24	27
Average	19.8	20.3	20.8	23.5	24.3	25.2	24.5

Table A.11 C6-58L-3R (Weeks 15-21)

Date	10/6/2011	10/13/2011	10/20/2011	10/27/2011	11/3/2011	11/10/2011	11/17/2011
A1	24	24	32	25	29	30	36
A2	23	19	19	24	20	22	28
A3	31	35	28	24	30	26	26
B1	25	28	26	26	26	28	25
B2	21	19	16	16	18	23	30
B3	28	19	20	21	20	37	28
Average	25.3	24.0	23.5	22.7	23.8	27.7	28.8

Table A.12 C6-58L-3R (Weeks 22-24)

Date	11/24/2011	12/1/2011	12/8/2011
A1	30	33	26
A2	22	23	24
A3	22	30	28
B1	24	43	29
B2	22	27	20
B3	21	34	33
Average	23.5	31.7	26.7

Table A.13 S6-48L-1R (Weeks 1-7)

Date	7/6/2011	7/13/2011	7/20/2011	7/27/2011	8/3/2011	8/10/2011	8/17/2011
A1	12	12	14	15	16	16	17
A2	12	13	13	14	14	14	15
A3	14	14	16	17	18	18	20
B1	14	14	14	15	16	16	17
B2	11	11	14	15	15	15	15
B3	13	14	16	18	18	18	19
Average	12.7	13.0	14.5	15.7	16.2	16.2	17.2

Table A.14 S6-48L-1R (Weeks 8-14)

Date	8/24/2011	8/31/2011	9/7/2011	9/14/2011	9/21/2011	9/28/2011	10/5/2011
A1	17	18	17	19	20	13	22
A2	17	17	18	19	21	17	21
A3	16	21	21	22	27	22	28
B1	19	19	21	21	22	22	20
B2	18	18	19	19	20	16	21
B3	19	20	22	23	25	25	25
Average	17.7	18.8	19.7	20.5	22.5	19.2	22.8

Table A.15 S6-48L-1R (Weeks 15-21)

Date	10/12/2011	10/19/2011	10/26/2011	11/2/2011	11/9/2011	11/16/2011	11/23/2011
A1	19	23	25	24	24	27	28
A2	20	15	15	25	21	16	28
A3	28	20	24	34	29	27	27
B1	28	24	27	24	22	19	26
B2	22	17	21	21	18	19	24
B3	26	21	27	28	32	27	23
Average	23.8	20.0	23.2	26.0	24.2	22.5	26.0

Table A.16 S6-48L-1R (Weeks 22-24)

Date	11/30/2011	12/7/2011	12/16/2011
A1	24	32	26
A2	31	23	20
A3	40	44	44
B1	26	39	40
B2	21	24	25
B3	30	26	23
Average	28.7	31.3	26.7

Table A.17 S6-48L-2R (Weeks 1-7)

Date	7/6/2011	7/13/2011	7/20/2011	7/27/2011	8/3/2011	8/10/2011	8/17/2011
A1	11	12	13	14	15	15	16
A2	10	11	11	13	11	11	16
A3	12	13	14	16	16	16	17
B1	11	12	12	14	14	14	15
B2	9.4	11	11	13	14	14	15
B3	11	13	13	14	14	14	16
Average	10.7	12.0	12.3	14.0	14.0	14.0	15.8

Table A.18 S6-48L-2R (Weeks 8-14)

Date	8/24/2011	8/31/2011	9/7/2011	9/14/2011	9/21/2011	9/28/2011	10/5/2011
A1	16	16	17	17	18	20	20
A2	14	14	18	19	19	18	19
A3	17	17	19	21	20	22	25
B1	18	15	17	19	20	22	20
B2	16	13	16	15	17	18	18
B3	17	17	17	20	19	21	20
Average	16.3	15.3	17.3	18.5	18.8	20.2	20.3

Table A.19 S6-48L-2R (Weeks 15-21)

Date	10/12/2011	10/19/2011	10/26/2011	11/2/2011	11/9/2011	11/16/2011	11/23/2011
A1	20	17	20	23	26	23	26
A2	19	17	15	17	21	19	22
A3	21	21	25	14	16	25	23
B1	20	25	22	14	17	20	24
B2	20	18	16	16	19	27	20
B3	24	19	25	18	22	25	26
Average	20.7	19.5	20.5	17.0	20.1	23.2	23.5

Table A.20 S6-48L-2R (Weeks 22-24)

Date	11/30/2011	12/7/2011	12/16/2011
A1	22	29	28
A2	21	19	24
A3	18	34	29
B1	19	33	28
B2	29	28	25
B3	25	33	31
Average	22.3	29.3	27.5

Table A.21 C10-58L-1R (Weeks 1-7)

Date	7/22/2011	7/29/2011	8/5/2011	8/12/2011	8/19/2011	8/26/2011	9/2/2011
A1	12	12	12	14	16	18	20
A2	11	11	12	14	17	18	19
A3	12	13	13	14	17	19	20
B1	12	13	14	16	16	19	20
B2	11	11	14	16	16	17	18
B3	12	12	13	15	17	18	20
Average	11.7	12.0	13.0	14.8	16.5	18.2	19.5

Table A.22 C10-58L-1R (Weeks 8-14)

Date	9/9/2011	9/16/2011	9/23/2011	9/30/2011	10/7/2011	10/14/2011	10/21/2011
A1	20	22	23	25	26	23	23
A2	19	21	23	22	25	25	27
A3	22	23	25	26	28	27	31
B1	16	21	20	25	28	18	28
B2	19	19	18	17	23	28	28
B3	21	22	26	21	24	35	29
Average	19.5	21.3	22.5	22.67	25.7	26.0	27.7

Table A.23 C10-58L-1R (Weeks 15-21)

Date	10/28/2011	11/4/2011	11/11/2011	11/18/2011	11/25/2011	12/2/2011	12/9/2011
A1	30	32	34	25	32	29	34
A2	27	30	28	29	25	28	33
A3	29	31	32	31	27	33	42
B1	22	25	32	36	30	27	46
B2	23	26	28	34	22	25	32
B3	25	30	37	37	30	36	27
Average	26.0	28.9	31.8	32.0	27.7	29.7	35.7

Table A.24 C10-58L-1R (Weeks 22-24)

Date	12/16/2011	12/23/2011	12/30/2011
A1	33	32	32
A2	22	24	24
A3	39	41	40
B1	33	34	33
B2	35	35	36
B3	27	28	28
Average	31.5	32.3	32.2

Table A.25 C10-58L-2R (Weeks 1-7)

Date	7/22/2011	7/29/2011	8/5/2011	8/12/2011	8/19/2011	8/26/2011	9/2/2011
A1	12	13	13	15	17	20	18
A2	11	11	11	13	15	16	17
A3	15	12	13	15	16	18	20
B1	12	11	13	16	17	20	20
B2	11	11	12	13	15	17	18
B3	13	12	14	15	18	20	22
Average	12.3	11.7	12.7	14.5	16.3	18.5	19.2

Table A.26 C10-58L-2R (Weeks 8-14)

Date	9/9/2011	9/16/2011	9/23/2011	9/30/2011	10/7/2011	10/14/2011	10/21/2011
A1	21	21	26	26	27	31	30
A2	17	19	21	20	19	27	21
A3	20	23	26	28	27	32	34
B1	20	21	21	25	25	25	28
B2	19	20	24	25	23	26	25
B3	23	24	26	28	29	29	30
Average	20.0	21.3	24	25.33	25.0	28.3	28.0

Table A.27 C10-58L-2R (Weeks 15-21)

Date	10/28/2011	11/4/2011	11/11/2011	11/18/2011	11/25/2011	12/2/2011	12/9/2011
A1	30	29	32	36	27	34	43
A2	23	21	24	26	21	25	28
A3	32	32	29	38	28	34	37
B1	27	25	24	35	35	33	36
B2	26	25	23	25	22	28	31
B3	32	31	23	41	26	33	35
Average	28.3	27.1	25.8	33.5	26.5	31.2	35.0

Table A.28 C10-58L-2R (Weeks 22-24)

Date	12/16/2011	12/23/2011	12/30/2011
A1	56	56	57
A2	27	28	27
A3	48	47	48
B1	40	42	42
B2	36	37	38
B3	37	38	38
Average	40.7	41.3	41.6

Table A.29 C10-58L-3R (Weeks 1-7)

Date	7/22/2011	7/29/2011	8/5/2011	8/12/2011	8/19/2011	8/26/2011	9/2/2011
A1	12	12	13	15	17	18	19
A2	11	12	13	16	17	20	20
A3	12	13	15	17	17	18	21
B1	12	13	14	15	18	19	22
B2	11	12	13	15	17	19	19
B3	13	13	15	16	19	21	23
Average	11.8	12.5	13.8	15.7	17.5	19.2	20.7

Table A.30 C10-58L-3R (Weeks 8-14)

Date	9/9/2011	9/16/2011	9/23/2011	9/30/2011	10/7/2011	10/14/2011	10/21/2011
A1	19	22	25	26	25	27	27
A2	22	22	24	27	24	27	28
A3	22	23	26	27	30	29	31
B1	20	22	24	25	27	28	28
B2	21	21	23	25	27	26	26
B3	24	25	23	28	29	31	32
Average	21.3	22.5	24.2	26.33	27.0	28.0	28.7

Table A.31 C10-58L-3R (Weeks 15-21)

Date	10/28/2011	11/4/2011	11/11/2011	11/18/2011	11/25/2011	12/2/2011	12/9/2011
A1	31	31	31	34	32	30	40
A2	30	32	30	32	24	37	36
A3	31	31	30	35	29	37	42
B1	28	30	31	36	37	40	39
B2	23	26	32	33	36	34	35
B3	34	32	33	34	39	42	42
Average	29.5	30.3	31.2	34.0	32.8	36.7	39.0

Table A.32 C10-58L-3R (Weeks 22-24)

Date	12/16/2011	12/23/2011	12/30/2011
A1	43	44	43
A2	38	39	41
A3	46	45	46
B1	41	42	41
B2	39	41	42
B3	47	48	48
Average	42.3	43.2	43.5

Table A.33 S10-48L-1R (Weeks 1-7)

Date	8/5/2011	8/12/2011	8/19/2011	8/26/2011	9/2/2011	9/9/2011	9/16/2011
A1	20	23	25	28	31	32	35
A2	18	20	22	25	28	30	33
A3	19	21	24	26	30	30	28
B1	18	19	21	25	28	24	28
B2	17	18	20	21	20	27	25
B3	20	22	25	27	30	23	34
Average	18.7	20.5	22.8	25.3	27.8	27.7	30.5

Table A.34 S10-48L-1R (Weeks 8-14)

Date	9/23/2011	9/30/2011	10/7/2011	10/14/2011	10/21/2011	10/28/2011	11/4/2011
A1	37	41	41	44	49	45	45
A2	32	38	38	41	42	44	43
A3	28	34	36	35	50	48	48
B1	35	30	24	32	51	45	44
B2	28	26	22	27	42	38	39
B3	30	34	28	31	48	42	44
Average	31.7	33.8	31.5	35.0	47.0	43.7	43.8

Table A.35 S10-48L-1R (Weeks 15-21)

Date	11/11/2011	11/18/2011	11/25/2011	12/2/2011	12/9/2011	12/16/2011	12/23/2011
A1	49	60	61	56	74	69	70
A2	34	40	38	44	58	61	60
A3	41	42	47	60	46	62	63
B1	51	44	40	55	52	59	60
B2	38	42	35	45	45	48	49
B3	51	46	38	60	64	70	71
Average	44.0	45.7	43.2	53.3	56.5	61.5	62.2

Table A.36 S10-48L-1R (Weeks 22-24)

Date	12/30/2011	1/6/2012	1/13/2012
A1	69	68	65
A2	61	61	54
A3	61	59	69
B1	58	57	54
B2	49	49	59
B3	68	67	54
Average	61.0	60.2	59.2

Table A.37 S10-48L-2R (Weeks 1-7)

Date	8/5/2011	8/12/2011	8/19/2011	8/26/2011	9/2/2011	9/9/2011	9/16/2011
A1	20	22	24	20	29	32	35
A2	18	19	21	23	23	25	30
A3	22	24	27	29	32	25	35
B1	20	23	25	29	30	30	35
B2	16	18	20	22	25	21	29
B3	18	21	22	26	28	29	33
Average	19.0	21.2	23.2	24.8	27.8	27.0	32.8

Table A.38 S10-48L-2R (Weeks 8-14)

Date	9/23/2011	9/30/2011	10/7/2011	10/14/2011	10/21/2011	10/28/2011	11/4/2011
A1	37	29	27	29	43	30	35
A2	27	32	34	31	40	32	34
A3	32	37	36	31	41	34	38
B1	29	33	27	27	39	36	39
B2	26	27	24	27	38	29	34
B3	30	27	29	32	37	36	38
Average	30.2	30.8	29.5	29.5	39.7	32.8	36.3

Table A.39 S10-48L-2R (Weeks 15-21)

Date	11/11/2011	11/18/2011	11/25/2011	12/2/2011	12/9/2011	12/16/2011	12/23/2011
A1	49	42	42	44	45	50	52
A2	38	36	32	38	37	44	45
A3	46	41	37	40	43	47	49
B1	38	45	38	48	47	55	56
B2	33	35	37	36	40	47	48
B3	34	45	35	46	45	58	59
Average	39.7	40.7	36.8	42.0	42.8	50.2	51.5

Table A.40 S10-48L-2R (Weeks 22-24)

Date	12/30/2011	1/6/2012	1/13/2012
A1	53	57	62
A2	47	49	50
A3	48	56	72
B1	57	54	51
B2	48	50	52
B3	61	54	50
Average	52.3	53.3	56.2

Table A.41 S10-48L-3R (Weeks 1-7)

Date	8/5/2011	8/12/2011	8/19/2011	8/26/2011	9/2/2011	9/9/2011	9/16/2011
A1	17	20	22	24	27	29	31
A2	16	17	19	21	22	25	28
A3	18	20	21	23	26	27	29
B1	16	20	20	21	24	27	32
B2	15	16	18	22	22	24	29
B3	17	20	20	25	25	28	32
Average	16.5	18.8	20.0	22.7	24.3	26.7	30.2

Table A.42 S10-48L-3R (Weeks 8-14)

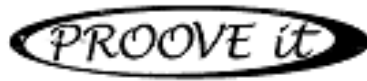
Date	9/23/2011	9/30/2011	10/7/2011	10/14/2011	10/21/2011	10/28/2011	11/4/2011
A1	34	35	36	39	42	43	44
A2	29	30	30	33	36	36	37
A3	32	33	31	36	42	34	34
B1	31	33	36	35	41	38	39
B2	28	27	31	32	37	39	40
B3	33	34	37	39	44	40	45
Average	31.2	32.0	33.5	35.7	24.3	38.3	39.9

Table A.43 S10-48L-3R (Weeks 15-21)

Date	11/11/2011	11/18/2011	11/25/2011	12/2/2011	12/9/2011	12/16/2011	12/30/2011
A1	49	51	49	52	52	57	58
A2	41	47	34	44	52	50	51
A3	41	40	39	39	47	58	56
B1	45	46	37	49	66	42	47
B2	36	35	33	35	53	58	54
B3	37	58	35	44	60	61	62
Average	41.5	46.2	37.8	43.8	55.0	54.3	54.6

Table A.44 S10-48L-3R (Weeks 22-24)

Date	12/30/2011	1/6/2012	1/13/2012
A1	56	53	51
A2	50	52	55
A3	54	52	52
B1	48	50	52
B2	52	46	44
B3	59	58	57
Average	53.2	51.8	51.8



ASTM C 1202-97



Test-compagny
Testing street 45
Compagny City
Some Country

Your own logo
Here



GERMAN INSTRUMENTS

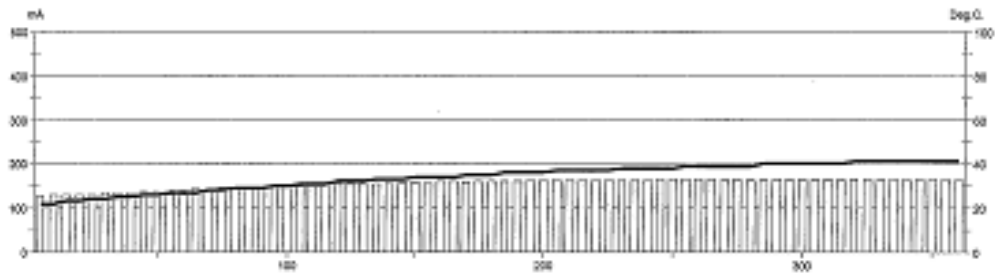
ASTM C 1202-97

ASTM C 1202-97

ASTM C 1202-97

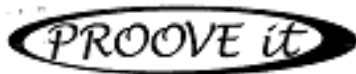
Test report

Voltage Used: 60
 Testing time: 06:00 hour
 Charge passed: 3352
 Adjusted Charge passed: 3025
 Permeability class: Moderate
 Instrument number: 071401
 Channel number: 1
 Report date: 8/10/2011
 Testing by: ZH/LG/TP
 Reference: EC-A1-28 DAY TEST-TOP LIFT
 Sample diameter: 100
 Comment: CALLED SET A



Time	°C	mA									
00:05	22	126.5	01:35	30	147.8	03:05	36	160.2	04:35	39	164.5
00:10	22	128.5	01:40	30	149.8	03:10	36	161.1	04:40	39	164.0
00:15	23	128.7	01:45	31	149.7	03:15	36	162.3	04:45	40	164.2
00:20	23	129.9	01:50	31	153.0	03:20	36	162.3	04:50	40	165.0
00:25	24	130.5	01:55	31	153.4	03:25	37	162.7	04:55	40	165.5
00:30	24	133.6	02:00	32	153.6	03:30	37	163.0	05:00	40	164.5
00:35	25	134.3	02:05	32	153.0	03:35	37	163.3	05:05	40	164.9
00:40	25	134.7	02:10	32	153.9	03:40	37	163.0	05:10	40	165.1
00:45	26	135.9	02:15	33	155.1	03:45	37	164.3	05:15	40	164.4
00:50	26	137.1	02:20	33	156.7	03:50	38	163.2	05:20	41	164.4
00:55	27	138.8	02:25	33	158.2	03:55	38	163.5	05:25	41	164.6
01:00	27	139.1	02:30	34	158.0	04:00	38	163.6	05:30	41	165.3
01:05	27	141.8	02:35	34	157.0	04:05	38	164.1	05:35	41	165.3
01:10	28	143.7	02:40	34	159.9	04:10	38	164.7	05:40	41	165.1
01:15	28	144.4	02:45	34	159.9	04:15	39	165.2	05:45	41	165.2
01:20	29	144.7	02:50	35	158.9	04:20	39	164.2	05:50	41	165.3
01:25	29	146.4	02:55	35	161.2	04:25	39	165.0	05:55	41	165.8
01:30	29	147.6	03:00	35	161.1	04:30	39	164.5	06:00	41	164.6

Figure A.1 – C6-58L-EC1TOP RCT Data



ASTM C 1202-97



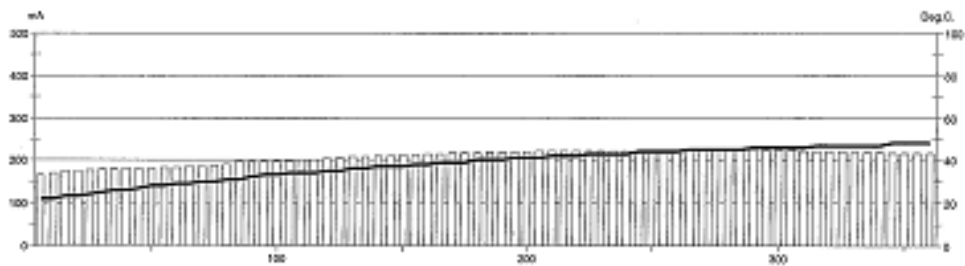
Test-company
Testing street 45
CompanyCity
Some Country



CEMEX
P.O. Box 1000
Tel: +31 20 231 2000
Fax: +31 20 231 2001
USA
P.O. Box 1000
Tel: +1 202 488 4888

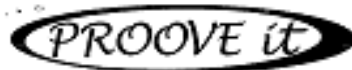
Test report

Voltage Used: 60
Testing time: 06:00 hour
Charge passed: 4488
Adjusted Charge passed: 4050
Permeability class: High
Instrument number: 071401
Channel number: 2
Report date: 8/10/2011
Testing by: LG/ZH/TP
Reference: EC-A1-28 DAY TEST-TOP LIFT
Sample diameter: 100
Comment: THIS SET IS CALLED SET B



Time	°C	mA									
00:05	22	165.9	01:35	33	195.4	03:05	40	218.0	04:35	45	224.6
00:10	22	170.5	01:40	33	196.2	03:10	40	218.3	04:40	45	224.5
00:15	23	173.0	01:45	34	198.7	03:15	41	218.9	04:45	45	224.3
00:20	23	175.1	01:50	34	200.7	03:20	41	219.6	04:50	46	224.4
00:25	24	176.7	01:55	34	202.0	03:25	41	220.1	04:55	46	224.0
00:30	25	178.0	02:00	35	203.3	03:30	42	220.5	05:00	46	222.9
00:35	26	179.1	02:05	35	204.6	03:35	42	220.8	05:05	46	222.8
00:40	26	180.0	02:10	36	206.5	03:40	42	221.0	05:10	46	221.7
00:45	27	180.7	02:15	36	207.8	03:45	43	221.1	05:15	47	221.4
00:50	28	181.8	02:20	37	209.6	03:50	43	221.2	05:20	47	221.1
00:55	28	182.8	02:25	37	210.9	03:55	43	221.2	05:25	47	220.4
01:00	29	184.0	02:30	37	211.8	04:00	43	221.3	05:30	47	219.8
01:05	29	185.1	02:35	38	212.7	04:05	44	221.1	05:35	47	219.0
01:10	30	185.7	02:40	38	213.7	04:10	44	221.1	05:40	47	218.3
01:15	30	186.5	02:45	39	215.3	04:15	44	220.8	05:45	48	217.6
01:20	31	189.7	02:50	39	215.9	04:20	44	221.9	05:50	48	216.9
01:25	31	196.8	02:55	39	216.4	04:25	45	224.7	05:55	48	216.7
01:30	32	196.1	03:00	40	217.5	04:30	45	224.8	06:00	48	217.2

Figure A.3 – C6-58L-EC2TOP RCT Data



ASTM C 1202-97



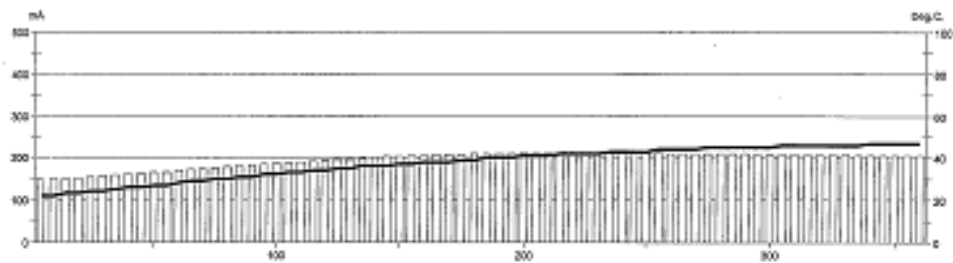
Test-compagny
Testing street 45
Compagny City
Some Country



GERMAN INSTRUMENTS
Phone: +49 201 7171
Fax: +49 201 7171
E-Mail: info@german-instruments.de
www.german-instruments.de

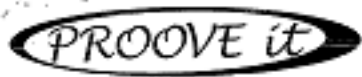
Test report

Voltage Used: 60
 Testing time: 06:00 hour
 Charge passed: 4222
 Adjusted Charge passed: 3810
 Permeability class: Moderate
 Instrument number: 071401
 Channel number: 4
 Report date: 8/16/2011
 Testing by: LG/ZH/TP
 Reference: EC-A1-28 DAY TEST-MIDDLE LIFT
 Sample diameter: 100
 Comment: CALLED SET B



Time	°C	mA									
00:05	22	146.9	01:35	32	184.9	03:05	40	210.3	04:35	45	210.4
00:10	22	148.8	01:40	32	186.6	03:10	40	210.1	04:40	45	209.7
00:15	23	149.8	01:45	33	188.5	03:15	40	210.8	04:45	45	209.4
00:20	23	151.4	01:50	33	190.7	03:20	41	211.2	04:50	45	209.1
00:25	24	155.1	01:55	34	192.4	03:25	41	211.8	04:55	45	208.6
00:30	24	157.2	02:00	34	193.7	03:30	41	211.8	05:00	45	208.7
00:35	25	159.3	02:05	35	195.8	03:35	42	211.8	05:05	46	207.9
00:40	26	161.7	02:10	35	197.2	03:40	42	212.2	05:10	46	207.5
00:45	26	163.5	02:15	36	199.3	03:45	42	212.0	05:15	46	207.2
00:50	27	165.2	02:20	36	200.3	03:50	42	212.1	05:20	46	207.1
00:55	27	166.2	02:25	36	202.3	03:55	43	211.9	05:25	46	206.8
01:00	28	169.6	02:30	37	203.2	04:00	43	212.0	05:30	46	206.5
01:05	29	172.1	02:35	37	204.5	04:05	43	211.7	05:35	46	206.1
01:10	29	173.6	02:40	38	205.6	04:10	43	211.7	05:40	47	206.0
01:15	30	175.9	02:45	38	206.6	04:15	44	211.2	05:45	47	205.9
01:20	30	179.0	02:50	38	208.0	04:20	44	210.9	05:50	47	205.7
01:25	31	180.4	02:55	39	208.1	04:25	44	210.7	05:55	47	205.6
01:30	31	183.5	03:00	39	209.3	04:30	44	210.8	06:00	47	204.9

Figure A.4 – C6-58L-EC2MIDDLE RCT Data



ASTM C 1202-97



Test-company
Testing street 45
CompanyCity
Some Country

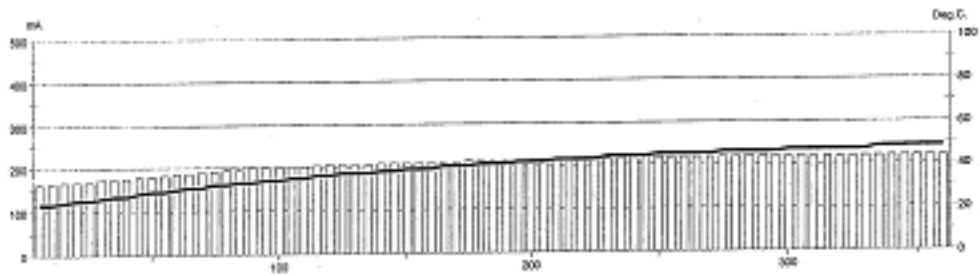
Vertical text on the right side of the TEST CO. logo.



Vertical text on the right side of the arrow logo.

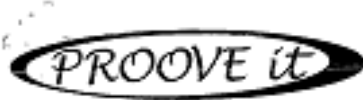
Test report

Voltage Used: 60
 Testing time: 06:00 hour
 Charge passed: 4421
 Adjusted Charge passed: 3990
 Permeability class: Moderate
 Instrument number: 071401
 Channel number: 5
 Report date: 6/29/2011
 Testing by: breeds
 Reference: SCC-EC1-Top 28 day
 Sample diameter: 100
 Comment: UMR Study



Time	°C	mA									
00:05	23	163.2	01:35	34	198.0	03:05	41	212.2	04:35	46	217.7
00:10	23	165.5	01:40	34	200.1	03:10	41	212.1	04:40	46	217.9
00:15	24	166.5	01:45	35	201.4	03:15	42	213.1	04:45	46	217.8
00:20	25	166.7	01:50	35	202.0	03:20	42	212.9	04:50	46	218.4
00:25	25	166.9	01:55	36	203.1	03:25	42	213.9	04:55	46	217.8
00:30	26	173.2	02:00	36	204.3	03:30	43	214.0	05:00	47	217.3
00:35	27	173.2	02:05	37	205.1	03:35	43	214.8	05:05	47	217.7
00:40	27	175.8	02:10	37	206.4	03:40	43	214.5	05:10	47	216.9
00:45	28	177.8	02:15	37	206.1	03:45	43	215.1	05:15	47	217.6
00:50	29	180.4	02:20	38	207.2	03:50	44	215.4	05:20	47	217.5
00:55	29	183.1	02:25	38	207.2	03:55	44	215.7	05:25	47	217.0
01:00	30	185.0	02:30	39	207.7	04:00	44	216.4	05:30	47	218.1
01:05	31	187.8	02:35	39	208.0	04:05	44	216.7	05:35	48	218.6
01:10	31	189.6	02:40	39	208.5	04:10	45	216.6	05:40	48	218.5
01:15	32	192.6	02:45	40	209.2	04:15	45	217.3	05:45	48	218.3
01:20	32	194.0	02:50	40	209.6	04:20	45	217.0	05:50	48	217.9
01:25	33	195.1	02:55	40	211.6	04:25	45	217.2	05:55	48	218.0
01:30	33	199.5	03:00	41	211.5	04:30	45	217.3	06:00	48	218.2

Figure A.5 – S6-48L-EC1TOP RCT Data



ASTM C 1202-97



Test-compagnay
Testing street 45
CompagnyCity
Some Country

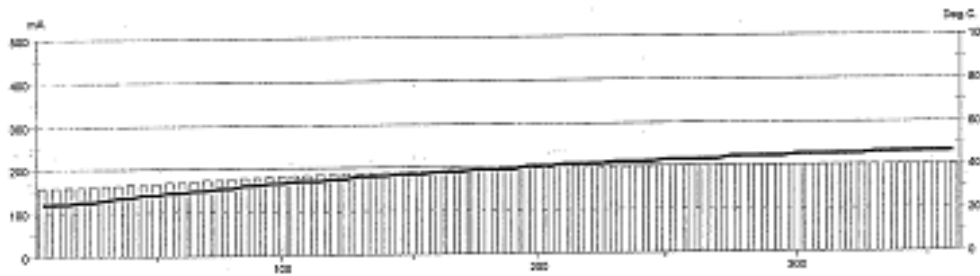
Vertical logo text



Small text block with contact information

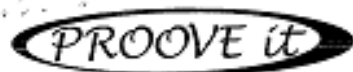
Test report

Voltage Used: 60
 Testing time: 06:00 hour
 Charge passed: 4079
 Adjusted Charge passed: 3681
 Permeability class: Moderate
 Instrument number: 071401
 Channel number: 6
 Report date: 6/29/2011
 Testing by: breeds
 Reference: SCC-EC1-Middle 28 day
 Sample diameter: 100
 Comment: UMR Study



Time	°C	mA									
00:05	24	157.4	01:35	33	180.4	03:05	39	195.8	04:35	44	200.7
00:10	24	159.3	01:40	33	181.3	03:10	39	196.0	04:40	44	201.0
00:15	24	159.5	01:45	34	182.4	03:15	40	196.6	04:45	44	201.2
00:20	25	158.8	01:50	34	183.6	03:20	40	197.0	04:50	44	201.6
00:25	25	160.4	01:55	34	184.5	03:25	40	197.4	04:55	44	201.7
00:30	26	162.0	02:00	35	185.5	03:30	41	197.7	05:00	45	201.3
00:35	27	163.7	02:05	35	186.6	03:35	41	198.1	05:05	45	201.9
00:40	27	165.1	02:10	36	187.4	03:40	41	198.6	05:10	45	201.5
00:45	28	166.2	02:15	36	188.4	03:45	41	198.6	05:15	45	201.2
00:50	28	167.2	02:20	36	189.3	03:50	42	198.9	05:20	45	201.9
00:55	29	169.2	02:25	37	190.0	03:55	42	199.1	05:25	45	201.2
01:00	29	170.5	02:30	37	190.8	04:00	42	199.4	05:30	46	200.9
01:05	30	172.3	02:35	37	191.5	04:05	42	199.7	05:35	46	200.8
01:10	30	173.5	02:40	38	192.5	04:10	43	200.4	05:40	46	201.2
01:15	31	175.1	02:45	38	193.1	04:15	43	199.8	05:45	46	200.5
01:20	31	176.5	02:50	38	193.7	04:20	43	200.0	05:50	46	200.4
01:25	32	177.6	02:55	39	194.5	04:25	43	200.1	05:55	46	200.4
01:30	32	178.8	03:00	39	195.2	04:30	43	200.2	06:00	46	200.5

Figure A.6 – S6-48L-EC1MIDDLE RCT Data



ASTM C 1202-97



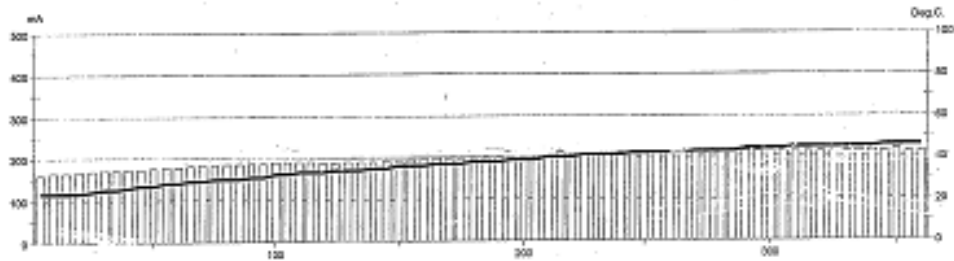
Test-company
Testing street 45
CompanyCity
Some Country



STANDARD INSURANCE
PROPERTY
FIRE & MARINE
INSURANCE CO. LTD.
100
PRINCE GEORGE
STREET
TORONTO, ONTARIO
M5H 1A5
CANADA
TEL: (416) 593-8888
FAX: (416) 593-8889

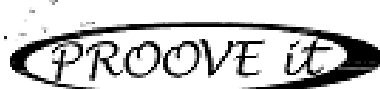
Test report

Voltage Used: 60
Testing time: 05:00 hour
Charge passed: 4262
Adjusted Charge passed: 3846
Permeability class: Moderate
Instrument number: (7190)
Channel number: 7
Report date: 6/28/2011
Testing by: broods
Reference: SCC-EC2-Top 28 day
Sample diameter: 100
Comment: UMR Study



Time	°C	mA									
00:05	23	160.8	01:35	31	188.0	03:05	38	199.0	04:35	43	212.6
00:10	23	164.3	01:40	32	188.7	03:10	38	200.7	04:40	43	214.5
00:15	23	166.1	01:45	32	189.0	03:15	39	201.0	04:45	43	213.2
00:20	23	167.8	01:50	33	189.0	03:20	39	201.6	04:50	44	213.7
00:25	24	169.7	01:55	33	188.8	03:25	39	203.2	04:55	44	213.6
00:30	25	171.3	02:00	33	188.2	03:30	40	204.0	05:00	44	216.1
00:35	25	172.5	02:05	34	188.4	03:35	40	211.1	05:05	44	214.6
00:40	26	173.3	02:10	34	189.3	03:40	40	208.3	05:10	45	214.4
00:45	27	175.0	02:15	34	190.6	03:45	41	205.6	05:15	45	214.0
00:50	27	176.7	02:20	35	190.7	03:50	41	205.2	05:20	45	214.3
00:55	28	178.2	02:25	35	192.3	03:55	41	207.6	05:25	45	215.3
01:00	28	179.6	02:30	36	192.0	04:00	41	211.3	05:30	45	214.4
01:05	29	181.1	02:35	36	193.1	04:05	42	208.2	05:35	45	217.3
01:10	29	182.6	02:40	36	195.9	04:10	42	208.6	05:40	45	217.0
01:15	30	183.9	02:45	37	198.8	04:15	42	210.1	05:45	46	215.0
01:20	30	185.1	02:50	37	197.0	04:20	42	209.5	05:50	46	217.7
01:25	30	186.2	02:55	37	197.0	04:25	42	214.3	05:55	46	214.9
01:30	31	187.2	03:00	38	198.8	04:30	43	212.5	06:00	46	214.6

Figure A.7 – S6-48L-EC2TOP RCT Data



ASTM C 1202-97



Test-company
Testing street 45
Company City
Some Country

Your contact
department



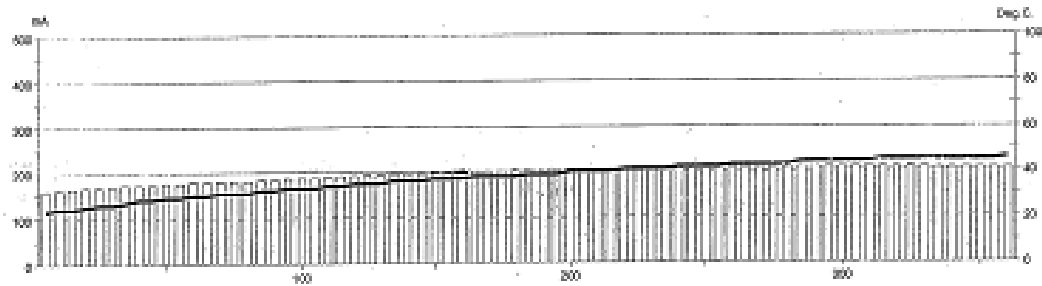
CLEARLY DEFINED

RESEARCH
PRODUCTS
FOR CONSTRUCTION

100
Years of
Service
to the Industry

Test report

Voltage Used: 60
 Testing time: 06:00 hour
 Charge passed: 4224
 Adjusted Charge passed: 3812
 Permeability class: Moderate
 Instrument number: 071401
 Channel number: 8
 Report date: 6/29/2011
 Testing by: broeds
 Reference: SCC-EC2-Middle 28 day
 Sample diameter: 100
 Comment: UMR Study



Time	°C	mA									
00:05	23	161.1	01:05	33	186.6	03:05	39	203.6	04:05	43	207.0
00:10	24	163.9	01:40	33	188.1	03:10	39	203.8	04:40	43	207.2
00:15	24	165.3	01:45	33	188.4	03:15	39	204.2	04:45	44	207.0
00:20	25	168.8	01:50	34	190.0	03:20	40	205.2	04:50	44	207.2
00:25	26	168.3	01:55	34	191.2	03:25	40	204.7	04:55	44	207.6
00:30	26	169.8	02:00	35	192.3	03:30	40	205.1	05:00	44	207.8
00:35	27	171.2	02:05	35	194.0	03:35	40	205.6	05:05	44	208.3
00:40	28	172.3	02:10	35	194.5	03:40	41	206.0	05:10	44	208.1
00:45	28	174.1	02:15	36	196.1	03:45	41	206.1	05:15	45	207.6
00:50	29	175.7	02:20	36	196.5	03:50	41	206.9	05:20	45	207.3
00:55	29	177.1	02:25	36	197.5	03:55	41	206.6	05:25	45	206.7
01:00	30	178.4	02:30	37	199.3	04:00	42	206.1	05:30	45	206.7
01:05	30	179.6	02:35	37	199.5	04:05	42	206.3	05:35	45	206.3
01:10	31	180.4	02:40	37	199.9	04:10	42	206.5	05:40	45	205.8
01:15	31	180.9	02:45	38	200.6	04:15	42	206.5	05:45	45	205.4
01:20	31	181.7	02:50	38	201.9	04:20	43	206.6	05:50	45	205.0
01:25	32	183.6	02:55	38	201.7	04:25	43	206.8	05:55	45	204.6
01:30	32	185.0	03:00	38	202.2	04:30	43	207.0	06:00	46	204.4

Figure A.8 – S6-48L-EC2MIDDLE RCT Data



ASTM C 1202-97



Test-compagny
Testing street 45
CompagnyCity
Some Country

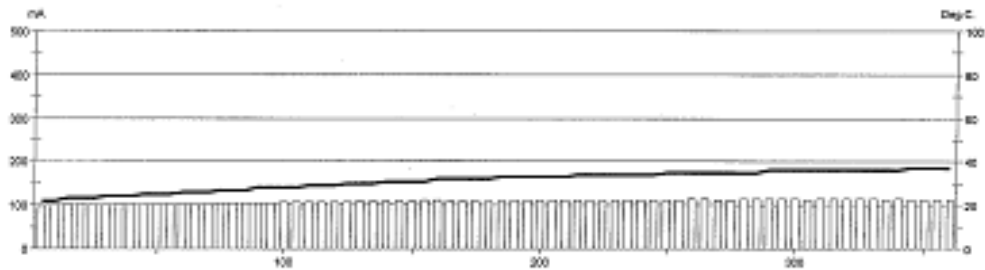
Your own logo
diam: 100 mm



CEMEX
Pavimento 2011
Pav. 100 mm x 100 mm
Pav. 100 mm x 100 mm

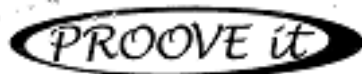
Test report

Voltage Used: 60
 Testing time: 06:00 hour
 Charge passed: 2355
 Adjusted Charge passed: 2125
 Permeability class: Moderate
 Instrument number: 071401
 Channel number: 1
 Report date: 7/29/2011
 Testing by: LG
 Reference: HS-SCC-1-TOP-28 DAY
 Sample diameter: 100
 Cement: ROLLA



Time	°C	mA									
00:05	22	99.1	01:35	28	105.2	03:05	33	110.4	04:35	35	112.3
00:10	22	101.2	01:40	28	106.2	03:10	33	111.1	04:40	35	113.2
00:15	23	102.0	01:45	28	106.4	03:15	33	111.6	04:45	35	114.8
00:20	23	101.6	01:50	29	107.6	03:20	33	111.6	04:50	36	113.4
00:25	23	100.8	01:55	29	107.8	03:25	33	111.2	04:55	36	113.1
00:30	24	101.5	02:00	29	107.8	03:30	33	111.1	05:00	36	113.3
00:35	24	101.8	02:05	30	107.9	03:35	34	111.2	05:05	36	112.1
00:40	24	102.1	02:10	30	108.4	03:40	34	110.7	05:10	36	113.9
00:45	25	102.4	02:15	30	109.0	03:45	34	112.2	05:15	36	113.6
00:50	25	102.7	02:20	31	108.7	03:50	34	112.7	05:20	36	113.5
00:55	25	102.7	02:25	31	108.4	03:55	34	112.6	05:25	36	113.0
01:00	26	102.9	02:30	31	108.4	04:00	34	112.7	05:30	36	113.1
01:05	26	102.9	02:35	31	110.7	04:05	34	112.6	05:35	36	112.6
01:10	26	103.5	02:40	32	110.7	04:10	35	112.6	05:40	36	112.8
01:15	27	104.0	02:45	32	110.1	04:15	35	112.4	05:45	37	112.7
01:20	27	104.1	02:50	32	110.2	04:20	35	113.3	05:50	37	112.7
01:25	27	104.8	02:55	32	110.2	04:25	35	112.9	05:55	37	112.4
01:30	28	105.1	03:00	32	110.3	04:30	35	112.7	06:00	37	111.8

Figure A.9 – C10-58L-EC1TOP RCT Data



ASTM C 1202-97



Test-compagny
Testing street 45
CompagnyCity
Some Country



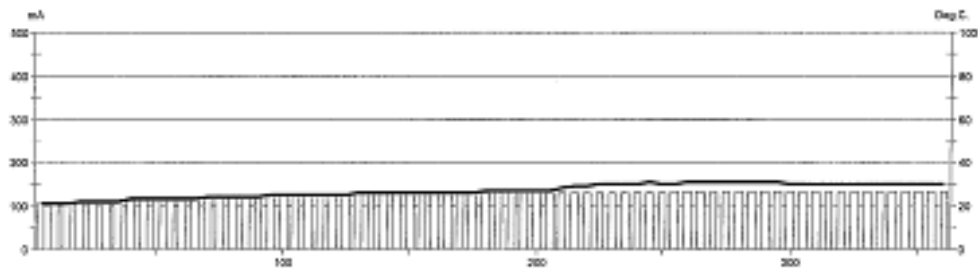
GERMAAD-DE-TRINIDADE

BOOMING
P.O. Box 1000
Tel: +31 (0) 20 247 1000

www.germanad.nl
For purchase

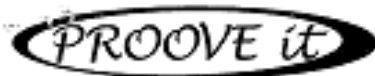
Test report

Voltage Used: 60
Testing time: 06:00 hour
Charge passed: 2706
Adjusted Charge passed: 2444
Permeability class: Moderate
Instrument number: 071401
Channel number: 2
Report date: 7/29/2011
Testing by: LG
Reference: HS-SCC-MIDDLE-I-28 DAY
Sample diameter: 100
Comment: ROLLA



Time	°C	mA									
00:05	21	104.8	01:35	25	121.3	03:05	27	130.6	04:35	31	130.6
00:10	21	107.0	01:40	25	122.2	03:10	27	130.7	04:40	31	130.9
00:15	21	108.2	01:45	25	122.9	03:15	27	130.8	04:45	31	130.9
00:20	22	109.1	01:50	25	123.7	03:20	27	130.7	04:50	31	131.0
00:25	22	109.9	01:55	25	124.5	03:25	27	130.5	04:55	31	130.9
00:30	22	110.7	02:00	25	125.0	03:30	28	130.1	05:00	30	131.2
00:35	22	111.4	02:05	25	125.7	03:35	29	129.9	05:05	30	131.3
00:40	23	112.2	02:10	26	126.4	03:40	29	130.0	05:10	30	131.3
00:45	23	113.0	02:15	26	126.9	03:45	30	130.0	05:15	30	131.2
00:50	23	113.8	02:20	26	127.6	03:50	30	130.1	05:20	30	131.3
00:55	23	114.6	02:25	26	128.0	03:55	30	130.2	05:25	30	131.4
01:00	23	115.3	02:30	26	128.6	04:00	30	130.2	05:30	30	131.3
01:05	23	116.1	02:35	26	128.9	04:05	31	130.4	05:35	30	131.3
01:10	24	116.8	02:40	26	129.4	04:10	30	130.5	05:40	30	131.1
01:15	24	117.6	02:45	26	129.6	04:15	30	130.6	05:45	30	131.1
01:20	24	118.6	02:50	26	130.0	04:20	31	130.6	05:50	30	130.9
01:25	24	119.5	02:55	26	130.3	04:25	31	130.7	05:55	30	130.7
01:30	24	120.5	03:00	27	130.4	04:30	31	130.7	06:00	30	131.0

Figure A.10 – C10-58L-EC1MIDDLE RCT Data



ASTM C 1202-97



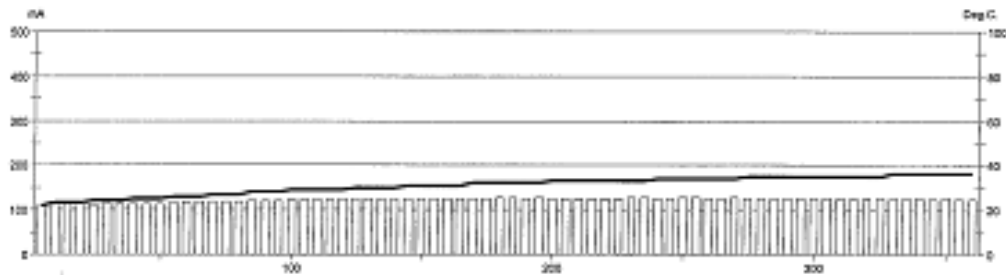
Test-compagny
Testing street 45
CompagnyCity
Some Country



CEMEX INSTRUMENTS
SERIAL NUMBER: 10210101
REV: 4.0 (2007)
CEMEX
P.O. Box 282800
Dallas, TX 75228

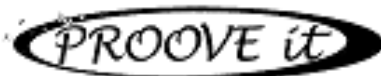
Test report

Voltage Used: 60
Testing time: 06:00 hour
Charge passed: 2649
Adjusted Charge passed: 2391
Permeability class: Moderate
Instrument number: 071401
Channel number: 3
Report date: 7/29/2011
Testing by: LG
Reference: HS-SCC-2-TOP-28 DAY
Sample diameter: 100
Comment: ROLLA



Time	°C	mA									
00:05	22	108.9	01:35	28	120.7	03:05	32	126.4	04:35	35	125.9
00:10	23	111.7	01:40	29	121.8	03:10	32	125.7	04:40	35	125.8
00:15	23	112.3	01:45	29	122.2	03:15	32	127.7	04:45	35	125.8
00:20	23	111.7	01:50	29	122.5	03:20	33	125.7	04:50	35	125.7
00:25	24	112.1	01:55	29	123.3	03:25	33	126.1	04:55	35	125.8
00:30	24	113.1	02:00	29	124.2	03:30	33	126.0	05:00	35	125.8
00:35	24	113.8	02:05	30	124.7	03:35	33	125.9	05:05	35	125.4
00:40	25	114.2	02:10	30	124.5	03:40	33	126.1	05:10	35	125.1
00:45	25	114.7	02:15	30	124.8	03:45	33	125.8	05:15	35	125.0
00:50	25	114.9	02:20	30	126.1	03:50	33	127.2	05:20	35	125.0
00:55	26	115.7	02:25	31	124.0	03:55	33	126.8	05:25	35	124.9
01:00	26	116.5	02:30	31	125.0	04:00	34	126.1	05:30	36	124.9
01:05	26	117.4	02:35	31	125.6	04:05	34	125.9	05:35	36	124.7
01:10	27	118.3	02:40	31	125.2	04:10	34	126.2	05:40	36	124.1
01:15	27	119.2	02:45	31	125.3	04:15	34	126.8	05:45	36	123.7
01:20	27	119.1	02:50	32	125.9	04:20	34	126.1	05:50	36	123.9
01:25	28	120.3	02:55	32	125.1	04:25	34	125.9	05:55	36	123.6
01:30	28	120.7	03:00	32	126.2	04:30	34	126.7	06:00	36	123.2

Figure A.11 – C10-58L-EC2TOP RCT Data



ASTM C 1202-97



Test-company
Testing street 45
CompagnyCity
Some Country

Some other logo
www.test-co.com
+33 1 23 45 67 89



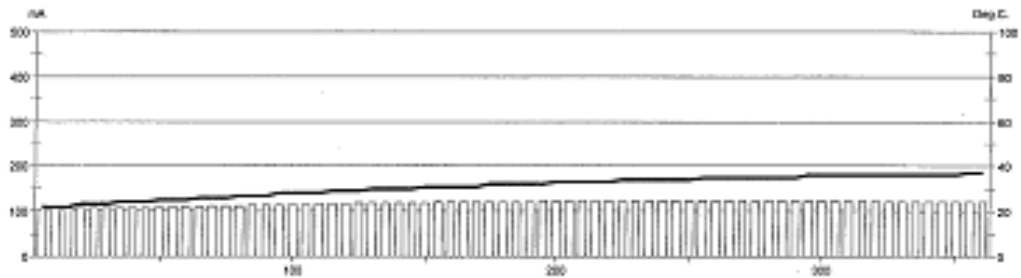
EDDADDD DDDDDDDDD

EDDADDD
From 10.000 to 10.000

From 10.000 to 10.000

Test report

Voltage Used: 60
Testing time: 06:00 hour
Charge passed: 2544
Adjusted Charge passed: 2296
Permeability class: Moderate
Instrument number: 071401
Channel number: 4
Report date: 7/29/2011
Testing by: LO
Reference: HS-SCC-2-MIDDLE-28 DAY
Sample diameter: 100
Comment: ROLLA



Time	°C	mA									
00:05	22	105.3	01:35	28	113.8	03:05	32	121.4	04:35	35	123.1
00:10	22	106.8	01:40	28	114.3	03:10	32	121.4	04:40	35	123.0
00:15	22	107.3	01:45	28	114.8	03:15	32	122.1	04:45	35	122.8
00:20	23	107.3	01:50	28	115.4	03:20	33	122.1	04:50	35	122.8
00:25	23	108.5	01:55	29	115.8	03:25	33	122.3	04:55	36	122.7
00:30	23	108.5	02:00	29	116.4	03:30	33	122.4	05:00	36	122.6
00:35	24	107.2	02:05	29	117.3	03:35	33	122.9	05:05	36	122.3
00:40	24	107.9	02:10	30	117.4	03:40	33	122.5	05:10	36	122.0
00:45	24	108.2	02:15	30	117.9	03:45	34	123.0	05:15	36	122.0
00:50	25	108.7	02:20	30	118.3	03:50	34	123.1	05:20	36	121.8
00:55	25	109.3	02:25	30	118.9	03:55	34	123.0	05:25	36	121.5
01:00	25	109.7	02:30	31	119.2	04:00	34	123.0	05:30	36	121.4
01:05	26	110.0	02:35	31	119.5	04:05	34	123.2	05:35	36	120.9
01:10	26	110.7	02:40	31	120.2	04:10	34	123.3	05:40	36	120.9
01:15	26	111.4	02:45	31	120.1	04:15	35	123.3	05:45	36	120.4
01:20	27	112.1	02:50	31	120.9	04:20	35	123.1	05:50	36	120.1
01:25	27	112.9	02:55	32	120.8	04:25	35	123.3	05:55	37	119.7
01:30	27	113.3	03:00	32	121.3	04:30	35	123.2	06:00	37	119.5

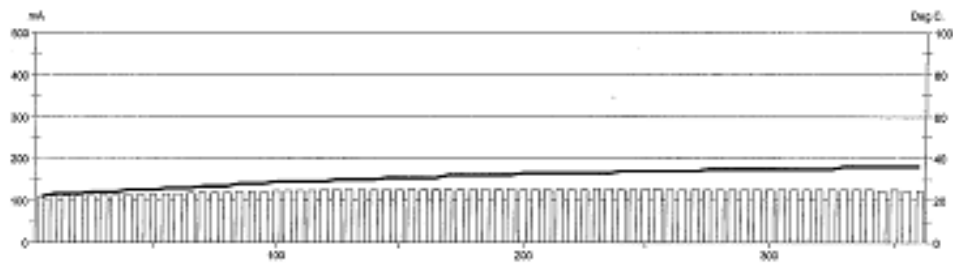
Figure A.12 – C10-58L-EC2MIDDLE RCT Data



Test report

Voltage Used: 60
 Testing time: 06:00 hour
 Charge passed: 2649
 Adjusted Charge passed: 2191
 Permeability class: Moderate
 Instrument number: 071401
 Channel number: 3
 Report date: 7/29/2011
 Testing by: LG
 Reference: HS-SCC-2-TOP-28 DAY
 Sample diameter: 100
 Comment: ROLLA

CERAMCO-REINFORCEMENTS
 BUREAU
 10000
 10000
 10000



Time	°C	mA									
00:05	22	108.9	01:35	28	120.7	03:05	32	126.4	04:35	35	125.9
00:10	23	111.7	01:40	29	121.8	03:10	32	125.7	04:40	35	125.8
00:15	23	112.3	01:45	29	122.2	03:15	32	127.7	04:45	35	125.8
00:20	23	111.7	01:50	29	122.5	03:20	33	125.7	04:50	35	125.7
00:25	24	112.1	01:55	29	123.3	03:25	33	126.1	04:55	35	125.8
00:30	24	113.1	02:00	29	124.2	03:30	33	126.0	05:00	35	125.8
00:35	24	113.8	02:05	30	124.7	03:35	33	125.9	05:05	35	125.4
00:40	25	114.2	02:10	30	124.5	03:40	33	126.1	05:10	35	125.1
00:45	25	114.7	02:15	30	124.8	03:45	33	125.8	05:15	35	125.0
00:50	25	114.9	02:20	30	124.1	03:50	33	127.2	05:20	35	125.0
00:55	26	115.7	02:25	31	124.0	03:55	33	126.8	05:25	35	124.9
01:00	26	116.5	02:30	31	125.0	04:00	34	126.1	05:30	36	124.9
01:05	26	117.4	02:35	31	125.6	04:05	34	125.9	05:35	36	124.7
01:10	27	118.3	02:40	31	125.2	04:10	34	126.2	05:40	36	124.1
01:15	27	119.2	02:45	31	125.3	04:15	34	126.8	05:45	36	123.7
01:20	27	119.1	02:50	32	125.9	04:20	34	126.1	05:50	36	123.9
01:25	28	120.3	02:55	32	125.1	04:25	34	125.9	05:55	36	123.6
01:30	28	120.7	03:00	32	126.2	04:30	34	126.7	06:00	36	123.2

Figure A.13 – S10-48L-EC1TOP RCT Data



ASTM C 1202-97



Test-compagny
Testing street 45
Compagny City
Some Country

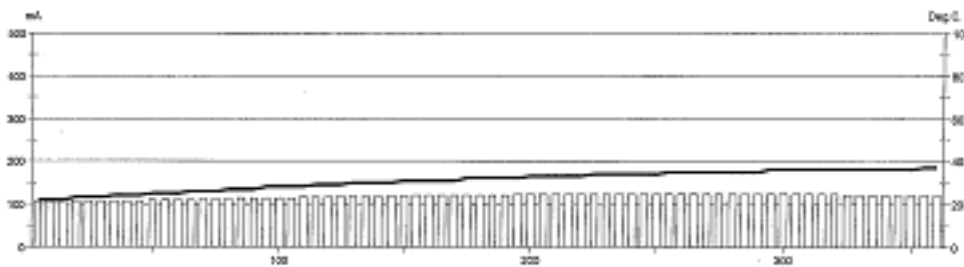
Year one log
file-0000000000



LABORATORY
MIDDLE
West-1202-97
The-1202-97
10
The-1202-97

Test report

Voltage Used: 60
 Testing time: 06:00 hour
 Charge passed: 2544
 Adjusted Charge passed: 2296
 Permeability class: Moderate
 Instrument number: 071401
 Channel number: 4
 Report date: 7/29/2011
 Testing by: LG
 Reference: HS-SCC-2-MIDDLE-28 DAY
 Sample diameter: 100
 Comment: ROLLA



Time	°C	mA									
00:05	22	105.3	01:35	28	113.8	03:05	32	121.4	04:35	35	123.1
00:10	22	106.8	01:40	28	114.3	03:10	32	121.4	04:40	35	123.0
00:15	22	107.3	01:45	28	114.8	03:15	32	122.1	04:45	35	122.8
00:20	23	107.3	01:50	28	115.4	03:20	33	122.1	04:50	35	122.8
00:25	23	106.5	01:55	29	115.8	03:25	33	122.3	04:55	36	122.7
00:30	23	106.5	02:00	29	116.4	03:30	33	122.4	05:00	36	122.6
00:35	24	107.2	02:05	29	117.3	03:35	33	122.9	05:05	36	122.3
00:40	24	107.9	02:10	30	117.4	03:40	33	122.5	05:10	36	122.0
00:45	24	108.2	02:15	30	117.9	03:45	34	123.0	05:15	36	122.0
00:50	25	108.7	02:20	30	118.5	03:50	34	123.1	05:20	36	121.8
00:55	25	109.3	02:25	30	118.9	03:55	34	123.0	05:25	36	121.5
01:00	25	109.7	02:30	31	119.2	04:00	34	123.0	05:30	36	121.4
01:05	26	110.0	02:35	31	119.5	04:05	34	123.2	05:35	36	120.9
01:10	26	110.7	02:40	31	120.2	04:10	34	123.3	05:40	36	120.9
01:15	26	111.4	02:45	31	120.1	04:15	35	123.3	05:45	36	120.4
01:20	27	112.1	02:50	31	120.9	04:20	35	123.1	05:50	36	120.1
01:25	27	112.9	02:55	32	120.8	04:25	35	123.3	05:55	37	119.7
01:30	27	113.3	03:00	32	121.3	04:30	35	123.2	06:00	37	119.5

Figure A.14 – S10-48L-EC1MIDDLE RCT Data

Table A.45 – C6-58L Chloride Content Data

Depth (in)	Chloride Content (%)		
	C6-58L-1P	C6-58L-2P	C6-58L-3P
0	0.29	0.23	0.23
0.25	0.05	0.09	0.07
0.75	0.02	0.03	0.02
1.5	0.01	0.01	0.01
2.0	0.01	0.01	0.01

Table A.46 – S6-48L Chloride Content Data

Depth (in)	Chloride Content (%)		
	S6-48L-1P	S6-48L-2P	S6-48L-3P
0	0.25	0.30	0.27
0.25	0.03	0.16	0.17
0.75	0.01	0.03	0.01
1.5	0.01	0.02	0.01
2.0	0.01	0.01	0.01

Table A.47 – C10-58L Chloride Content Data

Depth (in)	Chloride Content (%)		
	C10-58L-1P	C10-58L-2P	C10-58L-3P
0	0.27	0.22	0.24
0.25	0.05	0.19	0.09
0.75	0.01	0.01	0.02
1.5	0.01	0.01	0.01
2.0	0.01	0.01	0.02

Table A.48 – S10-48L Chloride Content Data

Depth (in)	Chloride Content (%)		
	S10-48L-1P	S10-48L-2P	S10-48L-3P
0	0.15	0.16	0.13
0.25	0.02	0.01	0.02
0.75	0.01	0.01	0.01
1.5	0.01	0.01	0.01
2.0	0.00	0.01	0.01

GM23		FREEZE & THAW LEDGER				Preliminary Testing Results @ Zero Cycles					
LAB NO:	UMR-A1	BEAM ID NO:		1	Agg. Description		Rolla				
35 Day Cure		Initial Weight in Air		9692.4	Initial bar reading		Starting Cycle Count		13153		
Initial Gage Reading		0.2495		Completion Date		Date Test Started		9/7/11			
Initial Frequency		1973		TERMINAL FREQUENCY		1184					
DATE	CYCLE # machine	Actual cycles	Weight	Ref. Bar	Gage reading	Corr. gage reading	Frqncy	RDM	Durab. Factor	% Gage Length Change	%Wght Change
9/8/11	13162	9	9693.0	0.2516	0.2509	0.2501	1911	93.81	2.81	0.0038	0.006
9/9/11	13171	18	9696.1	0.2523	0.2513	0.2498	1901	92.83	5.57	0.0019	0.038
9/12/11	13198	45	9704.4	0.2523	0.2522	0.2507	1856	88.49	13.27	0.0075	0.124
9/13/11	13207	54	9708.2	0.2523	0.2527	0.2512	1833	86.31	15.54	0.0106	0.163
9/15/11	13225	72	9718.6	0.2520	.	#VALUE!	1768	80.30	19.27	#VALUE!	0.270
9/16/11	13233	80	9722.3	0.2525	0.2558	0.2541	1741	77.87	20.76	0.0288	0.308
9/19/11	13260	107	9736.3	0.2521	0.2594	0.2581	1592	65.11	23.22	0.0538	0.453
9/21/11	13278	125	9747.4	0.2528	0.2627	0.2607	1454	54.31	22.63	0.0700	0.567
9/23/11	13296	143	9755.8	0.2522	0.2658	0.2644	1359	47.44	22.62	0.0931	0.654
9/26/11	13323	170	9764.8	0.2522	0.2705	0.2691	1217	38.05	21.56	0.1225	0.747
Totals		170						38.05	23.22	#VALUE!	0.01
Initial Measurements				Post Break Measurements							
WIDTH		DEPTH		WIDTH		DEPTH					
4.528		3.483		4.562		3.495		25.55 Avg. DF bms 1,2,3			
4.576		3.494		4.551		3.491		4.7907 Std. dev.			
4.539		3.498		4.574		3.495					
4.540		3.481									
4.546		3.489		4.562		3.494		Avg.			

Figure A.15 – C6-58L-FT1 Data

GM23		FREEZE & THAW LEDGER				Preliminary Testing Results @ Zero Cycles					
LAB NO:	UMR-A1	BEAM ID NO:		2	Agg. Description		Rolla				
35 Day Cure		Initial Weight in Air		9596.7	Initial bar reading		Starting Cycle Count		13153		
Initial Gage Reading		0.2445		Completion Date		Date Test Started		9/7/11			
Initial Frequency		1947		TERMINAL FREQUENCY		1168					
DATE	CYCLE # machine	Actual cycles	Weight	Ref. Bar	Gage reading	Corr. gage reading	Frqncy	RDM	Durab. Factor	% Gage Length Change	%Wght Change
9/8/11	13162	9	9598.7	0.2516	0.2472	0.2464	1886	93.83	2.81	0.0119	0.021
9/9/11	13171	18	9604.4	0.2523	0.2464	0.2449	1867	91.95	5.52	0.0025	0.080
9/12/11	13198	45	9616.5	0.2523	0.2491	0.2476	1819	87.28	13.09	0.0194	0.206
9/13/11	13207	54	9621.7	0.2523	0.2500	0.2485	1788	84.33	15.18	0.0250	0.261
9/15/11	13225	72	9633.9	0.252	0.2534	0.2522	1732	79.13	18.99	0.0481	0.388
9/16/11	13233	80	9638.7	0.2525	0.2560	0.2543	1702	76.42	20.38	0.0613	0.438
9/19/11	13260	107	9657.1	0.2521	0.2629	0.2616	1525	61.35	21.88	0.1069	0.629
9/21/11	13278	125	9668.1	0.2528	0.2677	0.2657	1414	52.74	21.98	0.1325	0.744
9/23/11	13296	143	9675.8	0.2522	0.2729	0.2715	1334	46.94	22.38	0.1688	0.824
9/26/11	13323	170	9683.4	0.2522	0.2800	0.2786	1177	36.54	20.71	0.2131	0.903
1/0/00	0	####		0							
1/0/00	0	####		0							
1/0/00	0	####		0							
1/0/00	0	####		0							
1/0/00	0	####		0							
1/0/00	0	####		0							
1/0/00	0	####		0							
1/0/00	0	####		0							
1/0/00	0	####		0							
1/0/00	0	####		0							
1/0/00	0	####		0							
1/0/00	0	####		0							
Totals		170						36.54	22.38	0.21	0.02
Initial Measurements				Post Break Measurements							
WIDTH		DEPTH		WIDTH		DEPTH					
4.558		3.482		4.547		3.491					
4.557		3.509		4.567		3.489					
4.555		3.487		4.556		3.492					
4.516		3.489									
4.547		3.492		4.557		3.491		Avg.			

Figure A.16 – C6-58L-FT2 Data

GM23		FREEZE & THAW LEDGER				Preliminary Testing Results @ Zero Cycles					
LAB NO:	UMR-A1	BEAM ID NO:		3	Agg. Description		Rolla				
35 Day Cure		Initial Weight in Air		9711.3	Initial bar reading		Starting Cycle Count		13153		
Initial Gage Reading		0.2606		Completion Date		Date Test Started		9/7/11			
Initial Frequency		1980		TERMINAL FREQUENCY		1188					
DATE	CYCLE # machine	Actual cycles	Weight	Ref. Bar	Gage reading	Corr. gage reading	Frqncy	RDM	Durab. Factor	% Gage Length Change	%Wght Change
9/8/11	13162	9	9710.6	0.2516	0.2597	0.2589	1933	95.31	2.86	-0.0106	-0.007
9/9/11	13171	18	9712.2	0.2523	0.2614	0.2599	1927	94.72	5.68	-0.0044	0.009
9/12/11	13198	45	9720.0	0.2523	0.2619	0.2604	1905	92.57	13.89	-0.0012	0.090
9/13/11	13207	54	9723.4	0.2523	0.2618	0.2603	1895	91.60	16.49	-0.0019	0.125
9/15/11	13225	72	9731.3	0.252	0.2611	0.2599	1867	88.91	21.34	-0.0044	0.206
9/16/11	13233	80	9734.5	0.2525	0.2640	0.2623	1851	87.39	23.31	0.0106	0.239
9/19/11	13260	107	9751.2	0.2521	0.2664	0.2651	1746	77.76	27.73	0.0281	0.411
9/21/11	13278	125	9763.6	0.2528	0.2689	0.2669	1666	70.80	29.50	0.0394	0.539
9/23/11	13296	143	9774.8	0.2522	0.2718	0.2704	1591	64.57	30.78	0.0612	0.654
9/26/11	13323	170	9786.2	0.2522	0.2768	0.2754	1466	54.82	31.06	0.0925	0.771
1/0/00	0	####		0							
1/0/00	0	####		0							
1/0/00	0	####		0							
1/0/00	0	####		0							
1/0/00	0	####		0							
1/0/00	0	####		0							
1/0/00	0	####		0							
1/0/00	0	####		0							
1/0/00	0	####		0							
1/0/00	0	####		0							
1/0/00	0	####		0							
1/0/00	0	####		0							
1/0/00	0	####		0							
Totals		170						54.82	31.06	0.09	-0.01
Initial Measurements				Post Break Measurements							
WIDTH		DEPTH		WIDTH		DEPTH					
4.542		3.494		4.569		3.485					
4.566		3.488		4.556		3.490					
4.566		3.492		4.562		3.493					
4.560		3.512									
4.559		3.497		4.562		3.489		Avg.			

Figure A.17 – C6-58L-FT3 Data

GM23		FREEZE & THAW LEDGER				Preliminary Testing Results @ Zero Cycles					
LAB NO:	UMR-SCC	BEAM ID NO:	2	Agg. Description	0						
35 Day Moist Cure		Initial Weight in Air	9701.3	Starting Cycle Count	12593						
Initial Gage Reading	N/A (No Studs)			Initial bar reading	N/A						
Initial Frequency	1979			Completion Date	Date Test Started	7/6/11					
				8/8/11	TERMINAL FREQUENCY	1187					
DATE	CYCLE # machine	Actual cycles	Weight	Ref. Bar	Gage reading	Corr. gage reading	Frqncy	RDM	Durab. Factor	% Gage Length Change	%Wght Change
7/7/11	12602	9	9701.8	0			1941	96.20	2.89		0.005
7/11/11	12638	45	9710.0	0			1909	93.05	13.96		0.090
7/14/11	12665	72	9720.8	0			1871	89.38	21.45		0.201
7/18/11	12701	108	9739.7	0			1775	80.45	28.96		0.396
		Flexural Strength = 696 psi									
		Tangent Modulus = 0.0825 Msi									
		Maximum Strain = 0.0098 in/in									
Totals		108						80.45	28.96	0.00	0.01
Initial Measurements				Post Break Measurements							
WIDTH		DEPTH		WIDTH		DEPTH					
				4.601		3.600					
				4.595		3.590					
				4.580		3.563					
0.000		0.000		4.592		3.584		Avg.			

Figure A.19 – S6-48L-FT2 Data

GM23		FREEZE & THAW LEDGER				Preliminary Testing Results @ Zero Cycles					
LAB NO:	UMR-SCC	BEAM ID NO:	3	Agg. Description	0						
35 Day Moist Cure		Initial Weight in Air	9666.1	Starting Cycle Count	12593						
Initial Gage Reading	N/A (No Studs)			Initial bar reading	N/A						
Initial Frequency	1902			Completion Date	Date Test Started	7/6/11					
				8/8/11	TERMINAL FREQUENCY	1141					
DATE	CYCLE # machine	Actual cycles	Weight	Ref. Bar	Gage reading	Corr. gage reading	Frqncy	RDM	Durab. Factor	% Gage Length Change	%Wght Change
7/7/11	12602	9	9667.8	0			1851	94.71	2.84		0.018
7/11/11	12638	45	9689.4	0			1783	87.88	13.18		0.241
7/14/11	12665	72	9705.8	0			1701	79.98	19.20		0.411
7/18/11	12701	108	9733.8	0			1353	50.60	18.22		0.700
		Flexural Strength = 548 psi									
		Tangent Modulus = 0.0455 Msi									
		Maximum Strain = 0.0204 in/in									
Totals		108						50.60	19.20	0.00	0.02
Initial Measurements				Post Break Measurements							
WIDTH		DEPTH		WIDTH		DEPTH					
				4.670		3.660					
				4.563		3.559					
				4.412		3.528					
0.000		0.000		4.548		3.582		Avg.			

Figure A.20 – S6-48L-FT3 Data

GM23		FREEZE & THAW LEDGER				Preliminary Testing Results @ Zero Cycles					
LAB NO:	HSC-Rolla	BEAM ID NO:	2	Agg. Description	0						
35 Day Cure		Initial Weight in Air	9729.1	Starting Cycle Count	12736						
Initial Gage Reading		Initial bar reading	0	Date Test Started	7/22/11						
Initial Frequency	1978	Completion Date	8/24/11	TERMINAL FREQUENCY	1187						
DATE	CYCLE # machine	Actual cycles	Weight	Ref. Bar	Gage reading	Corr. gage reading	Frqncy	RDM	Durab. Factor	% Gage Length Change	%Wght Change
7/25/11	12763	27	9727.8	0			1957	97.89	8.81		-0.013
7/27/11	12781	45	9728.4	0			1954	97.59	14.64		-0.007
7/29/11	12799	63	9728.1	0			1954	97.59	20.49		-0.010
8/1/11	12828	92	9728.9	0			1949	97.09	29.77		-0.002
8/3/11	12844	108	9721.6	0			1946	96.79	34.84		-0.077
8/5/11	12862	126	9720.0	0			1947	96.89	40.69		-0.094
8/9/11	12897	161	9723.8	0			1937	95.90	51.46		-0.054
8/11/11	12915	179	9724.0	0			1939	96.10	57.34		-0.052
8/15/11	12951	215	9726.7	0			1927	94.91	68.02		-0.025
8/17/11	12969	233	9728.3	0			1921	94.32	73.25		-0.008
8/19/11	12984	248	9729.1	0			1920	94.22	77.89		0.000
8/22/11	13009	273	9732.3	0			1915	93.73	85.30		0.033
8/23/11	13019	283	9734.3	0			1912	93.44	88.14		0.053
8/25/11	13036	300	9735.4				1908	93.05	93.05		0.065
Totals		300						93.05	93.05	0.00	-0.09
Initial Measurements				Post Break Measurements							
WIDTH		DEPTH		WIDTH		DEPTH					
0.000		0.000		0.000		0.000		Avg.			

Figure A.22 – C10-58L-FT2 Data

GM23		FREEZE & THAW LEDGER				Preliminary Testing Results @ Zero Cycles					
LAB NO:	HSC-Rolla	BEAM ID NO:		3	Agg. Description		0				
35 Day Cure		Initial Weight in Air		10038.1	Initial bar reading		Starting Cycle Count		12736		
Initial Gage Reading					Date Test Started		7/22/11				
		Completion Date		8/24/11	TERMINAL FREQUENCY		1193				
Initial Frequency		1988									
DATE	CYCLE # machine	Actual cycles	Weight	Ref. Bar	Gage reading	Corr. gage reading	Frqncy	RDM	Durab. Factor	% Gage Length Change	%Wght Change
7/25/11	12763	27	10037.7	0			1962	97.40	8.77		-0.004
7/27/11	12781	45	10039.7	0			1956	96.81	14.52		0.016
7/29/11	12799	63	10041.9	0			1957	96.91	20.35		0.038
8/1/11	12828	92	10044.5	0			1949	96.11	29.48		0.064
8/3/11	12844	108	10047.8	0			1947	95.92	34.53		0.097
8/5/11	12862	126	10050.8	0			1940	95.23	40.00		0.127
8/9/11	12897	161	10054.4	0			1930	94.25	50.58		0.162
8/11/11	12915	179	10058.7	0			1918	93.08	55.54		0.205
8/15/11	12951	215	10067.1	0			1888	90.19	64.64		0.289
8/17/11	12969	233	10067.0	0			1865	88.01	68.35		0.288
8/19/11	12984	248	10070.5	0			1847	86.32	71.36		0.323
8/22/11	13009	273	10076.7	0			1807	82.62	75.18		0.385
8/23/11	13019	283	10080.3	0			1787	80.80	76.22		0.420
8/25/11	13036	300	10084.1				1751	77.58	77.58		0.458
Flexural Strength = 654 psi											
Tangent Modulus = 0.0868 MSI											
Maximum Strain 0.0080 in/in											
Totals		300						77.58	77.58	0.00	0.00
Initial Measurements				Post Break Measurements							
WIDTH		DEPTH		WIDTH		DEPTH					
0.000		0.000		0.000		0.000		Avg.			

Figure A.23 – C10-58L-FT3 Data

GM23		FREEZE & THAW LEDGER				Preliminary Testing Results @ Zero Cycles					
LAB NO:	HS-SCC	BEAM ID NO:		1	Agg. Description		Rolla				
35 Day Cure		Initial Weight in Air		9819.9	Initial bar reading		Starting Cycle Count		12862		
Initial Gage Reading		Completion Date		9/7/11	Date Test Started		8/5/11				
Initial Frequency		2018		TERMINAL FREQUENCY		1211					
DATE	CYCLE # machine	Actual cycles	Weight	Ref. Bar	Gage reading	Corr. gage reading	Frqncy	RDM	Durab. Factor	% Gage Length Change	%Wght Change
8/9/11	12897	35	9819.7				1982	96.46	11.25		-0.002
8/11/11	12915	53	9821.8				1981	96.37	17.02		0.019
8/15/11	12951	89	9832.6				1950	93.37	27.70		0.129
8/17/11	12969	107	9841.0				1924	90.90	32.42		0.215
8/19/11	12984	122	9847.9				1905	89.11	36.24		0.285
8/22/11	13009	147	9862.1				1848	83.86	41.09		0.430
8/23/11	13019	157	9869.4				1830	82.24	43.04		0.504
8/25/11	13036	174	9882.0				1745	74.77	43.37		0.632
8/29/11	13072	210	9917.0				1376	46.49	32.55		0.989
Flexural Strength = 201 psi											
Tangent Modulus = 0.0292 Msi											
Maximum Strain = 0.0067 in/in											
Totals		210						46.49	43.37	0.00	0.00
Initial Measurements				Post Break Measurements							
WIDTH		DEPTH		WIDTH		DEPTH					
0.000		0.000		4.571		3.480		45.17 Avg. DF bms 1,2,3			
				4.569		3.440		15.5265 Std. dev.			
				4.570		3.460					
				4.570		3.460		Avg.			

Figure A.24 – S10-48L-FT1 Data

GM23		FREEZE & THAW LEDGER				Preliminary Testing Results @ Zero Cycles					
LAB NO:	HS-SCC	BEAM ID NO:	2		Agg. Description	Rolla					
Initial Weight in Air	35 Day Cure		9624.0		Initial bar reading	0	Starting Cycle Count	12862			
Initial Gage Reading					Completion Date	9/7/11	Date Test Started	8/5/11			
Initial Frequency	1998				TERMINAL FREQUENCY	1199					
DATE	CYCLE # machine	Actual cycles	Weight	Ref. Bar	Gage reading	Corr. gage reading	Frqncy	RDM	Durab. Factor	% Gage Length Change	%Wght Change
8/9/11	12897	35	9622.7	0			1978	98.01	11.43		-0.014
8/11/11	12915	53	9623.4	0			1982	98.40	17.38		-0.006
8/15/11	12951	89	9626.5	0			1973	97.51	28.93		0.026
8/17/11	12969	107	9628.6	0			1968	97.02	34.60		0.048
8/19/11	12984	122	9631.1	0			1967	96.92	39.41		0.074
8/22/11	13009	147	9637.7	0			1957	95.94	47.01		0.142
8/23/11	13019	157	9642.0	0			1948	95.06	49.75		0.187
8/25/11	13036	174	9648.0	0			1934	93.70	54.34		0.249
8/29/11	13072	210	9669.3	0			1873	87.88	61.52		0.471
Flexural Strength = 1081.5 psi											
Tangent Modulus = 0.1229 Msi											
Maximum Strain = 0.0101 in/in											
Totals		210						87.88	61.52	0.00	-0.01
Initial Measurements				Post Break Measurements							
WIDTH		DEPTH		WIDTH		DEPTH					
4.600		3.440		4.600		3.420					
4.600		3.420		4.610		3.400					
0.000		0.000		4.603		3.420		Avg.			

Figure A.25 – S10-48L-FT2 Data

GM23		FREEZE & THAW LEDGER				Preliminary Testing Results @ Zero Cycles					
LAB NO:	HS-SCC	BEAM ID NO:		3	Agg. Description		Rolla				
35 Day Cure		Initial Weight in Air		9132.1	Initial bar reading		Starting Cycle Count		12862		
Initial Gage Reading		Completion Date		9/7/11	Date Test Started		8/5/11				
Initial Frequency		2041		TERMINAL FREQUENCY		1225					
DATE	CYCLE # machine	Actual cycles	Weight	Ref. Bar	Gage reading	Corr. gage reading	Frqncy	RDM	Durab. Factor	% Gage Length Change	%Wght Change
8/9/11	12897	35	9133.6	0			1994	95.45	11.14		0.016
8/11/11	12915	53	9134.3	0			1983	94.40	16.68		0.024
8/15/11	12951	89	9147.1	0			1912	87.76	26.04		0.164
8/17/11	12969	107	9155.6	0			1852	82.34	29.37		0.257
8/19/11	12984	122	9163.5	0			1771	75.29	30.62		0.344
8/22/11	13009	147	9182.0	0			1516	55.17	27.03		0.546
8/23/11	13019	157	9192.5	0			1424	48.68	25.47		0.661
8/25/11	13036	174	9210.7	0			1290	39.95	23.17		0.861
8/29/11	13072	210	*	0			*	#####			#####
Flexural Strength = psi											
Tangent Modulus = Msi											
Maximum Strain = in/in											
* Beam broke into 2 pieces when pulled from the freezer											
Totals											
		210						#####	30.62	0.00	#####
Initial Measurements					Post Break Measurements						
WIDTH		DEPTH		WIDTH		DEPTH					
0.000		0.000		0.000		0.000 Avg.					

Figure A.26 – S10-48L-FT3 Data

REFERENCES

- ASTM C 39. (2010). Standard Test Method for Compressive Strength of Cylindrical Concrete Specimens. American Society of Testing and Materials, West Conshohocken, PA.
- ASTM C 78. (2010). Standard Test Method for Flexural Strength of Concrete (Using Simple Beam with Third-Point Loading). American Society of Testing and Materials, West Conshohocken, PA.
- ASTM C 192. (2007). Standard Test Method for Making and Curing Concrete Test Specimens in the Laboratory. American Society of Testing and Materials, West Conshohocken, PA.
- ASTM C 469. (2002). Standard Test Method for Static Modulus of Elasticity and Poissons Ratio of Concrete in Compression. American Society of Testing and Materials, West Conshohocken, PA.
- ASTM C 496. (2004). Standard Test Method for Splitting Tensile Strength of Cylindrical Concrete Specimens. American Society of Testing and Materials, West Conshohocken, PA.
- ASTM C 666. (2008). Standard Test Method for Resistance of Concrete to Rapid Freezing and Thawing. American Society of Testing and Materials, West Conshohocken, PA.
- ASTM C 1202. (2010). Standard Test Method for Electrical Indication of Concrete's Ability to Resist Chloride Ion Penetration. American Society of Testing and Materials, West Conshohocken, PA.
- ASTM C 1543. (2010). Standard Test Method for Determining the Penetration of Chloride Ion into Concrete by Ponding. American Society of Testing and Materials, West Conshohocken, PA.
- ASTM C 1610. (2010). Standard Test Method for Static Segregation of Self-Consolidating Concrete Using Column Technique. American Society of Testing and Materials, West Conshohocken, PA.
- ASTM C 1611. (2010). Standard Test Method for Slump Flow of Self-Consolidating Concrete. American Society of Testing and Materials, West Conshohocken, PA.

- ASTM C 1621. (2009). Standard Test Method for Passing Ability of Self-Consolidating Concrete by J-Ring, American Society of Testing and Materials, West Conshohocken, PA.
- American Concrete Institute ACI 237 R-07. (2007). Self-Consolidating Concrete, American Concrete Institute, Farmington Hills, Michigan.
- Bennenk, W., (2002). SCC in the Daily Precast Concrete Practice, Betonwerk and Fertigteiltechnik, V. 34, Issue 4.
- Berke, N.S. and Hicks, M.C. (1996). Predicting Times to Corrosion from Field and Laboratory Data, Techniques to Assess the Corrosion Activity of Steel Reinforced Concrete Structures, ASTM STP 1276. Neal S. Berke, Edward Escalante, Charles K. Nmai, and David Whiting, Eds., American Society for Testing and Materials.
- Broomfield, John P. (2007). Corrosion of Steel in Concrete: Understanding, Investigation and Repair. Taylor & Francis (Second Edition).
- Coppola, L., Cerulli, T., Salvioni, D. (2005). Sustainable Development and Durability of Self-Compacting Concretes, 11th International Conference on Fracture, Proceedings, Turin, Italy.
- Khayat, K.H. (1999). Workability, Testing, and Performance of Self-Consolidating Concrete. ACI Journal, Proceedings May-June, Vol. 96, No. 3, pp. 346-354.
- Khayat, K.H. (2002). Optimization and Performance of Air Entrained, Self-Consolidating Concrete. ACI Materials Journal, Vol. 97, No. 5, pp. 526-535.
- Mansfield, F. (1981). Recording and Analysis of AC Impedance Data for Corrosion Studies. Corrosion, Vol. 37, No. 5, pp. 301-307.
- Mortsell, E., and Rodum, E., (2001). Mechanical and Durability Aspects of SCC for Road Structures. Proceedings of the Second International Symposium on SCC, K. Ozawa and M. Ouchi, eds., Tokyo, pp. 459-468.
- Mindess, S., Young, J.F., and Darwin, D. (2003). Concrete. Pearson Education, Inc. (Second Edition).
- Neville, A. M. (1997). Properties of Concrete. John Wiley and Sons, Inc. (Fourth Edition).
- Office of Research, Development, and Technology, Office of Safety, RDT. (1997). User Guidelines for Waste and Byproduct Materials in Pavement Construction. Report No. FHWA-RD-97-148. Federal Highway Administration, Cortest Columbus Technologies.

- Oluokun, Francis A (1991). Prediction of Concrete Tensile Strength from Its Compressive Strength: Evaluation of Existing Relations for Normal Weight Concrete. *ACI Materials Journal*, Vol. 88, No. 3, pp. 302-309.
- Persson, B., (1999). Creep, Shrinkage and Elastic Modulus of Self-Compacting Concrete. 1st International RILEM Symposium on Self-Compacting Concrete Stockholm, Sweden.
- Powers, T.C. (1975). Freezing Effects in Concrete. SP-47, American Concrete Institute, Detroit, MI, pp. 1-12.
- Sengul, O. and Gjrv, O. (2009). Effect of Embedded Steel on Electrical Resistivity Measurements on Concrete Structures. *ACI Materials Journal*, 106(1), 11-18.
- Sonebi, M., and Bartos, P. J. M. (2001). Performance of Reinforced Columns Cast with Self-Compacting Concrete. *Recent Advances in Concrete Technology, Proceedings of the Fifth CANMET/ACI International Conference*, SP-200, V. M. Malhotra, ed., American Concrete Institute, Farmington Hills, Mich., pp. 415-431.
- Whiting, D.A. and Nagi, M.A. (2003). Electrical Resistivity of Concrete - A Literature Review. R&D Serial No. 2457. Portland Cement Association, Skokie, IL.

